UNCLASSIFIED

AD NUMBER

AD469994

NEW LIMITATION CHANGE

TO

Approved for public release, distribution unlimited

FROM

Distribution authorized to U.S. Gov't. agencies and their contractors; Administrative/Operational Use; AUG 1965. Other requests shall be referred to Air Force Weapons Lab., Kirtland AFB, NM.

AUTHORITY

AFWL ltr, 29 Apr 1985

THIS PAGE IS UNCLASSIFIED

AFWL TR-65-48

AFWL TR
65-48

CATALOGED BY DDC
469994

A COMPARISON OF THE DYNAMIC AND STATIC SHEAR STRENGTHS OF COHESIONLESS, COHESIVE AND COMBINED SOILS

B. B. Schimming, H. J. Haas, and H. C. Saxe

Department of Civil Engineering
University of Notre Dame
Notre Dame, Indiana

Contract AF29(601)-5174

TECHNICAL REPORT NO. AFWL TR-65-48

August 1965

AIR FORCE WEAPONS LABORATORY
Research and Technology Division
Air Force Systems Command
Kirtland Air Force Base
New Mexico

DDC
SEP 22 1965
DDC-IRA E

AFWL TR-65-48

Research and Technology Division
AIR FORCE WEAPONS LABORATORY
Air Force Systems Command
Kirtland Air Force Base
New Mexico

When U. S. Government drawings, specifications, or other data are used for any purpose other than a definitely related Government procurement operation, the Government thereby incurs no responsibility nor any obligation whatsoever, and the fact that the Government may have formulated, furnished, or in any way supplied the said drawings, specifications, or other data, is not to be regarded by implication or otherwise, as in any manner licensing the holder or any other person or corporation, or conveying any rights or permission to manufacture, use, or sell any patented invention that may in any way be related thereto.

This report is made available for study with the understanding that proprietary interests in and relating thereto will not be impaired. In case of apparent conflict or any other questions between the Government's rights and those of others, notify the Judge Advocate, Air Force Systems Command, Andrews Air Force Base, Washington, D. C. 20331.

Qualified users may obtain copies of this report from DDC.

Distribution is limited because of the technology discussed in the report.

A COMPARISON OF THE DYNAMIC AND STATIC SHEAR STRENGTHS OF COHESIONLESS, COHESIVE AND COMBINED SOILS

B. B. Schimming, H. J. Haas, and H. C. Saxe

Department of Civil Engineering
University of Notre Dame
Notre Dame, Indiana

Contract AF29(601)-5174

TECHNICAL REPORT NO. AFWL TR-65-48

FOREWORD

This report was prepared by the Department of Civil Engineering, University of Notre Dame, Notre Dame, Indiana, under AF Contract 29(601)-5174. The work was funded under DASA Subtask 13.144, Project 5710, Program Element 7.60.06.01.5. Inclusive dates of research were March 1962 through May 1965. The report was submitted on 27 July 1965. AFWL Project Officer was 1Lt John E. Seknicka (WLDC).

The authors wish to express their appreciation to Professor L. D. Graves, Professor C. C. Stevason, Mr. V. P. Drnevich, Mr. T. R. Kretschmer and Mr. R. S. LaRusso for their contributions to this project.

This report has been reviewed and is approved.

JOHN E. SEKNICKA
1Lt USAF
Project Officer

ROBERT E. CRAWFORD
Major USAF
Deputy Chief, Civil Engineering Branch

Frank M. McMullen Lt/C
for JOHN W. KODIS
Colonel USAF
Chief, Development Division

ABSTRACT

A direct shear device capable of applying maximum shear stresses to soil specimens in a period of time ranging from 1 millisecond to 20 minutes has been utilized to test a wide variety of soils.

The cohesionless materials, an Ottawa sand in the loose and dense condition, a powdered Nevada silt and a dry powder clay, did not exhibit any increase in maximum shear resistance due to an impact type dynamic shear force application as compared to a static force application. An increase of apparent friction angle from 45 degrees to approximately 60 degrees due to inertial confinement was observed in a dense Ottawa sand.

Cohesive materials, which included undisturbed and remolded clays and combined soils (mixtures of sand and clay), demonstrated an increase in maximum shear resistance under impact loads described solely by the apparent cohesion intercept of the failure envelope. The friction angle was essentially insensitive to test duration. The ratio of the apparent cohesion for a failure envelope involving failure times of 5 milliseconds to the corresponding intercept for failure times of nearly 1 minute was approximately 2. This ratio appeared to be relatively insensitive to moisture content, dry density, grain size and soil structure (flocculated or dispersed) for degrees of saturation in

excess of 85%. The apparent cohesion ratio appeared to decrease on the dry side of optimum for compacted soils.

Investigation of different pore fluids indicated that pore fluid viscosity was not primarily responsible for the increases in strength.

The simultaneous dynamic application of normal and shear forces did not alter the apparent cohesion ratio of the clays studied.

A preliminary discussion of repetitive force results on clays is included in the report.

CONTENTS

ILLUSTRATIONS

Figure		Page
III. 1	"Rapid Static" Failure Envelope for Dense Dry Ottawa Sand	123
III. 2	"Dynamic" Points Compared with "Rapid Static" Failure Envelope for Dense Dry Ottawa Sand	125
III. 3	"Dynamic" Saturated Points Compared with "Rapid Static" Failure Envelope for Dense Dry Ottawa Sand	127
III. 4	"Rapid Static" Failure Envelope for Loose Dry Ottawa Sand	129
III. 5	"Dynamic" Points Compared with "Rapid Static" Failure Envelope for Loose Dry Ottawa Sand	131
III. 6	Grain Size Distribution Curve for Jordan Buff Clay	134
III. 7	Failure Envelope for Air-dried Powdered Jordan Buff Clay: $w \approx 0\%$	135
III. 8	Failure Envelopes for Jordan Buff Clay: $w \approx 10\%$	137
III. 9	Failure Envelopes for Jordan Buff Clay: $w \approx 20\%$	139
III. 10	Failure Envelopes for Jordan Buff Clay: $w \approx 25\%$	142
III. 11	Failure Envelopes for Jordan Buff Clay: $w \approx 30\%$	145
III. 12	Failure Envelopes for Jordan Buff Clay: $w \approx 34\%$	148
III. 13	Normally Consolidated and Overconsolidated Jordan Buff Clay Test Results	150
III. 14	Failure Envelopes for Jordan Buff Clay + Salt Water: $w \approx 30\%$	153
III. 15	Failure Envelopes for Jordan Buff Clay + Glycerin: $w \approx 40\%$	155
III. 16	Failure Envelopes for Jordan Buff Clay + Glycerin: $w \approx 60\%$	157
III. 17	Failure Envelopes for Jordan Buff Clay + Kerosene: $w \approx 30\%$	159
III. 18	Failure Envelopes for Combined "Ideal" Soil: Jordan Buff Clay + Ottawa Sand + Water	162
III. 19	Failure Envelopes for Western Bentonite Clay: $w \approx 53\%$	165
III. 20	Failure Envelopes for Western Bentonite Clay: $w \approx 95\%$	167
III. 21	Failure Envelopes for Western Bentonite Clay + Benzene: $w \approx 40\%$	169
III. 22	Failure Envelope for Remolded Nevada Test Site Desert Alluvium	172
III. 23	Grain Size Distribution Curve for Chicago Blue Clay	175

TABLES

note: The following Table references of Appendix III are the summaries of test results for Figures of the same number.

ABBREVIATIONS AND SYMBOLS

A	$4k/\lambda$
A'	$4/\lambda$
A_c	cylinder cross-sectional area
a	acceleration
C_a	apparent cohesion; the cohesive intercept on Mohr failure envelope
$(C_a)_d$	"dynamic" test apparent cohesion
$(C_a)_{rs}$	"rapid static" test apparent cohesion
$\frac{(C_a)_d}{(C_a)_{rs}}$	"apparent cohesion" ratio
c	cohesion or intrinsic strength of soil
c_e	effective cohesion or cohesion component
c_u	ultimate cohesion component
c_v	rheologic strength component
D	energy required for dilation under the action of a unit interparticle normal force
ΔE_o	physico-chemical contribution to bond energy; the true cohesion expressed as an energy
e	void ratio
f	friction force
k	Boltzman constant

L. I.	liquidity index
m	mass
NR	no record
OCR	over consolidation ratio
p	normal stress on the failure plane
p_c	cylinder air pressure
p_i	intrinsic pressure
S	degree of saturation
S'	soil structure as represented by the number of interparticle contacts per unit cross-sectional area
s	shearing strength
T	temperature
t	time
u	pore water pressure
w	moisture content
γ_d	dry density
Δ_n	normal displacement
ϵ_s	shearing strain
$\dot{\epsilon}_1$	axial compressive strain rate in triaxial compression
λ	distance between successive interparticle equilibrium positions
σ_{ff}	total normal stress on the failure plane occurring simultaneously with the maximum shear stress level

$\bar{\sigma}_{ff}$	intergranular pressure normal to the surface of failure when failure is occurring
$\bar{\sigma}_i$	initial effective stress
σ_1	total axial stress in triaxial compression
σ'_1	effective axial stress in triaxial compression
σ_3	total lateral stress in triaxial compression
σ'_3	effective lateral stress in triaxial compression
τ	shearing stress on the failure plane
τ_d	surface energy (dilatation) component of measured shear strength
τ_f	measured shear strength
τ_m	maximum shear stress level
τ_ϕ	effective frictional component of measured shear strength
Φ	stress dependent interparticle bond energy under a unit normal force
Φ'	$2/\lambda(\Phi + D)$
ϕ	angle of internal friction
ϕ'	true friction angle
ϕ'_e	effective angle of internal friction
$(\phi)_d$	"dynamic" failure envelope friction angle
$(\phi)_{rs}$	"rapid static" failure envelope friction angle

Previous page was blank, therefore not filmed.

SECTION 1. INTRODUCTION

On March 1, 1962, the Civil Engineering Department of the University of Notre Dame was awarded United States Air Force Contract AF 29(601)-5174 to develop a direct shear apparatus for testing soils under both static and dynamic loads. Two previous reports concerning contract progress have been published by the Air Force. RTD-TDR-63-3050[1.1] contained preliminary design criteria and an annotated soil dynamics bibliography. RTD-TDR-63-3055[1.2] described the completed testing device. The purpose of this terminal report is to present the results of a rather extensive soil testing program utilizing the completed device.

The dominant theme of the testing program has been to attempt to relate, in terms of conventional soil mechanics parameters, the controlled-stress static strength to the maximum dynamic resistance for a wide variety of soils.

The basic feature of a direct shear device is maximum shear resistance determination, not strain measurements; thus, no particular attempt was made to examine stress strain behavior.

The range of application of the results of this study must be carefully understood to avoid misinterpretation. The effect of soil strength on the formation of a crater produced by the pressures developed from an underground explosion which forces failure to occur very rapidly is a potentially valid application. Utilization of dynamic strength properties for shock wave calculations such as the SOC code as reported by Butkovich[1,3] is another possible application. However, the ability of a soil to withstand a single dynamic pulse involving both rapid rise and decay times where the specimen is not necessarily forced to fail remains to be investigated as well as the effect of the passage of such a pulse on the subsequent static strength. The dwell period of a pulse is also pertinent. If for example, a specimen is subjected to a stress pulse with an amplitude slightly in excess of the static strength and a rise time of a few milliseconds which is then allowed to dwell, failure will occur as the strain rate effect is lost.

In addition, the effect of vibratory loads on maximum shear resistance should not be confused with the single-pass impact-type failure test.

With these interpretations as a guide, the following study is presented for review.

SECTION 1. REFERENCES

1.1 Woods, R. D., Preliminary Design of Dynamic-Static Direct Shear Apparatus for Soils and Annotated Bibliographies of Soil Dynamics and Cratering, Air Force Weapons Laboratory, Technical Documentary Report No. RTD-TDR-63-3050.

1.2 Saxe, H. C., L. D. Graves, C. C. Stevason, B. B. Schimming, V. P. Drnevich and T. R. Kretschmer, Development of an Apparatus for the Dynamic Direct Shear Testing of Soils, Air Force Weapons Laboratory, Technical Documentary Report No. RTD-TDR-63-3055.

1.3 Butkovich, T. R., "Calculation of the Shock Wave from an Underground Nuclear Explosion in Granite," Proceedings of the Third Plowshare Symposium, Engineering with Nuclear Explosives, April 1964, pp. 37-50.

SECTION 2. DESCRIPTION AND OPERATION OF DACHSHUND I

a. DACHSHUND I - Testing Device.

(1) General.

The initial objective of this research project was to develop a direct shear device on which the shearing resistance of the entire range of soil types could be measured under both static and dynamic testing conditions. The device, Figure 2.1, became operational in July 1963 and was given the name DACHSHUND I (Dynamically Applied Controlled Horizontal SHear - University of Notre Dame I).

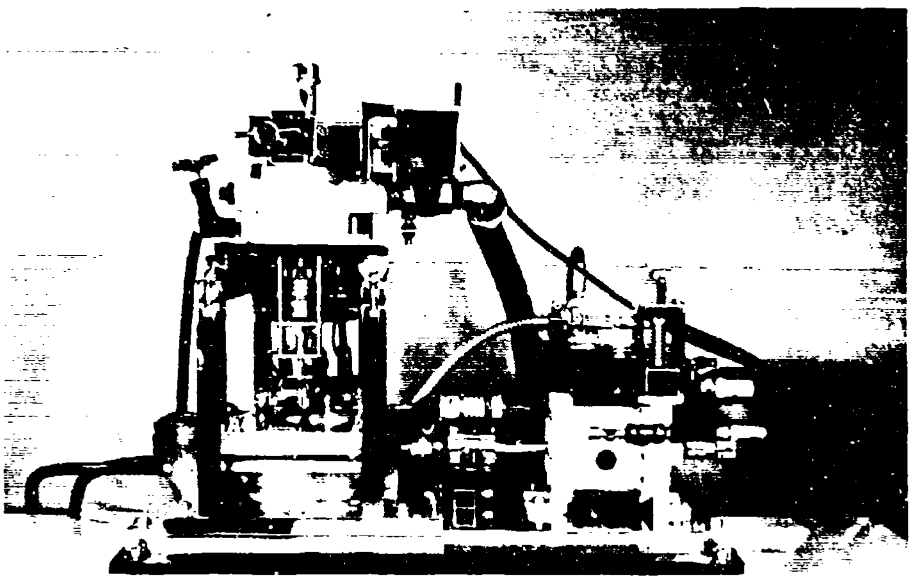

Figure 2.1 DACHSHUND I Direct Shear Device

Prior to discussion of the apparatus it is necessary to define a few terms which are used throughout this report.

Shear displacement: A measured displacement of the lower shear box relative to the upper shear box.

Shear force: The force imparting a shear displacement to the shear box and soil sample.

Normal displacement: An expansion or contraction of the soil sample in a direction perpendicular to the shear plane.

Normal force: The force applied to the soil sample on a plane parallel to the shear plane.

Reference to a shear or normal stress implies division of the respective forces by the initial cross-sectional area of the soil sample.

The following brief description of DACHSHUND I, schematically represented in Figure 2.2, summarizes its characteristics and capabilities. For a more detail description see Saxe, et al.[1,2]

(2) Shearing Mechanism.

(a) Shear Box.

The focal point of the shear device is the shear box in which a soil sample 3/4-inch-thick and 4 inches in diameter is placed. The shear box consists of a lower unit which moves relative to a restrained upper unit and produces a shearing deformation in the test sample. The moving portion of the shear box is cast of aluminum to

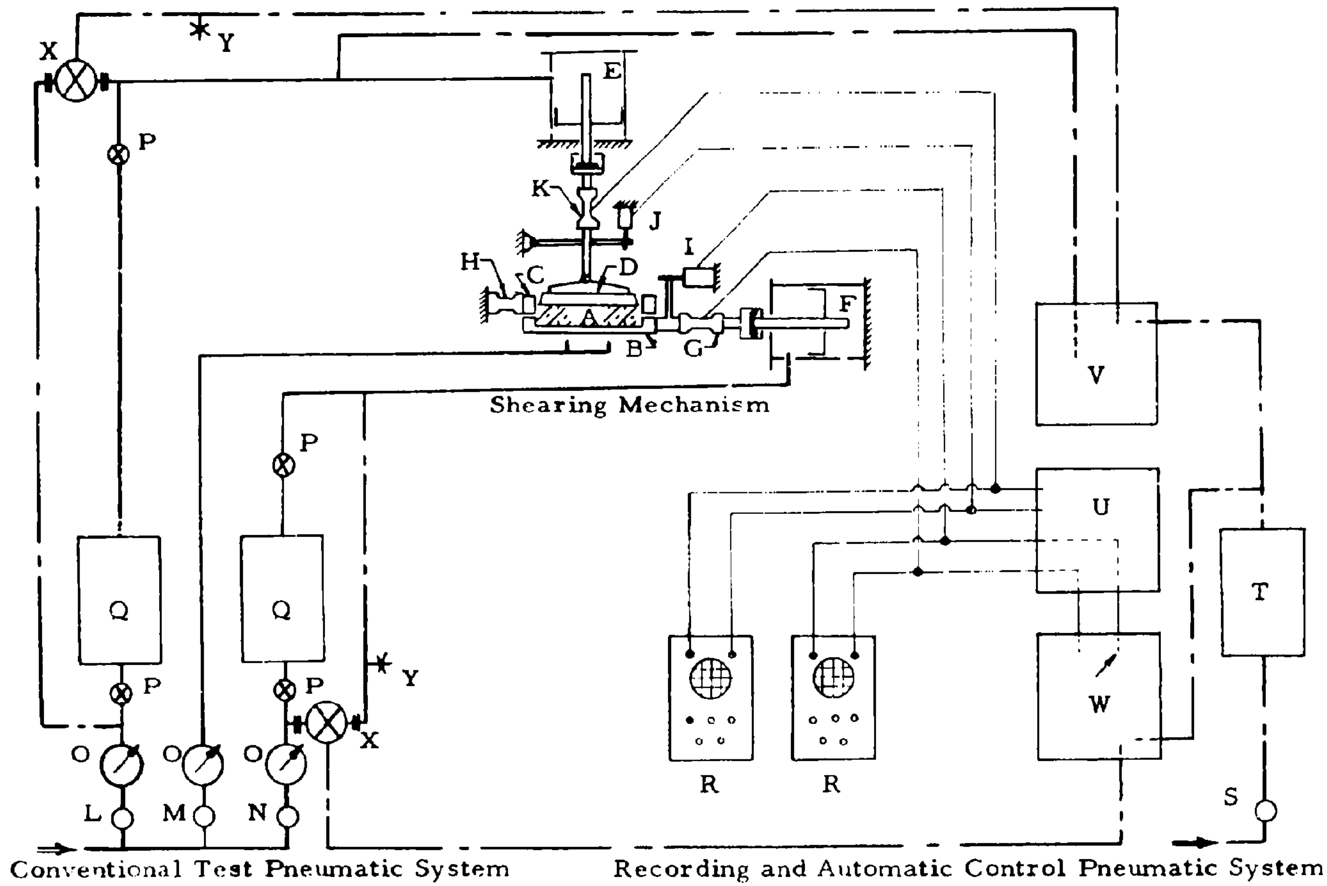

Figure 2. 2 Schematic Diagram of DACHSHUND I

Table 2.1

Symbols Used in Figure 2.2: Schematic Diagram of DACHSHUND I

Shearing Mechanism	Conventional Test Pneumatic System	Recording and Automatic Control Pneumatic System
A. Soil Sample	L. Normal Cylinder Pressure Regulator	R. Oscilloscopes
B. Lower Shear Box	M. Air Bearing Pressure Regulator	S. Automatic Control Pressure Regulator
C. Upper Shear Box	N. Shear Cylinder Pressure Regulator	T. Accumulator Tank
D. Upper Gripper Spacer and Loading Head	O. Pressure Gages	U. 4-Pen Strip Chart Recorder
E. Normal Force Air Cylinder	P. Gate valves (closed during automatic control tests)	V. Automatic Normal Force Programmer
F. Shear Force Air Cylinder	Q. Accumulator Tanks	W. Automatic Shear Force or Displacement Programmer
G. Action Shear Force Transducer (Lower Shear Force)		X. Pneumatically controlled gate valves
H. Reaction Shear Force Transducer (Upper Shear Force)		Y. Overflow needle valves
I. Shear Displacement Transducer	—— Conventional Test Pneumatic System	—-— Automatic Control Pneumatic System
J. Normal Displacement Transducer		···—· Recording System
K. Normal Force Transducer		

reduce inertial effects during dynamic tests. This lower unit contains seven 1/8-inch-high gripper blades to aid in the distribution of the shearing force throughout the sample. Porous bronze plates are located between the gripper blades and drainage paths are provided. A 1-inch-thick aluminum plate with a 4-inch-diameter hole to accommodate the soil sample, represents the upper unit. It is mounted on four flexible vertical cantilevers and restrained from lateral movement by the reactio shear force transducer. Ball bearings and an air bearing beneath the moving tray create a relatively frictionless surface between the lower shear box and its support.

An upper gripper spacer and a loading head permit application of the normal load to the sample. The upper gripper spacer is a 1/2-inch-thick, 4-inch-diameter aluminum plate with gripper blades positioned opposite those on the lower unit. The loading head, placed above the upper gripper spacer, is fitted with a socket which allows rotation in order to maintain a uniform pressure distribution on the sample during shear.

(b) Force and Displacement Transducers.

Force and displacement transducers were required to record the desired response as a function of time. The force transducers are thin-walled, spool-shaped steel cylinders. Four wire-resistance strain gages are cemented to the walls of the spool and connected in a wheatstone bridge circuit which permits an electronic readout of the applied force. The action shear force transducer is connected axially between the piston rod and the lower shear box. The reaction shear force transducer is designed for connection with an independent support which restrains the movement of the upper half of the shear box. The normal force transducer is located above the center of the sample. Linear potentiometers are used as displacement transducers and are connected indirectly to the piston rods.

(3) Recording System.

It was necessary to incorporate essentially two separate electronic recording systems in order to accommodate the range of test durations involved. Oscilloscopes with the appropriate Polaroid cameras and attachments are used to permanently record the test information for test durations ranging from milliseconds to 50 seconds. A Bristol "Dynamaster Four Pen Strip Chart Recorder" is used for test durations greater than 50 seconds.

(4) Pneumatic System.

DACHSHUND I, basically a stress-control direct shear apparatus, is also capable of controlled displacement tests when the desired rates of displacement are comparable to those available on standard laboratory direct shear devices. To accomplish this flexibility it was necessary to develop a pneumatic system which would permit various methods of shear and normal force application.

An air compressor, three accumulator tanks and two air cylinders represent the core of the pneumatic system. These components are supplemented by the necessary valving, piping, pressure regulators and gages required to transmit and control the air as desired. The two cylinders are made of cast iron with aluminum pistons designed to transmit maximum horizontal and vertical forces of 1000 pounds or the equivalent of 79.6 psi to the 4-inch-diameter sample.

(a) Conventional "Dynamic" and "Rapid Static" Tests.

The two accumulator tanks indicated in Figure 2.2 are used to provide a relatively large volume of air such that the volume change during the stroke of the piston does not appreciably affect the pressure on the soil sample.

Each air cylinder has a solenoid-actuated triggering device to hold the piston in position such that a preset pressure can be established behind the piston for dynamic force application. The basic difference between the "dynamic" test and the conventional "rapid static" test is that the piston in the latter case is unrestrained and the load is accumulated at the desired rate by manual control of the pressure regulators.

(b) Automatic Control Tests.

To perform either automatic controlled shear force or shear displacement tests which involve durations greater than

50 seconds, it is necessary to introduce the "Automatic Control Pneumatic System," Figure 2.2, and eliminate the conventional system accumulator tanks. As in the case of the conventional "rapid static" shear test the pistons are unrestrained from movement with a zero initial pressure in the cylinder. The entire system is automatically controlled on either a programmed rate of shear displacement or shear force application. The controlling signal is retransmitted from the four-pen strip chart recorder to the automatic shear force or displacement programmer, a Bristol "Dynamaster Air-Operated Controller." This controller pneumatically controls the opening and closing of the gate valve allowing air pressure to enter the air cylinder. The automatic normal force programmer, a Bristol "Pneumatic Free Vane Controller," is used to regulate the normal force on the soil sample by controlling the gate valve opening and flow into the air cylinder. An air pressure supply to the programming units is required to pneumatically control the gate valves. The accumulator tank in this system serves as a pressure stabilizer when a small volume of air is used by the controllers to operate the gate valves.

b. Test Description and Procedure.

(1) General.

The results of three basically different types of tests represent the bulk of all the data. They are referred to as the

1) Conventional "Dynamic" Test

2) Conventional "Rapid Static" Test

3) Automatic Control Tests.

In addition, a series of special tests have been run and are discussed in Section 5 of this report. In this subsection the testing procedures for the above three basic tests are outlined generally. All soils are tested in the manner described with variations arising only in sample preparation as detailed with the test results for each soil type in Appendix III of this report.

(2) <u>Conventional "Dynamic" Test.</u>

The term "conventional test" applies to the use of the conventional pneumatic system and the oscilloscopes as the recording system. In a conventional "dynamic" test the maximum shear force in the specimen is attained within a period of 1 to 5 milliseconds after imposition of the initial shear force. As was previously mentioned the basic difference between "dynamic" and "rapid static" tests is the method by which the shear force is applied. In the "dynamic" test the restrained piston is released by actuating the solenoid trigger mechanism. As a result of this release, an impact force is imposed on the soil resulting in very rapid rise times.

To perform a "dynamic" test, the recording system is prepared, the sample placed in the shear box, the normal force applied and the trigger mechanism cocked. An air pressure of sufficient magnitude to fail the sample is accumulated in the shear force cylinder. One switch simultaneously triggers the oscilloscope traces and the release mechanism to impose the shear force on the sample.

(3) Conventional "Rapid Static" Test.

"Rapid static" tests involve times to failure ranging from 30 seconds to nearly 50 seconds. A 50-second period is the upper limit because it is the maximum sweep time of the oscilloscope.

The general test procedure is to prepare the recording system, place the soil sample in the shear box, apply the normal force, trigger the oscilloscope traces and manually increase the shear force with the pressure regulator at the desired rate to achieve failure of the sample.

(4) Automatic Control Tests.

To perform tests with shear displacement rates or rates of shear force application comparable to those on the standard laboratory direct shear device a pneumatically controlled servomechanism was introduced. Test durations with the current arrangement can be varied from 1 to 20 minutes merely by using different cams. A change of cam motors would considerably increase the maximum time duration of tests.

Whether a controlled displacement or controlled force test is desired the general test procedure is essentially identical. The recording system is prepared, the sample is placed in the shear box, an air pressure is supplied to the servomechanism and the phenomenon to be controlled is selected on the programmer. Sufficient air pressures are established behind the closed gate valves to allow desired normal force application and failure of the soil in shear. The test is put on automatic control merely by starting the servomechanism and the strip chart recorder.

A more detailed description of the test procedures is given in Appendix I of this report.

Completion of the automatic control displacement apparatus late in the experimental phase of the project, the inherent ease with which "rapid static" tests were performed and the correlation of a "rapid static" test result with a controlled displacement test of comparable duration (Appendix II) dictated that the bulk of the static tests be conducted utilizing the "rapid static" technique.

c. Interpretation of Results.

(1) General.

The purpose of this section is to schematically indicate the maximum shear stress level (τ_m) and normal stress (σ_{ff}) interpretations of the various characteristic soil response traces. A detailed discussion of the reasoning involved and interpretation of test results is presented in Appendix II of this report.

(2) Conventional "Dynamic" Tests.

Figure 2.3 illustrates typical reaction shear force and normal force response for a "dynamic" test on a dense sand. It is noted that the applied normal force is evaluated at the time coincident with the maximum shear resistance offered by the soil. The initial peak in the reaction shear force response is attributed to inertial effects as described in Appendix II of this report.

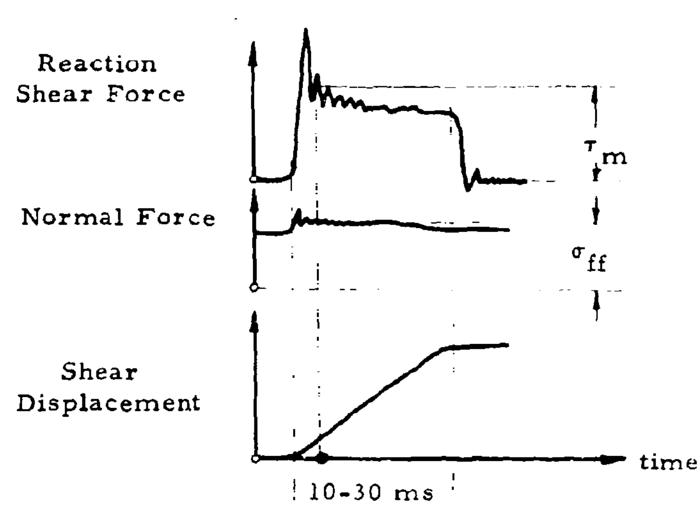

Figure 2.3 Characteristic Responses for "Dynamic" Test on Dense Sand

In the reaction shear force response for a "dynamic" test on a loose sand, Figure 2.4, it is seen that virtually no initial peak exists. The normal force is observed to be maintained at a constant level and is evaluated at the same time that the maximum shear resistance of the soil is offered.

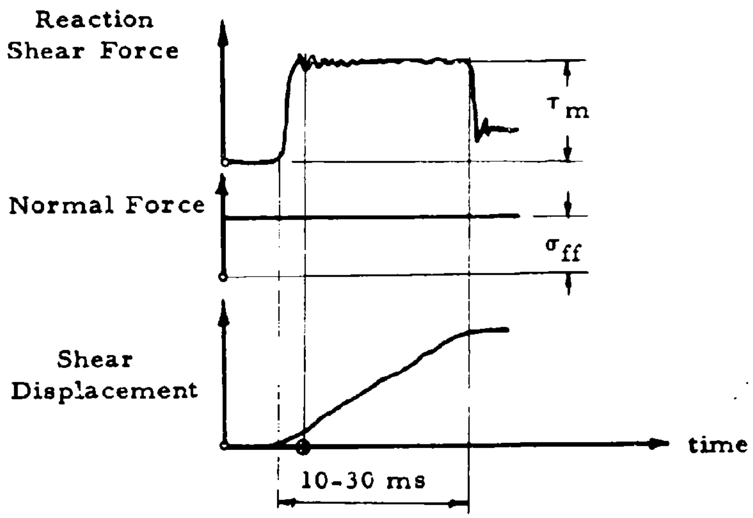

Figure 2.4 Characteristic Responses for "Dynamic" Test on Loose Sand

The response of a clay to "dynamic" loading, Figure 2.5, is similar to the loose sand response with a more gradual rise in shear force. Very little, if any, normal force variation is observed in "dynamic" tests on clay.

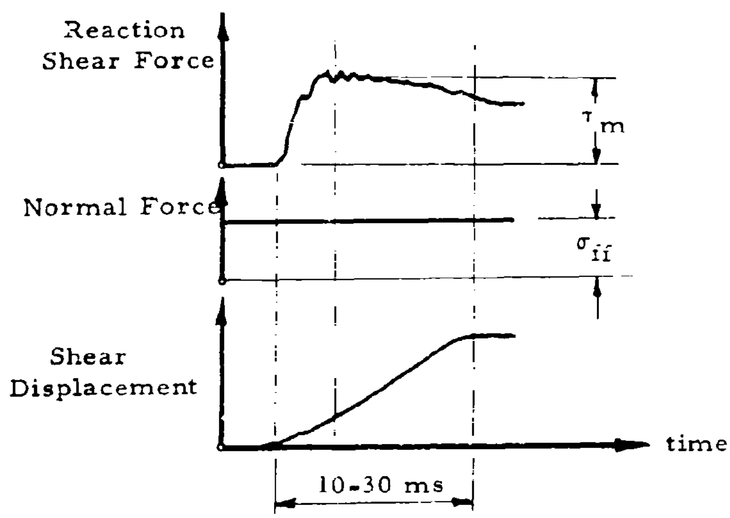

Figure 2.5 Characteristic Responses for "Dynamic" Test on Clay

(3) <u>Conventional "Rapid Static" Tests.</u>

Figure 2.6 shows the increase in applied shear force on a dense sand due to manual control of the pressure regulator. The shear resistance attains a maximum value, suddenly decays and approaches zero at exhaust to the atmosphere. An increase in normal force due to dilatation (Appendix II) is also observed during the "rapid static" shearing process.

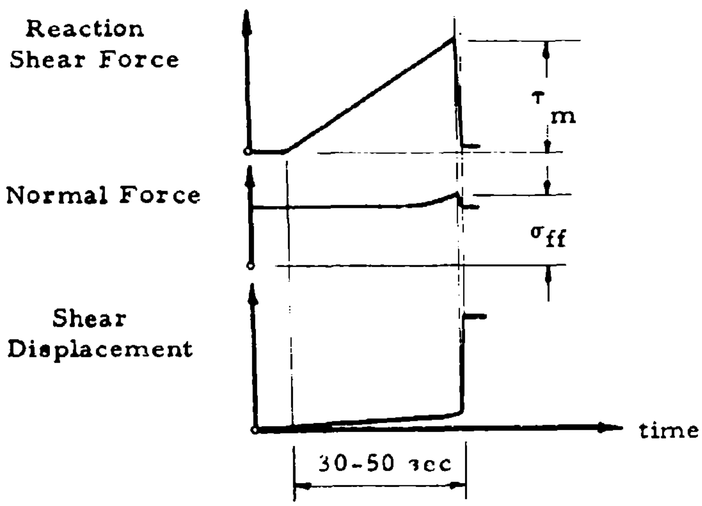

Figure 2.6 Characteristic Responses for "Rapid Static" Test on Dense Sand

A "rapid static" test on loose sand yields a reaction shear force response similar to that in Figure 2.6. Very little normal force variation has been observed in "rapid static" tests on loose sands.

The shear force response of a "rapid static" test on a clay soil is typified by a gradual increase in shear force and peak at failure as indicated in Figure 2.7. The maximum shear resistance offered by the soil, the peak force, apparently occurs as a result of the increased rate of displacement at "failure." Once again, for the clay soil, the normal force remains constant.

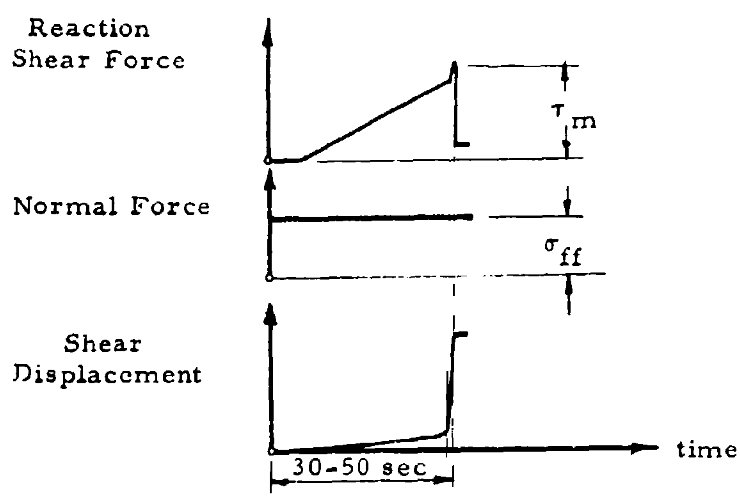

Figure 2.7 Characteristic Responses for "Rapid Static" Test on Clay

(4) Automatic Control Tests.

When performing an "automatic control test" by controlling the rate of shear force application, responses similar to those previously discussed for "rapid static" tests are observed.

"Automatic controlled displacement tests" on clay yield a reaction shear force curve similar to that illustrated in Figure 2.8. The normal force is automatically regulated at a preset level.

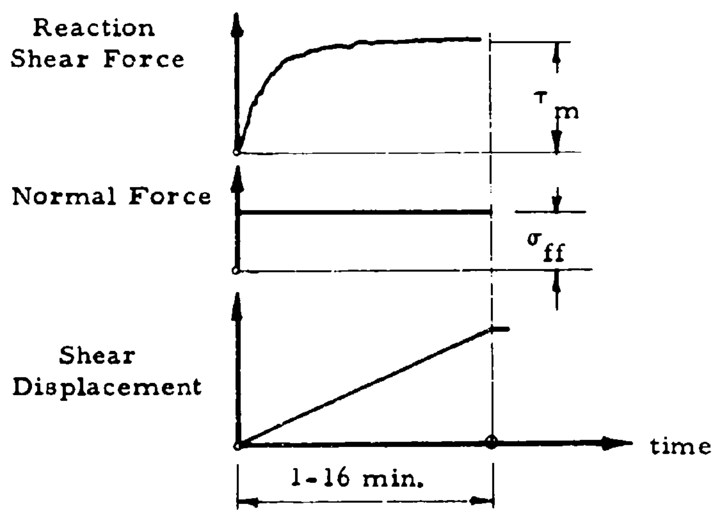

Figure 2.8 Characteristic Responses for "Automatic Controlled Displacement" Test on Clay

SECTION 3. HISTORICAL REVIEW

The following is a chronological review of the status of knowledge concerning the time-dependent shear strength of soils.

In 1776, Coulomb[3.1] suggested that the criteria for failure of a soil could be given by a relationship of the form, $\tau = c + p \tan \phi$, where τ is the shearing stress on the failure plane, p is the normal stress on the failure plane, ϕ is an angle of internal friction and c is the cohesion or intrinsic strength of the soil. The introduction by Teraghi[3.2] of the effective stress principle resulted in the modification of the Coulomb expression to include effective rather than total stress. One of the most comprehensive discussions of the cohesive and frictional components of soil resistance was given by Hvorslev[3.3] in 1960. In terms of total stresses, the Coulomb strength concept (in various forms) is, at the present time, one of the most commonly accepted and widely employed principles in soil mechanics.

Alexandre Collin[3.4], a French engineer, first recognized the time dependent nature of soil strength in 1846. Reference was made to "instantaneous" and "permanent" soil strengths. These implied, respectively, the resistance to temporary forces with a duration less than 30 seconds and permanent forces not significantly altered after a considerable lapse of time. Collin used a double-shear device and observed that the permanent strength of clay may be in the range of 24 to 34 percent of the instantaneous strength. As a result of this work Collin emphasized the importance of accurately evaluating the load duration as well as its magnitude. Collin also said, "Knowledge of the absolute instantaneous resistance is of no use in construction practice." For many years, only the "permanent" strength (long-term stability and creep problems) of soils received the attention of investigators.

Studies to determine the causes of sudden slope failures after long periods of apparent stability were conducted by Casagrande and Albert[3.5] in 1930. According to Jurgenson[3.6] this investigation by Casagrande and Albert definitely established the importance which rate of load application has upon the results of shear tests.

Casagrande[3.7], in the early 1940's, conducted triaxial tests on Atlantic muck at rates of loading which caused failure in periods of time ranging from 95 seconds to 1 hour. In these tests it was established that the more rapidly loaded samples yielded a strength about 40 percent greater than the slowly loaded samples.

In 1944, Taylor[3.8] reported on the results of investigations conducted for the Waterways Experiment Station and observed that undrained triaxial tests of 4-minute duration offered a 15-percent greater deviator stress on Boston blue clay than did 8-day tests.

Taylor[3.9], in 1947, reported the effect of strain rate on sands for rise times from 15 seconds to 5 minutes. These tests revealed no significant differences in the maximum compressive strengths.

The development of the atomic bomb near the end of World War II accelerated the need for the first real soil dynamics investigation. A law enacted by Congress in 1945 provided for a study of the security of the Panama Canal and for increasing its capacity. Concern for the security of the canal due partly to the possible instability of some of the deep-cut slopes if bomb blasts caused shock-type loadings. The basic characteristics of such a "transient impulsive" or "dynamic" load are rapid rise times and short duration. Soil dynamics as used herein is defined as the study of the engineering properties of soils as they are affected by one "dynamic" impulse load as opposed to a vibratory loading condition.

Casagrande and Shannon[3.10] initiated soil dynamics investigations in 1948 with research efforts directed at finding the effects of rate of loading upon soils common to the Panama Canal zone, i.e. clays, muck, shales, and dense dry sand. Consultation with Westergaard and Leet at Harvard University led to the decision of using minimum loading times of 10 milliseconds. Unconfined and triaxial compression tests on clay were performed with rise times varying from 0.01 second to 3000 seconds. The triaxial compression tests on clay were performed with lateral pressures of 3 kg/cm^2 or 6 kg/cm^2 while those on dry sand were confined in a vacuum with lateral pressures of 0.3 kg/cm^2 or 0.9 kg/cm^2. A "strain-rate" effect, defined as the ratio of maximum dynamic strength to the maximum static strength, was observed in all soils tested except the dry sand.

Four clays were tested with rise times varying from 0.02 second to 1000 seconds. The strain-rate effect upon the compressive strength exhibited by this group of clays ranged from 1.5 to 2.0 where the minimum shear strength considered was for the 10-minute test. The weakest and wettest clays exhibited the greatest strain-rate effect, and the strongest and dryest indicated the least strain-rate effect. The strain-rate effect from Atlantic muck unconfined tests was about 2.0 on the basis of the maximum shear strengths for the fastest test and a 10-minute test. On this same basis, Cucaracha shale, confined at 6 kg/cm^2, indicated a strain-rate effect of 1.6. It was observed that the compressive strengths of Manchester sand under transient and static loading conditions exhibited a possible strain-rate effect of 1.1.

Casagrande and Shannon also established the modulus of deformation as the slope of a line through the origin to a point on the stress-strain curve at which the stress is one-half the average static strength. This modulus of deformation for the clays, muck and shale showed a strain-rate effect of approximately 2, whereas this parameter appeared to be independent of the rate of loading for tests on sand.

In 1951, Casagrande and Wilson[3.11] extended the previous work to determine the effect of rate of loading on permanent soil strengths. The unconfined tests exhibited a soil resistance in the slowest tests (30 days) as low as 25 percent of the soil resistance offered in a test with a loading time of 1 minute. It is interesting to note how closely this compares with the 24 to 34 percent Collin had reported in 1846.

Seed and Lundgren[3.12] tested a coarse and fine-grained saturated sand in triaxial compression in 1954. All confining pressures were 2 kg/cm^2 and the rates of testing were such that the maximum loads were reached in 10-15 minutes, 4 seconds or 0.02 second. Both sands were tested in loose and dense states and in drained and undrained conditions. It was established that only undrained shear strengths could be used in determining the strain-rate effect. This conclusion resulted from the observation that no drainage took place during the 0.02-second test due to the inability of pore water to drain so rapidly.

Basically the same results were found in the coarse sand investigations as in the fine sand tests. The pertinent conclusions from these tests on saturated sands are that the strain-rate effect on saturated sands in the undrained condition is 1.15 to 1.20 due to development of a negative pore pressure and to the fact that the strain-rate effect decreases with increasing void ratios. It was also observed that the modulus of deformation strain-rate effect is 1.30 for equal void ratios.

Whitman and Taylor[3.13] and Whitman, et al.[3.14] performed a number of unconfined and triaxial compression tests on a wide variety of soils under contract with the Office of the Chief of Engineers and with the sponsorship of the Armed Forces Special Weapons Project.

Vacuum triaxial tests were conducted on three sands, soils having no strength when dry and unconfined, under confining pressures of 1/3 atmosphere and 1 atmosphere. The sands varied from coarse subrounded sand particles uniformly graded to a well-graded gravel-to-silt grain size distribution with irregular particles. The tested materials also had a complete distribution of interlocking capabilities. Strain rates were varied from 0.03 to 3000 percent strain per second and at no time did the strain-rate effect, considering loading times from 0.005 second to 5 minutes, exceed 1.1. Tests were also performed on these sands with the particle surfaces moistened. These results, once again, indicated no strain-rate effects exceeding 1.1. It therefore seemed reasonable for Whitman to conclude that at least for low confining pressures the compressive strength of sands was independent of strain rate.

A uniform coarse dense sand and a well-graded loose fine sand were tested under saturated undrained conditions at a lateral confining pressure of 60 psi and an initial pore water pressure of 30 psi. The coarse Ottawa sand exhibited a strain-rate effect of 1.1 while in the loose well-graded sand it was about 2.0. Whitman explained the large strain-rate effect of the well-graded fine sand by considering its low permeability and the inability of the pore water to migrate as would be necessary to establish a uniform pore pressure distribution following application of the force. It was also mentioned that a possible contribution to the effect was that the fine particles did give this material some unconfined strength.

A total of 5 different cohesive soils, defined as any soil which can be formed into an unconfined compression test specimen, were tested at M.I.T. and the results summarized along with results of tests previously performed at Harvard (Casagrande and Shannon[3.10]) on 6 cohesive soils. One soil, Boston blue clay, was common to both studies. The clays tested ranged from a remolded plastic clay loam to a stiff dry undisturbed clay. All tests were performed in either an unconfined state of stress or with a lateral pressure of 30, 42 or 85 psi. Only three of the ten soils were tested both unconfined and under one of the above confining pressures. Some variation in moisture content was attempted with apparent difficulties in reproducing soil samples on the dry side of the optimum moisture content.

Whitman observed that all cohesive soils displayed an increase in compressive strength with an increase in the applied strain rate. A variation in strain-rate effect from 1.3 to 2.0 was observed respectively for the strongest clay and the weakest clay once again applying loading times of 0.005 second and 5 minutes to determine these effects.

Examination of all test results led Whitman to the hypothesis that during failure two time effects establish the shear resistance of the soil. One is a continuous plastic deformation due to the highly viscous adsorbed water layer resisting rapid deformation and the other is the time interval required for the formation of discontinuities such as shear planes or cracks. Whitman observed that the soil can be affected by either one or both of these time effects and that the formation of discontinuities was reduced by confinement of the soil sample. It was also noted that the strain-rate effect for confined tests was apparently less than for unconfined tests. For quite plastic soils the stress-strain curves from unconfined tests show the strain-rate effect to be independent of the strain magnitude as is the case for all confined test results. This "true" strain-rate effect corresponds to the viscous component of resistance to continuous deformation. Whitman concluded, from the comparison of confined and unconfined tests, that the strain-rate effect should be evaluated from triaxial tests with confining pressures to prevent splitting or shear plane development before the maximum stress has been attained.

In attempting to unify the test results on cohesive soils Whitman commented that soil mechanicians do not know how the basic soil parameters effect cohesion, let alone strain rate and that the best current approach would be to relate the strain-rate effect to some simple standard classification. Initial attempts were made at relating this effect to the liquidity index (L. I.)* and the net conclusion was that there "appeared" to be a moderate increase in strain-rate effect with increasing plas ·city (higher value within the liquidity index).

In 1962, Whitman and Healy[3.15] reviewed all previous work on sands at MIT and expanded the study to include results of tests on satu- ·ated loose Ottawa sand. This sand exhibited a strain-rate effect of 1.4 between failure times of 5 seconds and 0.025 second. The investigators net conclusion was: "since friction angle was essencially independent of failure time, the undrained compressive strength of sand varied with time-to-failure when the excess pore pressures were time dependent." Compressive strength time dependency was only observed with saturated loose sands.

Whitman, Richardson and Nasim[3.16] reported a strain-rate effect of 1.6 for triaxial compression tests on saturated fat clay with loading times varying from 0.0025 second to 300 se ·ds. It is stated, as previously observed by Whitman,[3.14] that the maximum deviator stress as a function of the log of strain rate has a positive curvature with increasing slope toward high rates of strain.

---

*L. I. $= \dfrac{\text{Moisture Content - Plastic Limit}}{\text{Plasticity Index}}$

Healy[3.17], also in 1962, summarized a series of undrained saturated triaxial tests on a silty sand by saying that a strain-rate effect of from 1.1 to 1.2 could be expected going from the low to high rate of strain due to the "dilative tendency" of this material.

Kane, et al.[3.18] presented results of triaxial compression tests on a partly saturated clay in 1964. The soil had 34 percent by weight clay-size particles and a 70-percent degree of saturation. A strain-rate effect of 1.5 was noted when the time to failure was reduced from 100 seconds to 0.003 second and the lateral confining pressure was varied from 114 psi to 1010 psi.

In 1957, Whitman[3.19] commented: "there is relatively little understanding of the factors affecting the shear strength of cohesive soils" and "It is not surprising that the corresponding strain-rate effects are so poorly understood." In an attempt to clarify this effect a number of investigators including Crawford[3.20], Perloff[3.21], Olson[3.22], Healy[3.23], and Richardson and Whitman[3.24] have examined the pore pressure effect as a function of strain rate. Pore pressure variations with strain rate were observed in all but Olson's work. These studies, however, involved times to failure of one minute or longer (with the exception of the work by Healy, time to failure = 0.6 sec.) due to the fact that existing transducer technology does not allow pore pressure measurements involving a failure time of a few milliseconds.

Whitman[3.13] has related that the considerable range of strain-rate effects is undoubtedly dependent on the moisture content, grain size distribution, particle origin and chemical composition and the degree of consolidation. Other statements by Whitman[3.19] were "efforts must be directed to understanding fundamental principals" and "The greatest use of rapid tests will be as a part of this effort to unearth these fundamentals."

A summary of previous soil dynamics test results is presented in Tables 3.1 and 3.2 at the end of this chapter.

Despite all aforementioned investigations few individuals have attempted to postulate the inclusion of strain-rate effects in a modified failure envelope criterion.

In 1949, Taylor[3.25] reported that data had been obtained indicating that the plastic resistance at any given speed of shear in a given clay at various densities is approximately proportional to the intergranular pressure. On the basis of this relationship and assuming that the plastic resistance depends only on the intergranular pressure and speed of shear, it was conjectured that the shearing strength, s, of a specimen would be represented by the following expression:

$$s = (\bar{\sigma}_{ff} + p_i) \left\{ \tan \phi' + f\left(\frac{\partial \epsilon_s}{\partial t}\right) \right\}$$

in which p_i is the intrinsic pressure and ϵ_s is the shearing strain. The strain rate function which appears in this relationship may be obtained from a series of compressive strength tests at various strain rates.

Hvorslev[3.3], in 1960, presented a thorough discussion of parameters which possibly effect the shear strength of a cohesive soil. As suggested, the measured shear strength (τ_f) could be represented by the following relationship:

$$\tau_f = \tau_d + \tau_\phi + c_e .$$

The surface energy (dilatation) component, τ_d, has an effect of 1 to 2 degrees on the friction angle and decreases with increasing test duration approaching zero for very long tests. It is also zero for all undrained or constant volume tests. The effective friction component, $\tau_\phi = (\tau_f - u) \tan \phi'_e$, will only be affected by various strain rates if, u, the pore water pressure is a time-dependent variable. Hvorslev then proceeds to consider the effective cohesion component, $c_e = c_v + c_u$, as two independent quantities. The rheologic component, c_v, is the transient part of the effective cohesion component and decreases to zero with increasing test duration or reduced rate of deformation. If the test is performed at a rate such that c_v approaches zero the effective cohesion component approaches the ultimate cohesion component, c_u. The ultimate cohesion component is therefore a result of intrinsic pressures. This may or may not be in accord with Whitman[3.13] who states, "as yet no lower limiting strength has been observed and certainly there is no observable tendency for there to be an upper limit to the shearing strength."

Hvorslev closes by saying: "further research into the physico-chemical and rheologic properties of clays may suggest modifications of the definitions and/or introduction of other components."

A recent article by Mitchell[3.26] describing the shearing resistance of a soil as a rate process provides a wealth of fresh ideas regarding strain-rate effects. Of particular interest is the expression developed for shearing resistance which can be stated as follows:

$$
\begin{array}{lll}
(\sigma_1 - \sigma_3) = & & \text{- shearing resistance} \\
 & A'S'\Delta E_0 & \text{- interparticle bond strength term} \\
 & + AS'T \ln \dot{\epsilon}_1 & \text{- strain rate term} \\
 & - ABS'T & \text{- temperature term} \\
 & + \dfrac{(\sigma'_1 + 2\sigma'_3)}{3} \Phi' & \text{- frictional resistance term}
\end{array}
$$

As mentioned by Mitchell this relationship shows that variations in strain rate influence only the envelope intercept and not the frictional component of resistance for conditions of constant effective stress and frictional characteristics of particles.

On the basis of the previous discussion it becomes apparent that a considerable amount of research is required to evaluate the effect of strain rate on the conventional failure envelope parameters, especially in the dynamic range. The interdependence of time to failure, confinement and soil parameters such as moisture content, grain size, degree of saturation and stress history remains to be determined.

Table 3.1

Summary of Previous Dynamic Test Results - Sand

Date	Author	Test Type	Confining Pressures	Rise Times (used to determine Strain-Rate Effect)	Strain-Rate Effect on Comp. Strength	Soil and Condition
1948	Casagrande and Shannon	Vacuum Triaxial Compression	0.3 or 0.9 kg/cm^2	0.03 to 2100 seconds	1.1	dense dry medium grained
1954	Seed and Lundgren	Undrained Triaxial Compression	2 kg/cm^2	0.02 and 600 - 900 seconds	1.15 to 1.20	Saturated dense & loose; fine & coarse grained
1953 and 1954	Taylor, Whitman and others	Vacuum Triax.	1/3 & 1 atm	0.005 to 300 sec	1.1	3 comprehensive soils
		Undrnd. Triax.	$\bar{\sigma}_i$ = 30 psi	0.005 to 300 sec 0.2 to 180 sec	1.1 2.0	Sat. dense coarse Sat. loose fine
1962	Whitman and Healy	Vacuum Triaxial Compression	$\bar{\sigma}_i$ = 10 psi	0.025 to 5 sec	1.4	Same as above & Sat. loose coarse
1962	Healy	Triaxial Compression	5, 10, 20, 40 psi	0.013 to 4 sec	1.1 to 1.2	Fine silty sand

Table 3.2

Summary of Previous Dynamic Test Results - Clay

Date	Author	Test Type	Confining Pressures	Rise Times (used to determine Strain Rate Effect)	Strain-Rate Effect on Compressive Strength
1948	Casagrande and Shannon	Unconfined and Triaxial Compression	3 or 6 kg/cm^2	0.01 to 600 seconds	1.5 to 2.0
1953 and 1954	Taylor, Whitman and others	Unconfined and Triaxial Compression	30, 42 or 85 psi	0.005 to 300 seconds	1.3 to 2.0
1962	Whitman, Richardson and Nasim	Triaxial Compression	Norm. Cons. 60 psi and OCR = 3, 16	time to 1% strain 0.0015 to 300 seconds	1.57 to 1.71
1964	Kane Davisson and others	Triaxial Compression	114 to 1010 psi	0.003 to 100 seconds	1.5

SECTION 3. REFERENCES

3.1 Coulomb, C.A., "Essai sur une Application des Regles de Maximis et Minimus a Quelques Problemes de Statique, Relatifs a l'Architecture," Memoires de l'Academie des Sciences, (Savants Etrangers), Vol. 7, 1776, pp. 343-382.

3.2 Terzaghi, K., "The Shearing Resistance of Saturated Soils and the Angle Between the Planes of Shear, ' Proceedings of the First International Conference on Soil Mechanics and Foundation Engineering, Vol. 1, pp. 54-56.

3.3 Hvorslev, M.J., "Physical Components of the Shear Strength of Saturated Clays," ASCE Research Conference on Shear Strength of Cohesive Soils, June 1960, pp. 169-273.

3.4 Collin, A., Recherches Experimentales sur les Clissements Spontanes des Terrains Argileux, Paris (Translated by Schrinever as Landslides in Clay. University of Toronto Press, 1956), 1848.

3.5 Casagrande, A., and S.G. Albert, Research on the Shearing Resistance of Soils, MIT Unpublished Report, 1930.

3.6 Jurgenson, L., "The Shearing Resistance of Soils," Contributions to Soil Mechanics 1925-1940, Boston Society of Civil Engineers, 1940, pp. 184-226.

3.7 Casagrande, A., New Gatum Locks, Black Muck Design, for the Panama Canal Company, October 10, 1942.

3.8 Taylor, D. W., Reports on Cooperative Research on Stress, Deformation and Strength Characteristics of Soils, Unpublished Report submitted to WES, 1947, reviewed in 3.9 below.

3.9 Taylor, D. W., Soil Mechanics Fact Finding Survey, Progress Report, Triaxial Shear Research and Pressure Distribution Studies on Soil, prepared under auspices of and published by WES, April 1947.

3.10 Casagrande, A., and W. L. Shannon, "Strength of Soils Under Dynamic Loads," Proceedings of ASCE, Vol. 74, No. 4, April 1948, pp. 591-608.

3.11 Casagrande, A., and S. Wilson, "Effect of Rate of Loading on the Strength of Clays and Shales at Constant Water Contents," Geotechnique, Vol. II, 1950 and 1951, pp. 251-264.

3.12 Seed, H. B., and R. Lundgren, "Investigations of the Effect of Transient Loading on the Strength and Deformation Characteristics of Saturated Sands," Proceedings of ASTM, Vol. 54, 1954, pp. 1288-1306.

3.13 Taylor, D. W., and R. V. Whitman, The Behavior of Soils Under Dynamic Loadings, Report 2. Interim Report on Wave Propagation and Strain-Rate Effect, AFSWP-117, for Office of the Chief of Engineers, July 1953.

3.14 Whitman, R. V., J. F. Cheatham, J. A. Jackson, T. D. Landale, M. C. Soteriades, and W. S. Wang, The Behavior of Soils under Dynamic Loadings, Report 3. Final Report on Laboratory Studies, AFSWP-118, for Office of the Chief of Engineers, August 1954.

3.15 Whitman, R. V., and K. A. Healy, The Response of Soils to Dynamic Loadings, Report 9: Shearing Resistance of Sands During Rapid Loadings, for U. S. Army Engineers, Waterways Experiment Station, May 1962.

3.16 Whitman, R. V., A. M. Richardson, Jr., and N. M. Nasim, The Response of Soils to Dynamic Loadings, Report 10: Strength of Saturated Fat Clay, for U. S. Army Engineers, Waterways Experiment Station, June 1962.

3.17 Healy, K. A., The Response of Soils to Dynamic Loadings, Report 11: Triaxial Tests upon Saturated Fine Silty Sand, for U. S. Army Engineers, Waterways Experiment Station, September 1962.

3.18 Kane, H., M. T. Davisson, R. E. Oleson, and G. K. Sinnamon, A Study of the Behavior of a Clay under Rapid and Dynamic Loading in the One-Dimensional and Triaxial Tests, for Air Force Weapons Laboratory, Report No. RTD-TDR-63-3116, June 1964.

3.19 Whitman, R. V., "Testing Soils with Transient Loads," Mexico City Conference on Soils for Engineering Purposes, ASTM Special Technical Publication STP No. 232, December 1957, pp. 242-254.

3.20 Crawford, C. B., "The Influence of Rate of Strains on Effective Stresses in a Sensitive Clay," ASTM Special Technical Publication STP No. 254, 1959, pp. 36-61.

3.21 Perloff, H. P., The Effect of Stress History and Strain Rate on the Undrained Shear Strength of Cohesive Soils, Ph. D. Thesis, Northwestern University, Evanston, Illinois, June 1962.

3.22 Olson, R. E., "Shear Strength Properties of a Sodium Illite," Journal of the Soil Mechanics and Foundations Division, ASCE, Vol. 89, February 1963, pp. 183-208.

3.23 Healy, K. A., The Response of Soils to Dynamic Loadings, Report 15: Undrained Strength of Saturated Clayey Silt, for U.S. Army Engineers, Waterways Experiment Station, March 1963.

3.24 Richardson, A. M., and R. V. Whitman, "Effect of Strain-Rate upon Undrained Shear Resistance of a Saturated Remoulded Fat Clay," Geotechnique, Vol. XIII, No. 4, December 1963, pp. 310-324.

3.25 Taylor, D. W., Fundamentals of Soil Mechanics, Wiley and Sons, New York, N. Y., 1948, pp. 377-378.

3.26 Mitchell, J. K., "Shearing Resistance of Soils as a Rate Process," Journal of the Soil Mechanics and Foundations Division, ASCE, Vol. 90, January 1964, pp. 29-62.

SECTION 4. CONVENTIONAL DIRECT SHEAR TEST RESULTS

a. Background.

The principal effort of this research program, as previously described, has been directed at the comparison of the "dynamic" and "rapid static" shear resistances of a representative group of soils. Specifically, an attempt has been made to formulate this comparison in terms of the well-established failure envelope parameters, cohesion and friction, as a function of soil properties.

Conventional direct shear test results reported herein were obtained by systematically following the "dynamic" and "rapid static" test procedures described in Appendix I of this report.

The spectrum of soils studied ranges from pure ideal clays to an Ottawa sand. In order to further discuss the test results the following definitions (Committee on Glossary of Terms and Definitions[4.1]) are presented:

Cohesionless Soil: A "soil" that when unconfined has little or no strength when air-dried, and that has little or no "cohesion" when submerged.

Cohesive Soil: A "soil" that when unconfined has considerable strength when air-dried, and that has significant "cohesion" when submerged.

These definitions have been interpreted to imply that the soil classification prior to stress application is appropriate.

The cohesive soils discussed in this report will include both "cohesive soils ($\phi \approx 0$)" and "combined soils ($\phi > 0$)."

In excess of 575 tests have been conducted during the study indicating a recurrent behavioral pattern over a wide range of soil properties. This consistency has permitted a rather concise statement of results as shown in the following subsection. Subsection c further discusses the significance of the indicated test results.

b. Characteristic Failure Envelopes.

(1) General.

The commonly accepted total stress failure envelopes are presented in Figure 4. 1. As shown, soils can offer frictional resistance alone (cohesionless soil), pure cohesive resistance (cohesive soil), or a combination of both frictional and cohesive resistance (combined soil). Whether cohesion is in reality a frictional phenomenon will not be discussed here. Essentially all soils can be categorized by one of the aforementioned envelopes. Thus, if the effect of time to failure can be related to the "apparent cohesion (C_a)" and "friction angle (ϕ)" there exists the potential to postulate a unified description of the effect of test duration on maximum shear resistance for all soils.

(2) Cohesionless Soil.

As previously indicated, a cohesionless soil has little or no strength when air-dried and unconfined. The "rapid static"

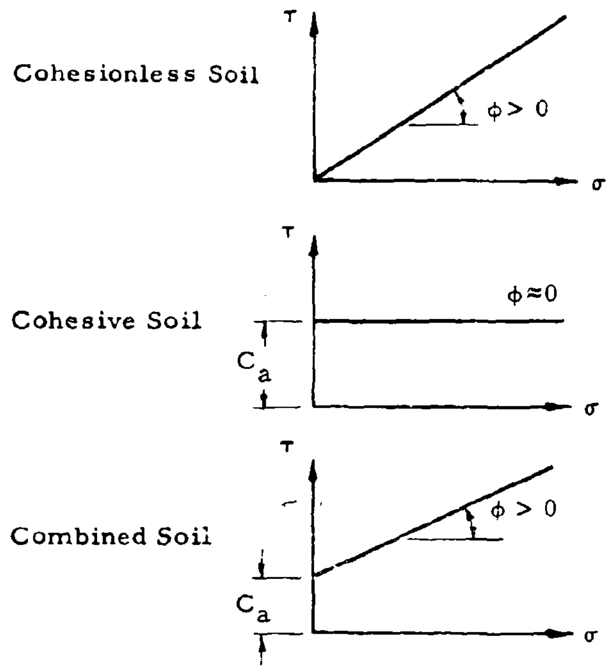

Figure 4.1 Total Stress Failure Envelopes

failure envelope for such a material is characteristically a straight line passing through or near the origin, Figure 4.2. The concise, conclusive statement, "dynamic effects are minimal," is applicable to all cohesionless soils studied during this investigation. This conclusion for sands is in good agreement with other investigators, Table 3.1.

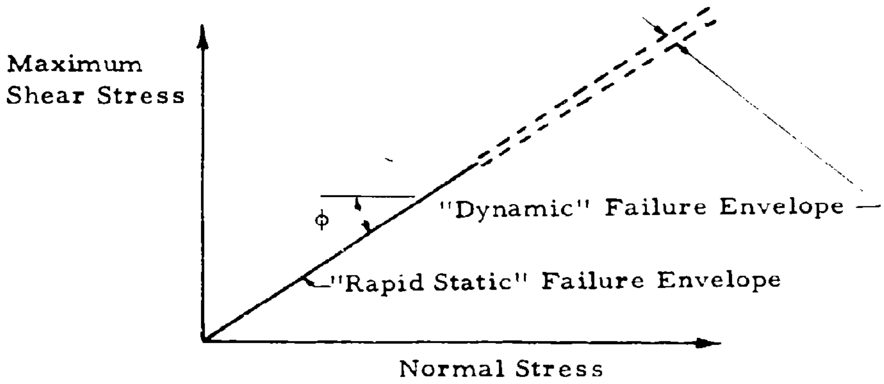

Figure 4.2 Characteristic Failure Envelope: Cohesionless Soil

A summary of the cohesionless soils tested is presented in Table 4.1. The actual test results and soil conditions are graphically illustrated and tabulated in Appendix III of this report. Tests on fine loose saturated sands, which Whitman[3.14] observed to have a considerable strain-rate effect, have not been included in this investigation.

Table 4.1

Representative Tests and References: Cohesionless Soils

Soils		Number of Conclusive Test Results		Appendix III Reference Figures
		Dynamic	Rapid Static	
ASTM C-190 Standard Ottawa Sand	Dense Dry	13	8	1,2
	Dense Sat.[a]	5	-	3
	Loose Dry	4	4	4,5
NTS Desert Alluvium (remolded powdered silt)		3	5	22
Air-dried Powdered Jordan Buff Clay		5	5	7

[a]Drainage unrestricted--see page 54 for discussion.

(c) Cohesive Soil.

Cohesive soil, as discussed in this section is characterized exclusively by apparent cohesion as indicated by the "rapid static" failure envelope in Figure 4.3. The outstanding "dynamic" response trend for these soils was merely a parallel shift of the failure envelope to a level at which the intercept exhibited an apparent cohesion approximately twice as large as that for the "rapid static" test conditions.

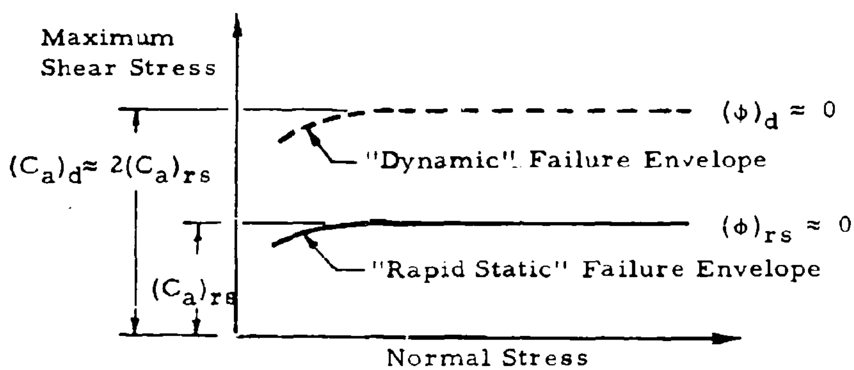

$(\phi)_{rs}$ = "rapid static" friction angle
$(\phi)_d$ = "dynamic" friction angle
$(C_a)_{rs}$ = "rapid static" apparent cohesion
$(C_a)_d$ = "dynamic" apparent cohesion

Figure 4.3 Characteristic Failure Envelopes: Cohesive Soil

The cohesive soils tested are summarized in Table 4. 2. The referenced figures of Appendix III present the actual test results and soil conditions.

(4) Combined Soils.

The "rapid static" failure envelope for a combined soil, Figure 4. 4, exhibits both a friction angle and an apparent cohesion, respectively the individual characteristics of a cohesionless soil and a cohesive soil. Once again the "dynamic" failure envelope indicated the significantly consistent response of a doubling of the apparent cohesive intercept while the friction angle remained unchanged.

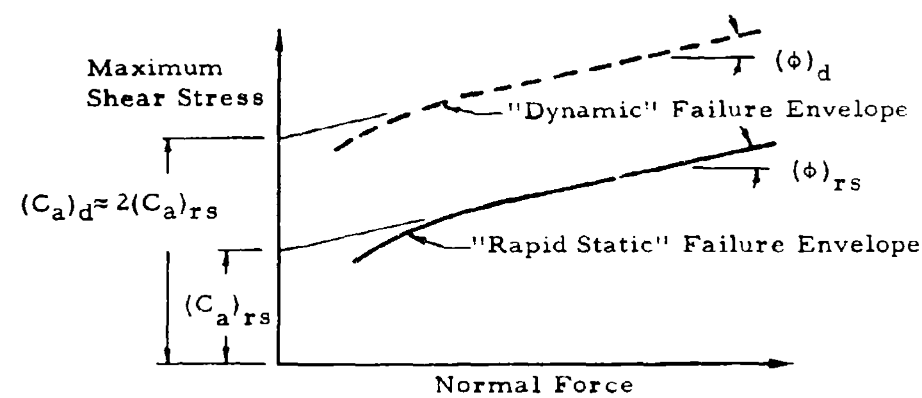

Figure 4. 4 Characteristic Failure Envelopes: Combined Soil

Table 4.2

Representative Tests and References: Cohesive Soils

Soils	w (%)	Number of Conclusive Test Results			Appendix III Reference Figures
		Dynamic	Rapid Static	Automatic Controlled Shear Displacement	
Jordan Buff Clay (compacted)	20.7	4	5	-	9
	24.5	8	4	9	10
	30.2	17	10	-	11
	33.7	3	3	-	12
Western Bentonite Clay (compacted)	53.3	5	5	-	19
	95.1	6	6	-	20
Chicago Blue Clay (undisturbed)	29.9	5	6	-	24

Failure response of this type was observed for those soils listed in Table 4.3. Once again, the specific test results are reported in the indicated appendix.

(5) Summary of Envelope Response.

The regularity of the previously described failure envelope trends allows a very concise, comprehensive, presentation of the results in terms of the friction angles and the following ratio.

$$\text{"apparent cohesion" ratio} = \frac{(C_a)\ \text{dynamic}}{(C_a)\ \text{rapid static}}$$

This information is indicative of the dynamic effect on the apparent cohesion and the friction angle. Frequent reference is made to the apparent cohesion ratio as either a "dynamic-static strength" ratio or merely a "strength" ratio.

Tables 4.4a, b, and c present a summary of this investigation for the previously described, cohesionless, cohesive, and combined soils together with an abbreviated summary of the average soil properties.

c. Discussion of Results.

(1) General.

The following discussion presents the results of this investigation in an orderly manner for the purpose of discussing the correlations that have been observed.

Table 4.3

Representative Tests and References: Combined Soils

Soils	Number of Conclusive Test Results		Appendix III Reference Figures
	Dynamic	Rapid Static	
Jordan Buff Clay + Ottawa Sand	5	6	18
Rochester Sandy Silt (undisturbed)	4	5	26
Notre Dame Lake Marl (undisturbed)	8	4	28

Table 4.4a

Summary of Results: Cohesionless Soils

Soil		w (%)	γ_d (pcf)	S (%)	$(c_a)_{rs}$ (psi)	$(\phi)_{rs}$ (deg)	$(c_a)_d$ (psi)	$(\phi)_d$ (deg)	$\frac{(c_a)_d}{(c_a)_{rs}}$
ASTM C-190 Standard Ottawa Sand	Dense Dry	0	107.4	0	0	46	0	43	-
	Dense Sat.[a]	20.2	107.4	100	-	-	0	46	-
	Loose Dry	0	98.1	0	0	35	0	35	-
NTS Desert Alluvium (remolded powdered silt)		6.2	79	15	5	28	5	28	1.0
Air-dried Powdered Jordan Buff Clay		0	74.8	0	2.4	30	2.4	30	1.0

[a]Drainage unrestricted--see page 54 for discussion.

Table 4.4b

Summary of Results: Cohesive Soils

Soil	w (%)	γ_d (pcf)	S (%)	$(C_a)_{rs}$ (psi)	$(\phi)_{rs}$ (deg)	$(C_a)_d$ (psi)	$(\phi)_d$ (deg)	$\frac{(C_a)_d}{(C_a)_{rs}}$
	20.7	104.8	89.8	-	-	-	-	1.8-2.0[a]
Jordan Buff Clay	24.5	98.2	90.7	8.9	4	22.5	4	2.5[b]
(compacted)	30.2	88.0	88.0	6.7	0	13.9	0	2.1
	33.7	83.0	87	2.8	0	5.6	0	2.0
Western Bentonite Clay	53.3	66.0	90.7	8.7	0	16.0	0	1.35
(compacted)	95.1	45.8	93.6	2.9	0	5.4	0	1.85
Chicago Blue Clay (undisturbed)	29.9	93.1	94.2	5.2	0	8.8	0	1.7

[a] Approximate ratios of shear strengths--see page 57 for discussion.

[b] Established on the basis of various static tests--see page 56 for discussion.

Table 4.4c

Summary of Results: Combined Soils

Soil	w (%)	γ_d (pcf)	S (%)	$(C_a)_{rs}$ (psi)	$(\phi)_{rs}$ (deg)	$(C_a)_d$ (psi)	$(\phi)_d$ (deg)	$\frac{(C_a)_d}{(C_a)_{rs}}$
Jordan Buff Clay + Ottawa Sand	16.1	107.9	76	7.0	15	14.1	15	2.0
Rochester Sandy Silt (undisturbed)	13.4	106	61	6.8	38.5	14.6	35.5	2.15
Notre Dame Lake Marl (undisturbed)	89.4	40	74	4.9	20.5	6.9	20.5	1.4

Commercially available soils or "ideal soils" were utilized throughout the duration of this investigation. Natural soils were tested periodically, as obtained, providing verification of "ideal soil" response.

(2) Cohesionless Soils.

The ideal cohesionless soil used for all tests was the ASTM C-190 Standard 20-30 Ottawa sand. Tests were performed on this sand in both loose and dense states.

The "dynamic" and "rapid static" loose dry sand test results offered no interpretation problems and showed excellent agreement with each other (Appendix III - Figures 4 and 5) exhibiting a unique failure envelope passing through the origin.

The dense dry sand "dynamic" and "rapid static" failure envelopes (Appendix III - Figures 1 and 2) were also characteristic of cohesionless soils. The "dynamic" failure envelope, however indicated a slightly lower friction angle than that of the "rapid static" response. This could well be the result of interpretation difficulties for "dynamic" dense sand tests. As indicated by the shear force versus shear displacement response the maximum shear resistance in "rapid static" tests was offered at shear displacements of approximately 0.06 in. The interpretation procedure used for "dynamic" dense sand test results yielded a maximum shear resistance value at shear displacements of approximately 0.08 in. If in fact, the shear displacement at maximum dynamic resistance is comparable to that for a "rapid static" test, 0.06 in., the true "dynamic" maximum shear resistance is masked by the previously mentioned initial inertial peak.

The "rapid static" failure envelopes, Table 4.5, agree favorably with those reported by Burmister[4.2] for this sand at the indicated relative densities.

Table 4.5

Comparison with Burmister Ottawa Sand Results

Sand	Relative Density	Burmister	ND
Dense Sand	87%	43°	46°
Loose Sand	37%	37°	35°

"Dynamic" saturated dense sand test results (Appendix III - Figure 3) indicate good agreement with the "rapid static" dry dense sand failure envelope. These maximum shear resistances are slightly greater than those indicated for the "dynamic" dry dense sand tests in which similar interpretation procedures were used. This slight increase in shear resistance is probably due to incomplete drainage, although unrestricted, and the effect of dilatation in developing some negative pore pressure.

On the basis of this discussion the net conclusion regarding a "cohesionless" coarse clean sand is that no "test-duration effect" is observed with the exception of a small effect for a saturated condition.

(3) Cohesive Soils.

Two cohesive soils were used throughout this investigation to determine the dynamic-static strength ratio.

Jordan Buff clay, basically a kaolinite, was used as the principal cohesive material. "Dynamic" and "rapid static" failure envelopes were formed with this soil using various moisture contents, preparation processes and pore fluids. It was obtained in dry powdered form from the United Clay Mines Corporation, Trenton, New Jersey. The Atterberg limits are as indicated below. Other specific soil properties are recorded in Appendix III of this report.

Liquid Limit	≈	54%
Plastic Limit	≈	26%
Plasticity Index	≈	28%
Shrinkage Limit	≈	22%

Western Bentonite clay, a montmorillonite, was used to amplify and determine the grain size effect on failure envelope criterion. It is available in dry powdered form from Baroid Chemicals, Incorporated, Houston, Texas. The Atterberg limits

Liquid Limit	≈	543%
Plastic Limit	≈	51%
Plasticity Index	≈	492%

are in good agreement with those obtained by Seed, et al.[4.3] These values, much greater than those for Jordan Buff clay, are indicative of the predominant presence of montmorillonite clay minerals. Other specific information regarding this soil is reported in Appendix III.

To facilitate sample preparation and production a modified standard proctor procedure was adopted and used extensively. Detailed sample preparation and placement techniques are described with the tabulated summaries of all test results in Appendix III.

(a) Moisture Content.

"Dynamic" and "rapid static" failure envelopes were developed for the Jordan Buff clay at moisture contents of approximately 0, 10, 20, 25, 30 and 34 percent, respectively Figures 7, 8, 9, 10, 11 and 12 in Appendix III. The apparent cohesion ratio was evaluated for this entire range of soil consistencies.

As inferred from Table 4.4 the highly saturated ($S \approx 90\%$) clays ($w \approx 20, 30, 34\%$) exhibit a strength ratio very nearly equal to 2 with the exception of the series at a moisture content of 25%. This variation is partially a result of utilizing "automatically controlled shear displacement" tests as well as "rapid static" tests to form the indicated static failure envelope, Appendix III - Figure 10. The "automatically controlled shear displacement" tests with a duration of approximately 8 minutes appeared to yield slightly lower shear strengths than under "rapid static" conditions. This slight reduction in strength tends to lower the static envelope and hence increase the apparent cohesion ratio. However, even if the "rapid static" tests were the sole criterion for forming the static envelope, the apparent cohesion ratio, for this particular soil, would still be in excess of 2.

Scott[4.4] discusses nonsaturated soils and indicates that the total stress failure envelopes will not be a straight line but will have a varying slope becoming horizontal at high pressures, which according to Means and Parcher[4.5] implies that the remaining air is then dissolved in the pore fluid. This type of response is characteristic of that obtained from the Jordan Buff clay. It is particularly evident at a moisture content of 20% (Appendix III - Figure 9) at which the horizontal level is not approached due to the fact that the normal force is never sufficiently high to dissolve the existing air. Instead of attempting to establish apparent cohesion intercepts for the 20% moisture content the dynamic-static strength ratio was determined to range from 1.8 to 2.0 for various values of normal stress.

It is interesting to note that as the moisture content is decreased a friction angle is introduced subsequently attaining a value of 30° when the dry powder is investigated. This increase in friction angle with reduction in moisture content is likely the result of the limited amount of pore water permitting more direct interparticle action and effective stress variation as a function of confining pressure. At moisture contents above the plastic limit the friction angle is virtually nonexistent.

Figure 4.5 graphically illustrates the interdependence between apparent cohesion and degree of saturation. Apparently on the wet side of the optimum moisture content, relatively high degrees of structural dispersion, the apparent cohesion ratio is very consistent at 2 dropping off to 1 at zero moisture content. The decrease in strength ratio appears to start at moisture contents less than the optimum, below which there is a greater tendency toward flocculation in compacted samples, Leonards[4.6]. The indicated range of dry densities (83 pcf to 105 pcf) at similar degrees of saturation ($S \approx 87\%$ to 91%) varies substantially the number of interparticle contacts per unit area. It is readily observed that on the wet side of the optimum moisture content the apparent cohesion ratio is independent of the aforementioned number of interparticle contacts. This is in accordance with the hypothesis advanced by Mitchell[3.26] from which the particle contact term would be cancelled if placed in ratio form for two different rates of strain.

Although both Taylor and Whitman[3.13] and Schimming and Saxe[4.7]

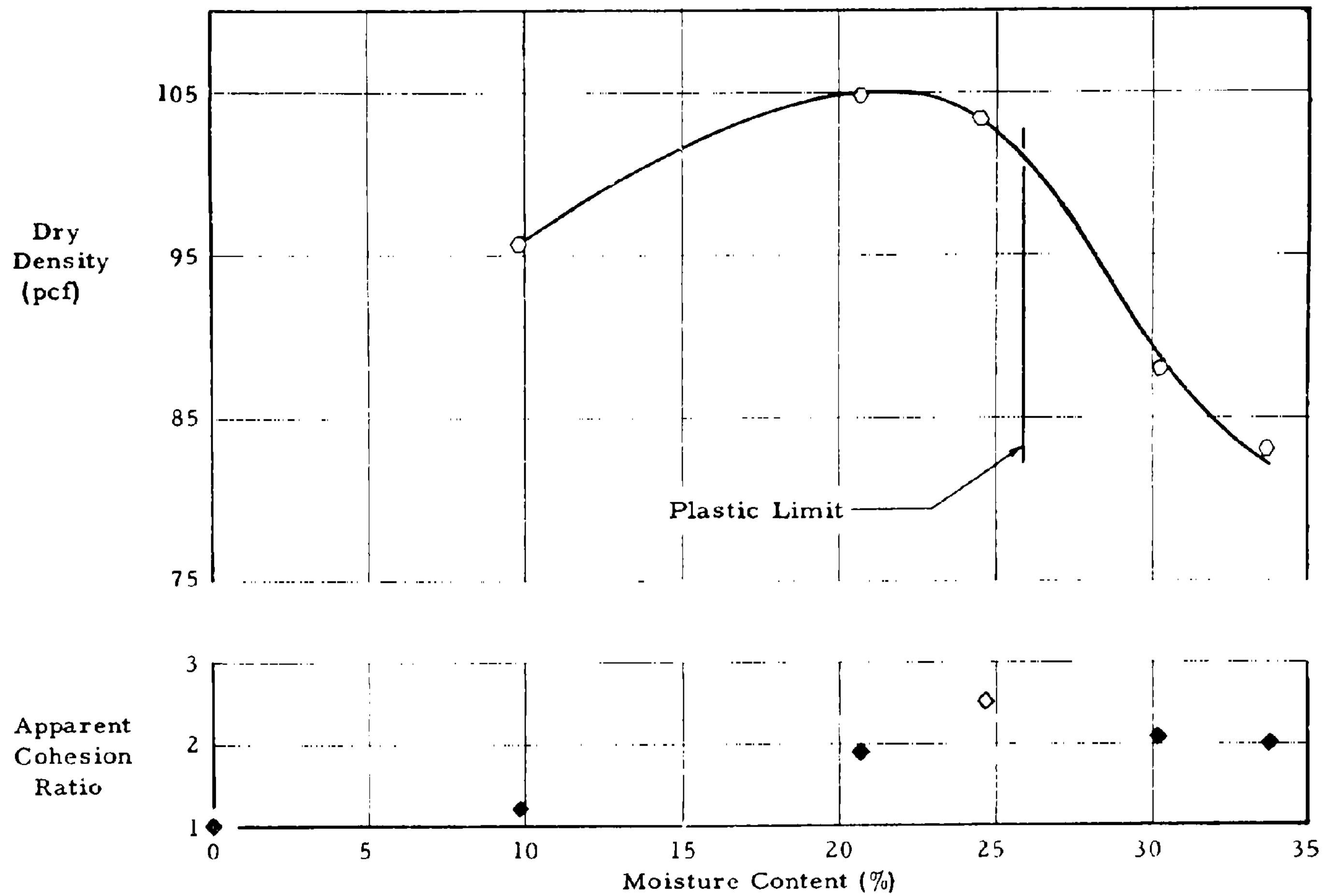

Figure 4.5 Dry Density, Apparent Cohesion Ratio Relation - Jordan Buff Clay

reported an "apparent" correlation between the strength ratio and the position of the soil in the plastic range as indicated by the liquidity index, it must be kept in mind that both investigators based their tentative conclusions on a limited number of confined tests, not the apparent cohesion intercepts as developed from the great number of tests reported herein. For the Jordan Buff clay within a liquidity index range from -0.21 to + 0.29 no marked strength ratio variation was observed.

(b) Structural Effects.

Fresh water deposits can provide dispersed structures although flocculated clays are more predominant in nature. Due to structural differences the flocculated clays would not necessarily yield the same response trends that the aforementioned dispersed structures have under "dynamic" shear force application.

As previously indicated the dispersed soil structure yields a strength ratio in terms of apparent cohesion of 2. For compacted soils having a tendency toward flocculation, those below the optimum moisture content and partially saturated, the strength ratio varied from 1 to 2. To observe the strength ratio for saturated soils with flocculated structures a number of tests were performed on samples consolidated under various conditions. The test results are presented in Figure 4.6, with an exaggerated vertical scale, as well as in Figure 13 of Appendix III which also contains a tabulated summary of soil conditions. The indicated

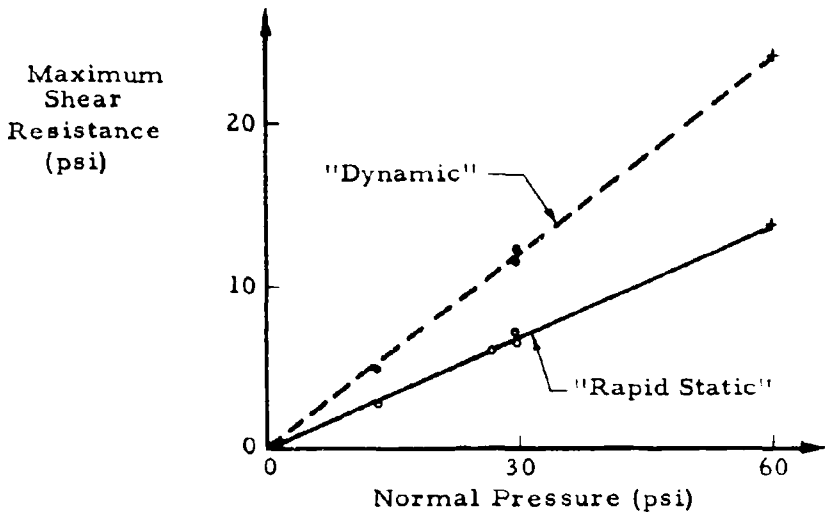

a. Normally Consolidated Envelopes

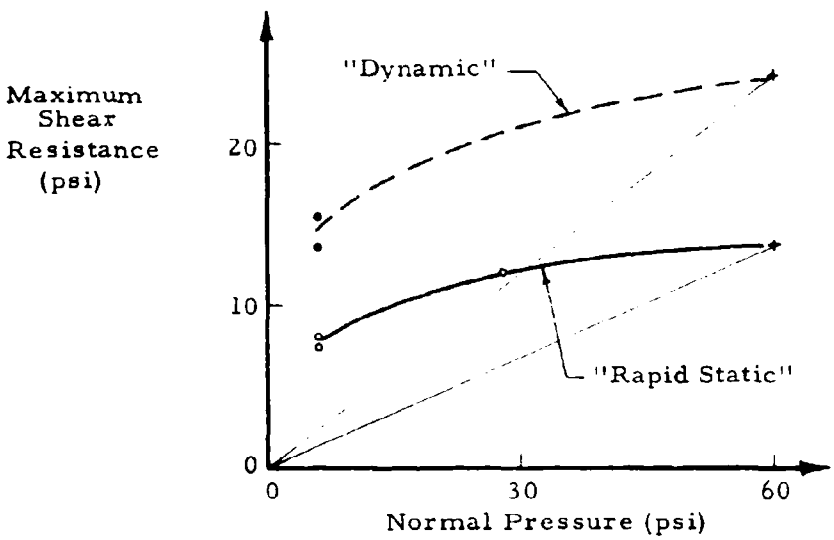

b. Overconsolidated Envelopes

Figure 4.6 Shear Tests on Consolidated Samples - Jordan Buff Clay "rapid static" stress envelopes take the form of those suggested by Hvorslev[3.3].

It is interesting to note that the flocculated structure appears to exhibit a greater "rapid static" resistance (7.2 psi) than that of a more dispersed structure (6.7 psi, Appendix III - Figure 11), although the latter has a slightly greater dry density (88 pcf as compared to 86.5 pcf).

Under the given normal consolidation pressures of 13.1 psi and 29.9 psi, Figure 4.6a, the strength ratio was 1.75. Had normally consolidated direct shear tests been performed at pressures of 60 psi the indicated (+) values of shear resistance would have been expected. With reference to Figure 4.6b it can be seen that samples normally consolidated to 60 psi and rebounded to 6 psi indicated a dynamic-static strength ratio of 1.9, which is slightly higher than that for the normally consolidated samples. This value tends to approach the time-to-failure effect for dispersed soils indicating that perhaps an overconsolidated sample is more dispersed than a normally consolidated sample.

The general conclusion from these observations on a variety of consolidated samples can once again be stated very concisely in that the preparation process and type of structures cause only a slight deviation from the strength ratio observed for the previously discussed compacted soils.

(c) Grain Size Effect.

Western Bentonite clay, a montmorillinite, was used to observe whether or not grain size variation in the cohesive range affected the apparent cohesion ratio.

"Dynamic" and "rapid static" failure envelopes were developed at two moisture contents ($w \approx 53\%$ and 95%) within the plasticity index. All failure envelopes (Appendix III - Figures 19 and 20) were readily interpreted to be purely cohesive in nature indicating an apparent cohesion ratio of 1.85 for both the low and high moisture contents. As for the Jordan Buff clay no variation in the strength ratio is observed for a considerable change in moisture content at these high degrees of saturation ($S \approx 91\%$ and 94%). The apparent cohesion ratio is also, once again, constant for a considerable variation in dry density (66 pcf to 46 pcf). This merely confirms the observation for Jordan Buff clay that the strength ratio is independent of the number of interparticle contacts.

Since the Western Bentonite and Jordan Buff exhibited similar responses it appears that the strength ratio is relatively insensitive to grain size in the cohesive range.

Figure 4.7 presents an all encompassing view of the consistency established in apparent cohesion ratios for the soil-water combinations tested within the indicated moisture content range.

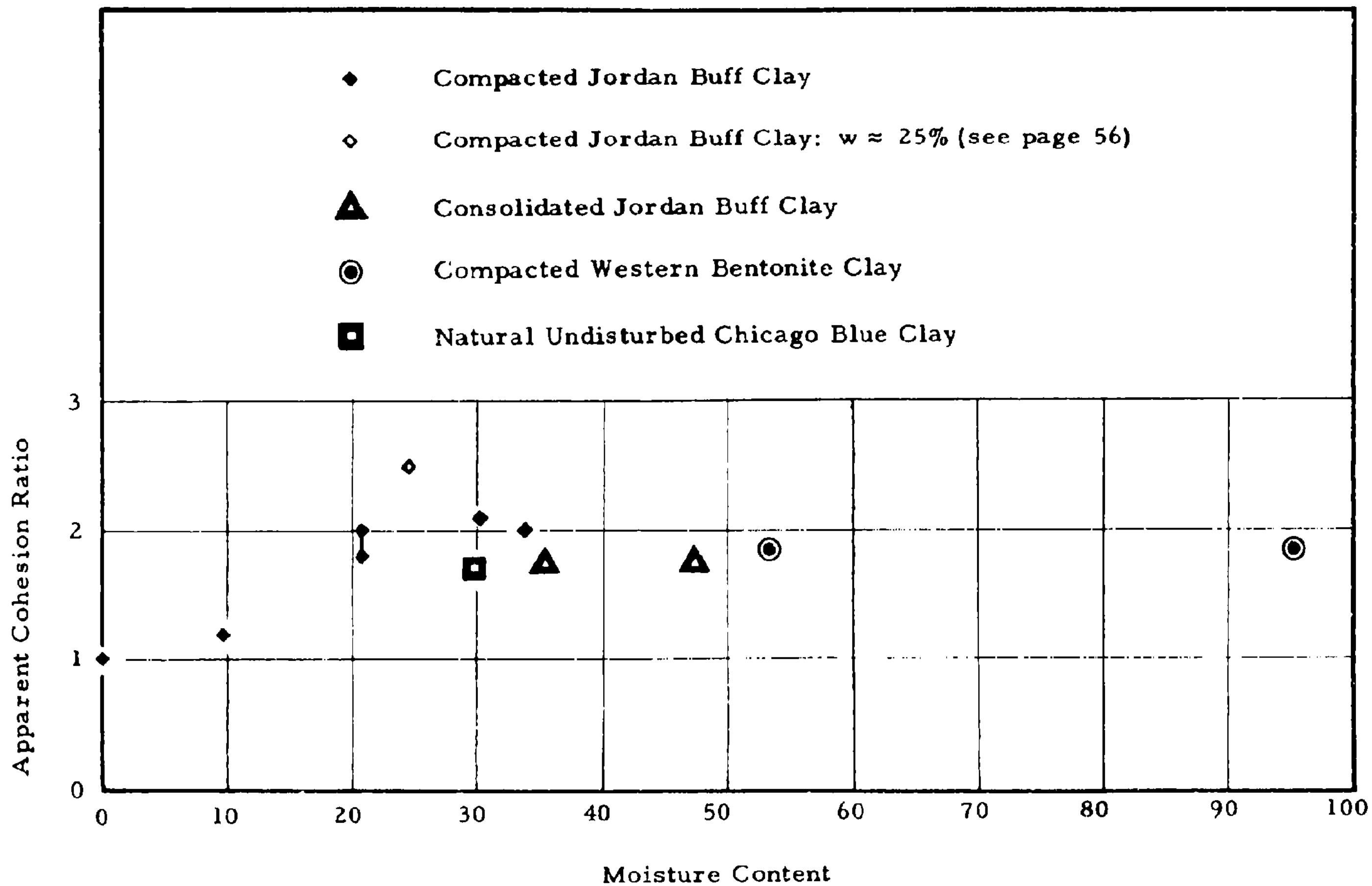

Figure 4.7 Apparent Cohesion Ratio Response for Various Soil-Water Combinations

(d) Pore Fluid Variation.

With respect to the previous discussions for cohesive soils the time-to-failure effect has been studied as a function of moisture content, dry density (number of interparticle contacts), degree of saturation, history in the form of preparation process (basic particle to particle structure) and effective grain size. A very consistent set of response characteristics has been observed. Deviation from the strength ratio of approximately 2, was only particularly noted at extremely low degrees of saturation ($S \approx 0\%$ and 34%), where there would be a marked deficiency of pore water. This seemed to implicate the pore water as being an influencing factor in creating the unique response trends. In an effort to gain some insight into the pore water effect it was decided to test Jordan Buff and Western Bentonite clays mixed with various fluids having electrical and viscous properties unlike those of water. Table 4.6 is a summary of the average soil properties and test results from the "dynamic" and "rapid static" failure envelopes of the indicated soil mixtures.

Prior to discussion of the significance of these results in terms of fluid properties it is necessary to be aware of the nature of diffuse double layers and the electrical nature of colloidal particles. Scott[4.4] presents a discussion of clay-water relationships and the tendency to formation of the diffuse double layer. It is mentioned that the valence,

Table 4.6

Summary of Results: Pore Fluid Variation

Soil	w (%)	γ_d (pcf)	S (%)	$(C_a)_{rs}$ (psi)	$(\phi)_{rs}$ (deg)	$(C_a)_d$ (psi)	$(\phi)_d$ (deg)	$\frac{(C_a)_d}{(C_a)_{rs}}$
Jordan Buff Clay + Salt Water	30.0	89.6	89.9	4.5	2	9.9	2	2.2
Jordan Buff Clay	40	84.1	84.6	18.2	0	72.4	0	4.0
+ Glycerin	60	69.1	89.1	4.4	0	15.8	0	3.6
Jordan Buff Clay + Kerosene	30.5	77.5	87	5.1	15	9.2	15	1.8
Western Bentonite Clay + Benzene	40	77.3	99.5	3.7	20	7.3	20	2.0

concentration and size of the counterions in the dissolved electrolyte as well as the surface charge of the particle, the dielectric constant of the fluid and the temperature affect the degree of diffusion of ions from the surfaces of the charged particles. At some distance from the particle surface the ions have a minimal tendency for diffusion. The double layer "thickness" can be defined as a distance at which the potential for diffusion has fallen to a given level.

Salt water was used as a pore fluid to determine the effect an electrolytic solution would have on the strength ratio. The apparent cohesion intercepts (Appendix III - Figure 14) indicated a slightly larger dynamic-static strength ratio for the salt water mix than for the fresh water mix, respectively 2.2 and 2.1. It must be kept in mind that these ratios are quite sensitive to interpretation of the "apparent cohesion" values.

Van Olphen[4.8] indicates that a suspension of kaolinite clay in salt water would offer a lower shear resistance than a similar fresh water kaolinite mixture. A weaker structure was actually observed, as the salt water mix ($\gamma_d \approx 90$ pcf, $w \approx 30\%$) indicated a "rapid static" apparent cohesion of 4.5 psi while a fresh water mix of Jordan Buff clay ($\gamma_d \approx 88$ pcf, $w \approx 30\%$) yielded an apparent cohesion of 6.7 psi. As described, this response is apparently due to a compression of the particle edge and face double layers permitting the dominance of face to face attractive forces and essentially reducing the number of interparticle edge to face contacts which contribute significantly to a soils yield stress.

Glycerin was used to magnify the pore fluid viscosity as related to the strength ratio. On the basis of the overall electrical similarities between glycerin and water, respective dielectric constants of 42.5 and 78.5, similar diffuse double layers should be anticipated. Two moisture contents (40% and 60%) were investigated indicating characteristic "purely cohesive" failure envelopes, Appendix III - Figures 15 and 16. The dry density and degree of saturation for the glycerin-soil mix ($\gamma_d \approx$ 84 pcf, S $\approx$ 85%) compared favorably with another Jordan Buff clay-water mix ($\gamma_d \approx$ 83 pcf, S $\approx$ 87%). A six-fold increase in "rapid static" shear resistance was observed for the glycerin samples. This may be partially attributed to the difference in pore fluid viscosities (glycerin viscosity = 939 centipoises, water viscosity = 1 centipoise at 20°C). The desired strength ratios were evaluated as 4.0 and 3.6 respectively for the 40% and 60% moisture contents. These values imply an incremental increase in "dynamic" shear resistance of 3.0 and 2.6 times the "rapid static" shear resistance. The corresponding increase for a water-soil mix would be approximately 1. This incremental increase in strength is certainly not proportional to the increase in viscosity thus indicating that "dynamic" strength increases cannot be explained exclusively by the pore fluid viscosity.

Kerosene, a nonpolar long chain hydrocarbon was used in an attempt to see if the strong dielectric nature of water affected the apparent cohesion ratio. In comparison to a water-soil mix, a nonpolar fluid (dielectric constant $\approx$ 0) would have a significantly decreased tendency to form a diffuse double layer adjacent to the charged soil particle. The "dynamic" and "rapid static" failure envelopes were, surprisingly, similar to those for combined soils in that a constant friction angle and cohesion were indicated, Appendix III - Figure 17. A strength ratio of 1.8 was established on the basis of considerable apparent "dynamic" and "rapid static" cohesions. These intercepts were unexpected as the soil-kerosene mix had no adhesion for physical objects.

"Dynamic" and "rapid static" failure envelopes were also formed for the Western Bentonite clay and benzene, another nonpolar pore fluid. As for kerosene the weak dielectric nature of benzene should inhibit the formation of any diffused double layers. Similar to the kerosene-soil mix, failure envelopes characteristic of combined soils were obtained (Appendix III - Figure 21) and an apparent cohesion ratio of 2.0 was observed.

For the viscous and electrically similar pore fluids, kerosene and benzene, the strength ratio is again indicated to be independent of grain size.

When attempting to correlate the "rapid static" apparent cohesions of the bentonite-benzene mix and ordinary bentonite-water mixes, comparable dry densities were never obtained. However, the bentonite-benzene mix ($\gamma_d \approx 77$ pcf) had a lower "rapid static" apparent cohesion (3.7 psi) than did a bentonite-water mix (8.7 psi) at a lower dry density ($\gamma_d \approx 67$ pcf) indicating that if comparable densities were obtained a greater difference would have been observed. This reduction in apparent cohesion for the special mix is probably due to a greater number of inter-particle contacts having been established in the fresh water-bentonite mix than in the benzene-bentonite mix.

For the particular cohesive soils investigated this last study has indicated that the high dielectric constant of water has a significant effect on the formation of the horizontal ($\phi = 0$) total stress envelopes.

(4) Combined Soils.

To extend this investigation to the inclusion of combined ideal soils Jordan Buff clay was mixed with the Standard 20-30 Ottawa sand and water in the following proportions by weight.

Jordan Buff Clay	:	4.8/10
Standard Ottawa Sand	:	3.6/10
Water	:	1.6/10

This provides a moisture content of 16% for the entire mix and approximately 30% for the clay part of the structure.

"Dynamic" and "rapid static" failure envelopes were formed (Appendix III - Figure 18) indicating a parallel shift of the envelopes and an apparent cohesion ratio of 2.0. As previously mentioned, Mitchell[3.26] concurs with this type of response.

(5) Natural Soils.

A variety of natural soils were obtained and tested in an attempt to determine whether or not the response trends for the ideal soils would be applicable to natural soils.

Nevada Test Site desert alluvium, a silt, was obtained in an undisturbed form but was extremely dry and brittle and had to be remolded in the shear box. No differentiation was observable between "dynamic" and "rapid static" response (Appendix III - Figure 22) indicating that this soil applied to the cohesionless category despite the relatively dry "apparent cohesion (5 psi)." A considerable friction angle (28°) was present.

A natural purely cohesive soil utilized in this test program was an undisturbed Chicago Blue clay from which parallel horizontal "dynamic" and "rapid static" failure envelopes were obtained, Appendix III - Figure 24. A strength ratio of 1.7 was observed which was slightly less than but otherwise in good agreement with the ideal consolidated (flocculated) Jordan Buff clay test results.

The combined soil effect was observed on two undisturbed natural soils. The first, a sandy silt (Appendix III - Figure 26), exhibited a strength ratio of 2.15 with a lower angle of friction (35.5°) for the "dynamic" failure envelope than for the "rapid static" failure envelope (38.5°). This slight reduction in "dynamic" friction angle was also observed for the tests on dense Ottawa sand. The non-homogeneity of this natural soil cannot be overlooked as a possible contributor to the observed response.

Undisturbed Notre Dame Lake Marl (Appendix III - Figure 28) was also investigated indicating a parallel shift of the failure envelope and a strength ratio of 1.4. The apparent friction angle was 20.5°. As described by Fitz Hugh, Miller and Terzaghi[4, 9], a marl has clay and fine silt particles firmly united in hard clusters which behave similar to sand grains during undisturbed shear testing of the soil. They also state that after the flocks are destroyed the character of the marl changes from that of a sand to that of a clay. If this "cementation" represents part of the initial "rapid static" apparent cohesion it would probably remain constant for the "dynamic" apparent cohesion as indicated previously for the intercepts of Nevada Test Site Desert Alluvium and dry Jordan Buff clay. Such a small reduction from both "dynamic" and "rapid static" apparent cohesions would effectively increase the apparent ratio.

(6) Shear Stress versus Shear Displacement Response.

The basic feature of a direct shear device is maximum shear resistance determination and not strain measurement. A limited number of shear force versus shear displacement responses were recorded however, to further reveal any significant soil characteristics.

Typical "dynamic" and "rapid static" shear force versus shear displacement responses for dense dry sands and cohesive soils are presented and discussed in Appendix II of this report. The salient features of these responses are the excellent agreement between "dynamic" and "rapid static" dense sand test results and the maximum shear resistance occurring at larger displacements for "dynamic" tests than "rapid static" tests on cohesive soils.

SECTION 4. REFERENCES

4.1 Committee on Glossary of Terms and Definitions, "Glossary of Terms and Definitions in Soil Mechanics," Journal of the Soil Mechanics and Foundations Division, ASCE, Vol. 84, October 1958, p. 1826-10.

4.2 Burmister, Donald M., "The Place of the Direct Shear Test in Soil Mechanics," Symposium on Direct Shear Testing of Soils, ASTM Special Technical Publication, No. 131, June 1952, pp. 3-18.

4.3 Seed, H. B., R. J. Woodward Jr., and R. Lundgren, "Clay Mineralogical Aspects of the Atterberg Limits," Journal of the Soil Mechanics and Foundations Division, ASCE, Vol. 90, July 1964, p. 110.

4.4 Scott, R. F., Principles of Soil Mechanics, Addison-Wesley Publishing Company, Inc., Reading, Massachusetts, 1963.

4.5 Means, R. E., and J. V. Parcher, Physical Properties of Soils, Charles E. Merrill Books, Inc., Columbus, Ohio, 1963, p. 356.

4.6 Leonards, G. A., Foundation Engineering, McGraw-Hill Book Company, Inc., New York, N. Y., 1962.

4.7 Schimming, B. B., and H. C. Saxe, "Inertial Effects and Soil Strength Criteria," Symposium on Soil-Structure Interaction, University of Arizona, Engineering Research Laboratory, Tucson, Arizona, September 1964, pp. 118-128.

4.8 van Olphen, H., An Introduction to Clay Colloid Chemistry, Interscience Publishers - a division of John Wiley and Sons, New York, N. Y., 1963, pp. 98-103.

4.9 Fitz Hugh, M. M., J.S. Miller, and K. Terzaghi, "Shipways with Cellular Walls on a Marl Foundation," Transactions of ASCE, Vol. 112, 1947, pp. 300-301.

SECTION 5. SPECIAL TESTS

a. General.

During the course of this investigation some of the unique characteristics of DACHSHUND I were utilized to perform various types of exploratory tests. All of these tests were performed on either the ASTM C-190 Standard Ottawa sand or the Jordan Buff clay.

b. Inertial Confinement.

Whitman[5.1] has referred to a "lateral inertia effect" under triaxial conditions associated with dynamic impact loads. He describes it as follows: "Lateral strains must occur before failure can take place, and in very rapid tests inertia delays the development of lateral strains. Thus, it is possible to develop, during very short periods of time, stresses far in excess of the peak resistance."

DACHSHUND I permitted the examination of this effect under boundary conditions quite different from those of the triaxial test.

It has been well established for static tests on dense sand, that if the specimen is not allowed to expand completely, failure cannot be achieved without shearing individual sand grains. In the direct shear device expansion can only take place in a direction normal to the plane of failure and must cause a displacement of the normal force loading system in dynamic as well as static tests. This condition allowed the "lateral inertia" to be treated as a variable. To accentuate this dilatational inertial effect, failure envelopes were formed by applying the normal force with a large mass (lead weights) as well as with the pneumatic system (virtually no mass). As shown in Figure 5.1, the dynamic friction angle (60°) for the lead weight confinement is considerably greater than that (43°) for pneumatic normal force application. Thus, when considering a material with a tendency toward dilatation it is indicated that the inertial forces normal to the failure plane may alter the apparent dynamic strength of the soil.

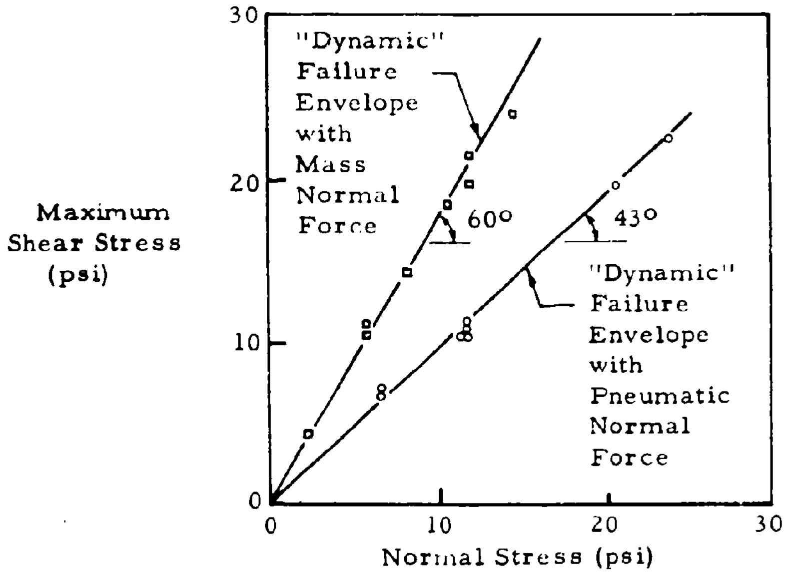

Figure 5.1 Test Results: Inertial Confinement of Dense Ottawa Sand

c. <u>Simultaneous "Dynamic" Shear and Normal Force Application.</u>

The characteristics of this particular pneumatic system permit simultaneous "dynamic" application of both the shear and normal forces.

In an effort to observe the effect of simultaneously applying both the confining force and the shear force a series of conventional "dynamic" and "rapid static" tests were conducted on the Jordan Buff clay for reference purposes. The photographic records of particular simultaneous test responses indicated that in general the shear and normal forces commenced within 1 ms of each other. Virtually all simultaneous tests exhibited a slower rate of increase in normal force than shear force. The limited simultaneous loading results of Figure 5.2 merely indicate duplication of the conventional "dynamic" test results.

This excellent agreement between simultaneous and conventional test results and the consistency of the conventional test response leads to no anticipation of variation in soil response due to this unique loading technique for a soil characterized by a horizontal failure envelope.

For materials characterized by a friction angle, which have been shown to be insensitive to dynamic effects, it could be anticipated that failure will occur whenever the shear versus normal force stress path contacts the static failure envelope. Whether or not the stress path remains beneath the envelope is related to the relative moduli (shear and compression) involved.

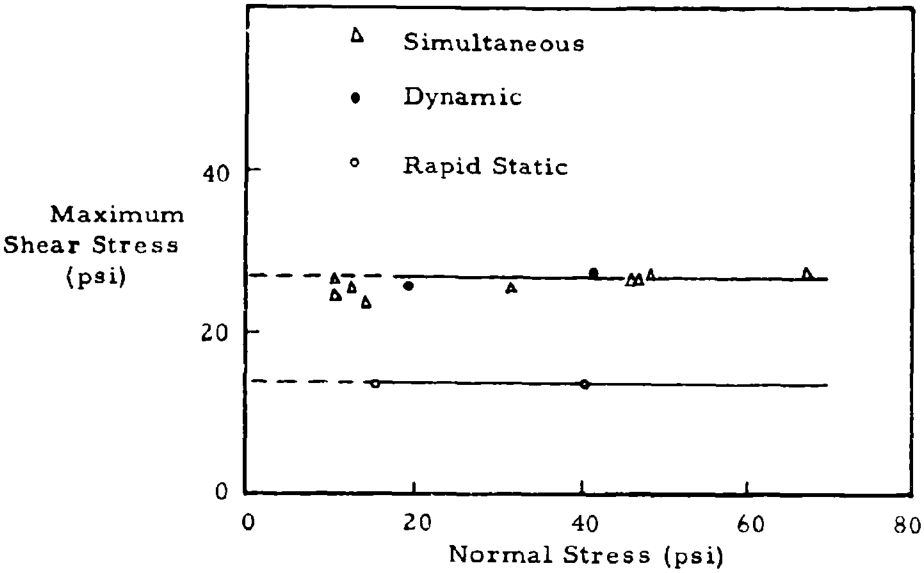

Figure 5.2 Test Results: Simultaneous "Dynamic" Shear and Normal Force Application - Jordan Buff Clay

d. Repetitive Shear Force Application.

An electrically controlled poppet-type pilot-operated valve inserted in the air supply line ahead of the shear force cylinder permitted the application of shear force pulses at frequencies up to 4 cps.

The shear force input pulses, Figure 5.3, had rise times of approximately 30 ms and decay (to atmospheric pressure) times approaching 8 ms. It is interesting to note the consistent linearity (k) of the net shear displacement per pulse as a function of time for the plastic ($w \approx 28\%$) Jordan Buff clay. Even after considerable displacements have taken place this phenomenon is observed. The plastic displacements per pulse for

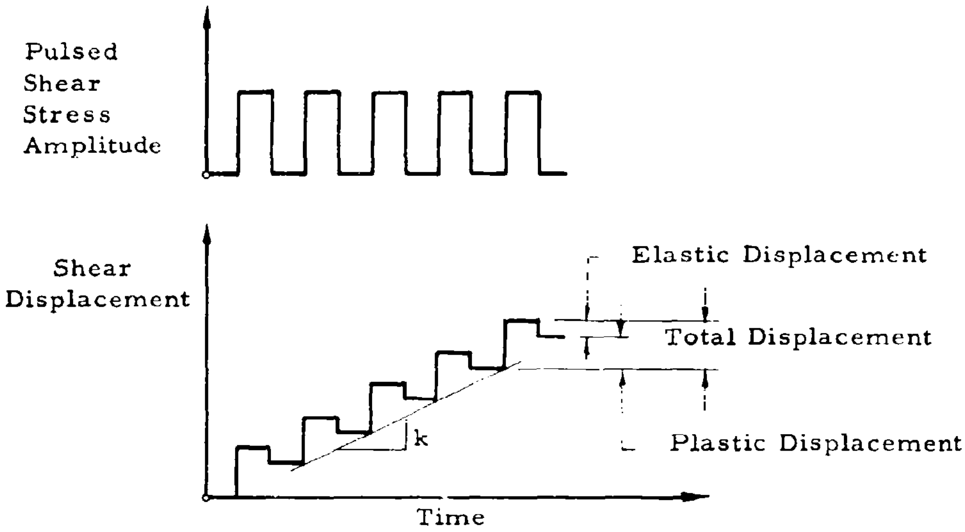

Figure 5.3 Schematic Diagram of Clay Response to Repetitive Shear Force Application

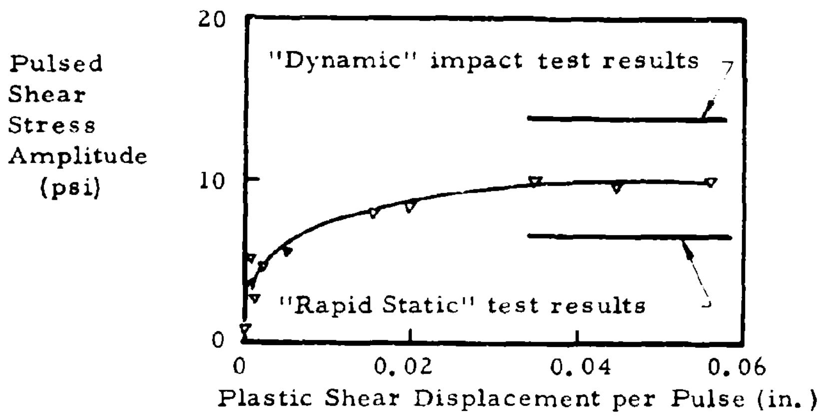

Figure 5.4 Test Results: Repetitive Shear Force Application - Jordan Buff Clay

various shear force magnitudes are given in Figure 5.4. It is readily observed that the maximum shear stress amplitude of this "stress-displacement" plot lies between the conventional "dynamic" and "rapid static" test results.

A tabular summary of all special tests is presented in Appendix IV of this report.

SECTION 5. REFERENCE

5.1 Whitman, R. V., "The Behavior of Soils under Transient Loading," Fourth International Conference on Soil Mechanics and Foundation Engineering, Proceedings, Vol. I, 1957, pp. 207-210.

SECTION 6. CONCLUSIONS

Based on the results of this investigation the following conclusions may be drawn:

a. Coarse cohesionless materials do not exhibit an increase in maximum shear resistance due to "dynamic" shear force application. This is true in both the dry and saturated states for the drainage conditions present in the direct shear box.

b. Cohesive and combined soils exhibit an increase in maximum shear resistance as indicated by an increase in apparent cohesion for the following conditions.

   (1) The apparent cohesion ratio is independent of moisture content, dry density and grain size for degrees of saturation in excess of approximately 85%.

   (2) Low degrees of saturation, the dry side of optimum for compacted soils, tend to reduce the apparent cohesion ratio.

   (3) Soil structure, whether flocculated or dispersed, does not appear to have a significant effect on the apparent cohesion ratio.

(4) The effect of an investigated electrolytic solution is to reduce the maximum shear resistance of the soil; however, the apparent cohesion ratio is not significantly altered.

(5) Examination of pore fluid viscosity indicates that for viscosities near that of water the apparent cohesion ratio remains unchanged. However, if the pore fluid viscosity is radically different than that of water the apparent cohesion ratio is altered but not in proportion to the respective fluid viscosities.

c. The consistent failure envelope trends provide a basis for estimating the dynamic shear resistance if the static failure envelope is available, thus minimizing the need for specialized laboratory tests in an applied situation.

d. Corroboration of Mitchell's[3.26] "rate process theory" on the basis of failure envelope parameters has been observed for the distinct times to failure involved in the "dynamic" and "rapid static" tests.

e. The relatively uniform apparent cohesion ratio for the wide variety of soils investigated certainly questions the explanation that variations in pore pressure development are entirely responsible for strength variations as a function of strain rate.

f. Inertial confinement effects can alter the maximum shear resistance of soils which tend to dilate.

g. The "dynamic" application of normal force simultaneous with shear force did not alter the apparent cohesion ratio for the clays studied.

h. The previous conclusions indicate that with respect to application to a dynamic phenomenon such as cratering

For soils whose strengths are dependent on body forces, such as sand, the descriptive dimensionless term,

$$\frac{\text{Explosive Energy}}{(\text{Soil Density}) \times (\text{Characteristic Length})^4}$$

Sedov[6.1], will not assume different dynamic and static values. However, for materials whose strengths are independent of body forces, such as pure cohesive soils, the descriptive dimensionless term,

$$\frac{\text{Explosive Energy}}{(\text{Characteristic Soil Strength}) \times (\text{Characteristic Length})^3}$$

will assume different static and dynamic values.

i. The effect of duration of a stress controlled pulse on maximum shear resistance and subsequent static strength remains to be investigated. The residual strain as related to maximum shear resistance in the presence of a dynamic loading history would be of interest.

j. The consistent performance of DACHSHUND I has demonstrated it to be an efficient dynamic direct shear device.

SECTION 6. REFERENCE

6.1 Sedov, L.I., Similarity and Dimensional Methods in Mechanics, Academic Press Inc., New York, N.Y., 1961, p.256.

APPENDIX I. DETAILED TEST PROCEDURE

a. General.

The following are standard test procedures used throughout the DACHSHUND I experimental program. Variations of these techniques are used to perform the "special" tests indicated in Section 5 of this report.

Prior to testing, it is necessary to turn the equipment on for a minimum of one-half hour to obtain a stabilized condition of all electrical components. Calibrated input voltages to the force transducers must be checked as well as the recorder response for each of the test variables.

b. Conventional "Dynamic" Test Procedure.

1. General preparation of oscilloscopes

a) Trigger mode on auto sweep

1) Set the appropriate sweep time (normally 50 ms) and voltage scale for transducer calibration.

2) Focus the traces and set the proper polarity.

3) Set the scale illumination just above f 2.8 and the trace intensity such that there is an illumination band 2 cm wide centered on each of the traces. (This is for a time exposure of approximately 1 minute.)

4) Check for film in cameras with lens setting of f 2.8 and the shutter speed at B (bulb).

2. Cock the trigger mechanism on the horizontal air cylinder to restrain the piston during cylinder pressurization.

3. Place the prepared soil sample in the shear box seating the upper gripper spacer on top with the gripper teeth perpendicular to the direction of shear displacement.

4. Place the loading head on the upper gripper spacer and pivot the vertical loading assembly into a testing position, being careful to center the loading head and assembly on the upper gripper spacer.

5. With the horizontal piston restrained and the vertical piston free to move prepare the pneumatic system as follows:

    a) Open to atmosphere the stop cocks controlling the exhaust side of the air cylinders.

    b) Open the quick-opening gate valves ahead of the pressure side of the cylinder to allow pressure accumulation within the air cylinder.

    c) Close the stop cocks at the quick-opening gate valves.

6. Set the trace base lines at their chosen zero location on the oscilloscope.

7. Set the desired vertical pressure with the pressure regulator. <u>Note:</u> The time length of vertical pressure

   application prior to shearing varies with the preparation technique for the soil being tested.

8. Set the trigger sweep mode on the oscilloscope to the "arm" position and arm the oscilloscope.

9. Close the viewing ports and lock the camera shutters in the open position.

10. Set the air bearing at a pressure of 60 psi and accumulate a shear force cylinder pressure of sufficient magnitude to fail the sample.

11. With the sample now prepared for testing the load is applied by depressing the "Fire Both" or "Fire Horizontal" switch which simultaneously activates the traces on the oscilloscope and the solenoid actuated trigger thus freeing the piston.

12. Immediately after failure of the soil sample release the camera shutters and develop the Polaroid pictures which are to be attached to prepared data sheets as a permanent record of the test.

c. Conventional "Rapid Static" Test Proceedure.

1. General preparation of oscilloscope

   a) Trigger mode on auto sweep

      1) Set the appropriate sweep time (normally 50 sec.) and voltage scales for transducer calibration.

      2) Focus the traces and set the proper polarity.

      3) Set the scale illumination just above f 2.8 and the trace intensity such that the traces are just visible. (This is for a time exposure of approximately 1 minute.)

      4) Check for film in cameras with lens setting of f 2.8 and the shutter speed at B (bulb).

2. Set the horizontal pressure regulator with the release of air impending.

3. Place the prepared soil sample in the shear box seating the upper gripper spacer on top with the gripper teeth perpendicular to the direction of shear displacement.

4. Place the loading head on the upper gripper spacer and pivot the vertical loading assembly into a testing position, being careful to center the loading head and assembly on the upper gripper spacer.

5. With both the horizontal and vertical pistons free to move prepare the pneumatic system as follows:

   a) Open to atmosphere the stop cocks controlling the exhaust side of the air cylinders.

   b) Open the quick-opening gate valves ahead of the pressure side of the cylinder to allow pressure accumulation within the air cylinder.

   c) Close the stop cocks at the quick opening gate valves.

6. Set the trace base lines at their chosen zero location on the oscilloscope.

7. Set the desired vertical pressure with the pressure regulator. Note: The time length of vertical pressure application prior to shearing varies with the preparation technique for the soil being tested.

8. Set the trigger sweep mode on the oscilloscope to the "arm" position and arm the oscilloscope.

9. Close the viewing ports and lock the camera shutters in the open position.

10. Set the air bearing at a pressure of 60 psi.

11. Trigger the traces by depressing the "Fire Both" switch.

12. Build up the shear force at the desired rate with the pressure regulator.

13. Immediately after failure of the soil sample, release the camera shutters and develop the Polaroid pictures which are to be attached to prepared data sheets as a permanent record of the test.

d. <u>Automatic Control Test Procedure.</u>

1. General preparation of recording system

   a) Set the appropriate voltage scales for displacement calibration.

   b) Check the pens for recording purposes on the 4-pen strip chart recorder.

2. Accumulate an air supply pressure of 25 psi to the servomechanism controls.

3. Select the phenomenon to be controlled on the "Horizontal Programming Force or Displacement Pressure Regulator."

4. Eliminate the conventional test accumulator tanks from the system by closing the gate valves ("P" in Figure 2.2).

5. Set the appropriate values of RESET and PROPORTIONAL BAND on the programming unit for the consistency of

the particular soil being tested. Note: There is an optimum operating condition for either displacement rate or rate of force application for each soil type which can only be established by trial and error tests at various settings of the programmers RESET and PROPORTIONAL BAND.

6, 7, and 8. Same as 3, 4, and 5 of the Conventional "Rapid Static" Test.

9. Accumulate the desired vertical and horizontal pressure behind the pneumatically controlled gate valves. The horizontal (shear force) pressure should be slightly greater than that required to fail the sample.

10. Set the air bearing pressure at 60 psi.

11. Start the test by switching on the controlling cam clock and the chart drive on the recorder.

12. After the test is over remove the chart with the desired information such that it can be retained as a permanent record of the test.

APPENDIX II. INTERPRETATION OF TEST RESULTS

a. Response Interpretation.

(1) General.

The purpose of this section is to clarify some details regarding the interpretation of typical soil response traces.

(2) Conventional "Dynamic" Tests.

With "dynamic" test time durations (from zero to total displacement) varying from 10 to 30 milliseconds it is easy to conceive of acceleration and deceleration forces entering the response. To allow for this possibility the moving components of the shear box mechanism were shaped and constructed of materials to minimize their mass.

(a) Shear Force.

Preliminary tests on a dense Ottawa sand indicated a large spike in the action cell trace upon application of the shear force. This spike was concluded to be an inertial force because the magnitude was considerably larger than that available when considering the pressure within the air cylinder and the area of the piston. The dynamic equilibrium immediately after release of the restrained piston is indicated in Figure II. 1 below.

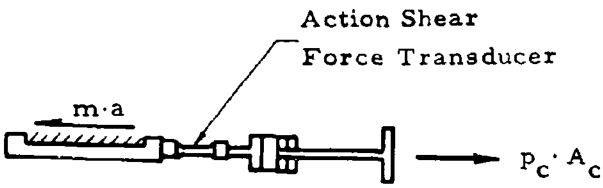

Figure II. 1 Inertial Effect on Action Shear Force Transducer

To clarify this situation the reaction shear force transducer was added to the system. With such an arrangement it is possible to record the actual force transmitted through the soil specimen.

The shear force response of the dense Ottawa sand exhibited a large peak in the reaction shear force transducer as well as in the action shear force transducer. A test on this dense Ottawa sand with zero normal force yielded the traces in Figure II. 2. As can be seen, both traces exhibit the high initial peak. This peak is likely a combined

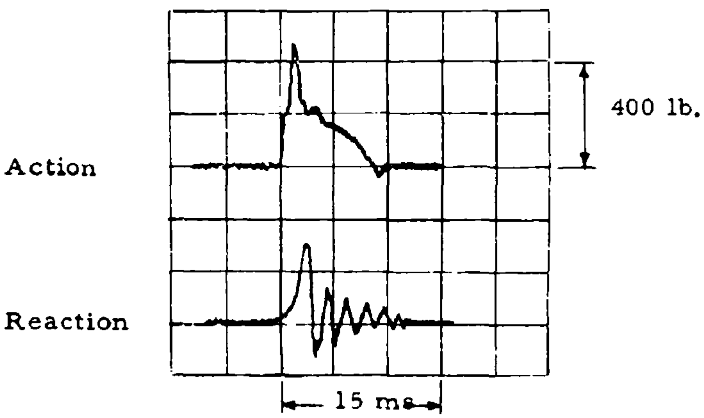

Figure II. 2 Action and Reaction Shear Force Transducer Response - Unconfined Dense Ottawa Sand effect of the excess air pressure in the cylinder which induces "over-shoot" in the reaction transducer and "dilatational inertia" which is a phenomenon similar to the "lateral inertia effect" referred to by Whitman [5.1]. In the test results of cohesive soils and loose sands the first spike is almost eliminated from the reaction shear force transducer response but still remains in the action shear force transducer.

The inertial effects were eliminated from the interpretation of the results by reading the reaction shear force trace as an average of the small amplitude oscillations immediately following the first peak.

(b) Normal Force.

Variation in normal force is principally due to the dilatation tendency of some materials which as a result changes the direction of the friction force component on the piston as indicated in Figure II. 3. In addition to the friction force direction change "dynamic" tests on dense sand exhibit an initial inertial force (A), Figure II. 4,

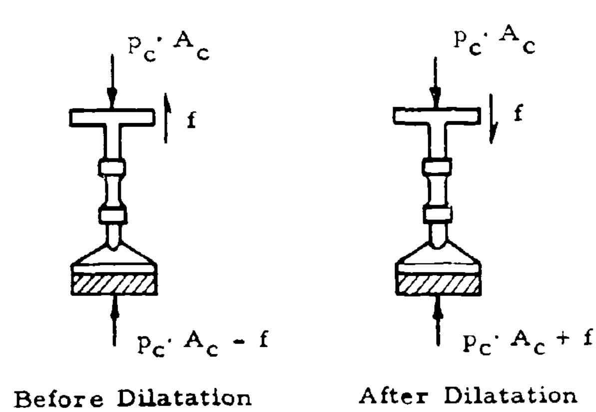

Figure II. 3 Effect of Sample Dilatation on Normal Force

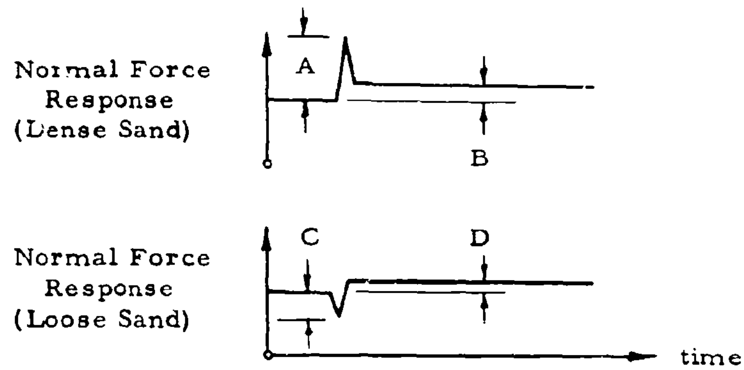

Figure II. 4 "Dynamic" Test Effect on Normal Force

acting in the same direction of the friction force "after dilatation," Figure II. 3, effectively increasing the normal force applied to the specimen. This peak is due to the vertical acceleration resulting from dilatation and has dissipated such that the dilatation friction force component (B) is the only remaining effect on the normal force by the time the maximum shear resistance has been attained. "Dynamic" tests on loose sand also exhibit an apparent inertial force (C), Figure II. 4, which reduces the normal forces as a result of an instantaneous contraction. The dynamic equilibrium of this situation is indicated in Figure II. 5. If the initial contraction creates a void ratio less than the critical void ratio, dilatation will have to occur for further shear displacement to take place. This dilatation will reverse the direction

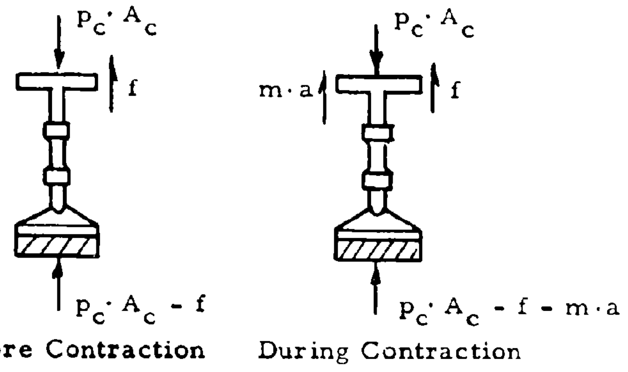

Figure II. 5 Normal Dynamic Equilibrium Before and During Contraction

of the friction force and effectively increase the value of the normal force (D), Figure II. 4. The inertial normal force effect for loose sands has also dissipated by the time the maximum shear resistance is attained.

Very little normal force fluctuation is observed in "dynamic" tests on cohesive soils.

The appropriate normal force to use in interpretation of the results is that which exists at the time the peak shear resistance is recorded.

(3) Conventional "Rapid Static" Tests.

(a) Shear Force.

A number of tests on clay yielded a shear force and shear displacement response as indicated in Figure II. 6.

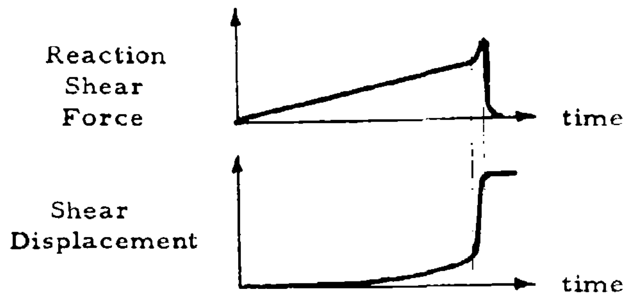

Figure II. 6 Characteristic Conventional "Rapid Static" Test Shear Response for Cohesive Materials

It is noted that the rate of shear displacement increases slowly until a simultaneous marked increase in shear force and shear displacement rate occur. The characteristic shear force versus shear displacement response, Figure II. 7, for a "rapid static" test on clay indicates that the maximum shear resistance offered by the soil is the peak recorded

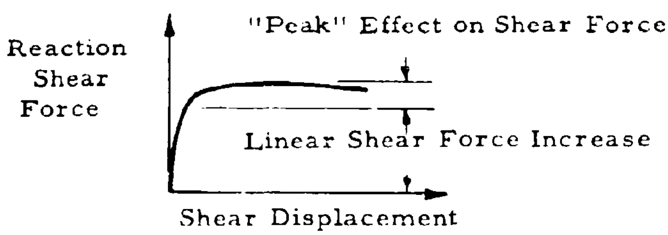

Figure II. 7 Characteristic Conventional "Rapid Static" Test Shear Force versus Shear Displacement Response for Cohesive Materials shear force. This resistance is offered at displacements during the increased rate of shear deformation. The analagous situation exists in "automatically controlled tests" in which the rate of shear force application is programmed.

Figure II. 8, a plot of shear force versus shear displacement for two tests of 4 minutes duration shows the agreeable comparison of maximum shear resistance provided by Chicago Blue clay specimens under both controlled displacement and controlled force test conditions. The relative agreement of the above test results and the ease of performing conventional "rapid static" tests seems to justify the use of maximum values of shear resistance for tests with a 30-50 second duration.

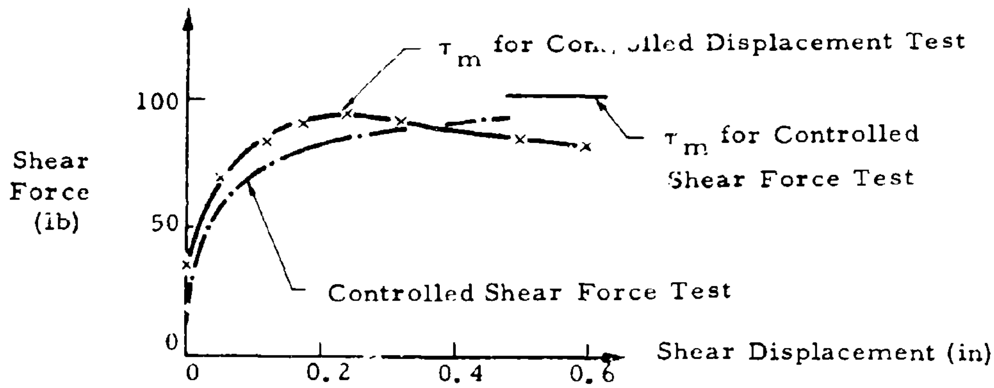

Figur.. .. 8 Effect of '4 minute" Test Procedure on Maximum Shear Resistance

(b) Normal Force.

Variation in normal force is observed in "rapid static" tests as well as in "dynamic" tests. This is particularly true of tests on dense sand in which dilatation does occur and the direction of the friction force component is reversed as indicated in Figure II. 3. Once again, the interpreted value of normal force is that which is on the specimen at the time the soil offers its maximum shear resistance.

b. Typical Test Results.

(1) General.

For the proper interpretation of the test results it is necessary to present typical values of the measured variables. In order that these values quantitatively represent the forces and displacements, the respective transducers must be calibrated periodically as described by Saxe, et al.[2.1] The calibrated input voltages to the force transducers must be recorded to facilitate a daily calibration merely by setting the same voltage input as that established in the calibration process. The standard transducer calibrations are as indicated in Table II-1.

(2) Dense Cohesionless Material.

All tests used to represent cohesionless material test results have been performed on the 20-30 Ottawa sand with ASTM designation C-190.

Table II.1

Transducer Calibrations

Recording System	Transducer	Voltage Scale	Readout Calibration
Oscilloscope	Normal Force	10 mv	100 lb/cm
	Shear Force	10 mv	100 lb/cm
	Normal Disp.	10 mv	0.01 in/cm
	Shear Disp.	20 mv	0.20 in/cm
4-Pen Strip Chart Recorder	Normal Force	-	10 lb/division
	Shear Force	-	5 lb/division
	Normal Disp.	4 mv	0.002 in/division
	Shear Disp.	2 mv or 4 mv	variable

The preparation process, Appendix III, used for the following tests on dense sand yielded a consistent void ratio of 0.535, the equivalent of an 87% relative density.

(a) Conventional "Dynamic" Test.

The "Dynamic" test results of Figure II.9 show that upon application of the normal force (A = 235 lb.), prior to testing, a compression (B = 0.006 in.) of the specimen takes place. The imposed impact shear force develops the inertial peaks (C and D) due to the combined effect of overshoot and dilatation prior to the time the soil has

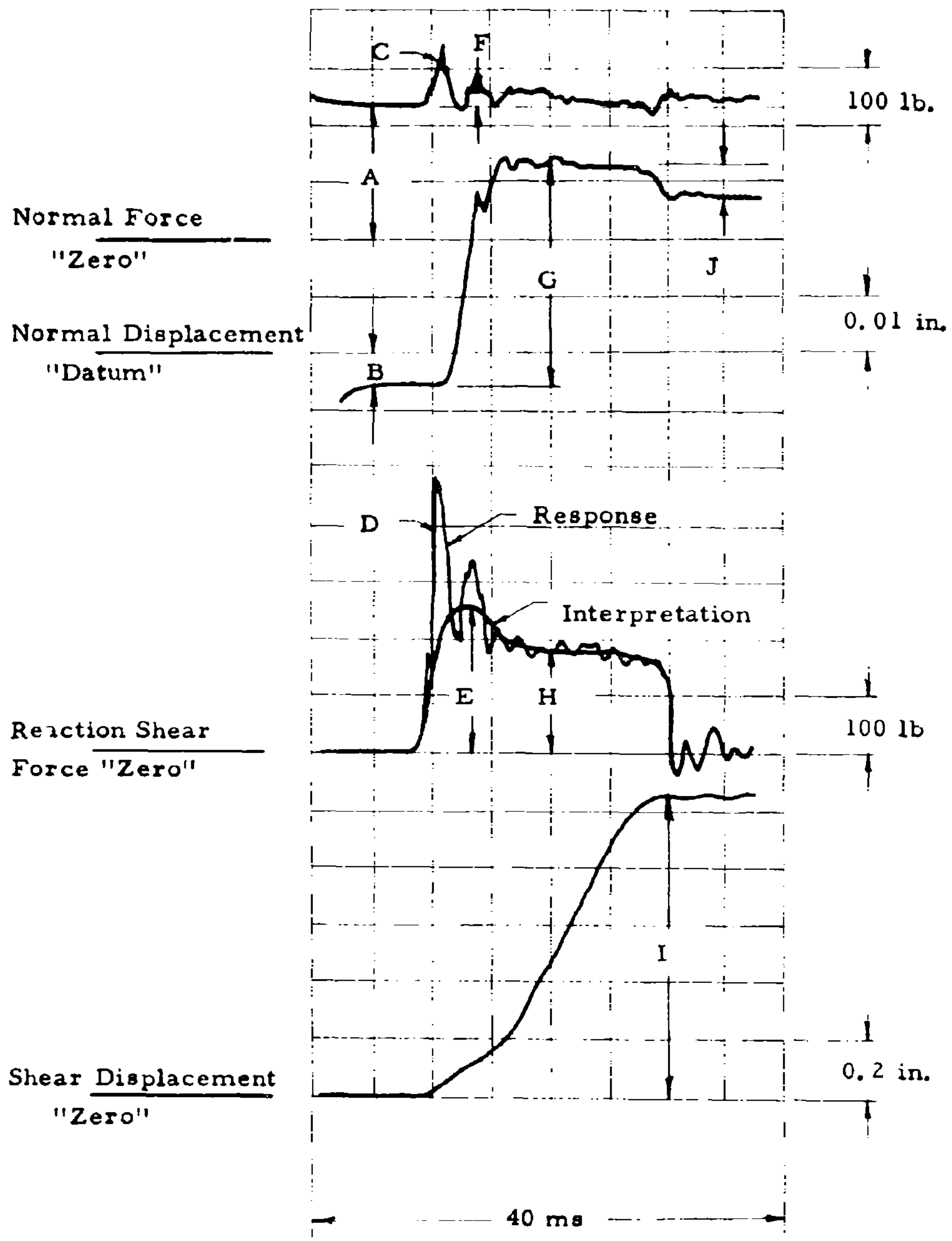

Figure II.9 Typical Conventional "Dynamic" Dense Sand Test Results developed its maximum shear resistance (E = 250 lb.). This shear resistance occurs as dilatation is reversing the direction of the normal friction force, effectively increasing the normal force (F = 25 lb., A+ F = 260 lb.) on the sample. A constant dilatation (G = 0.04 in.) is maintained at the critical void ratio and the shear force required to continue shearing is substantially reduced (H = 180 lb.). At exhaust and total shear displacement (I = 1.05 in.) the sample is compressed (J = 0.004 in.) to a density greater than that at the critical void ratio. The shear force versus shear displacement response, Figure II. 10, of another test with a comparable normal force merely exemplifies the characteristic similarities of "dynamic" shear tests on dense sand and "static" controlled displacement tests performed by other investigators [II. 1].

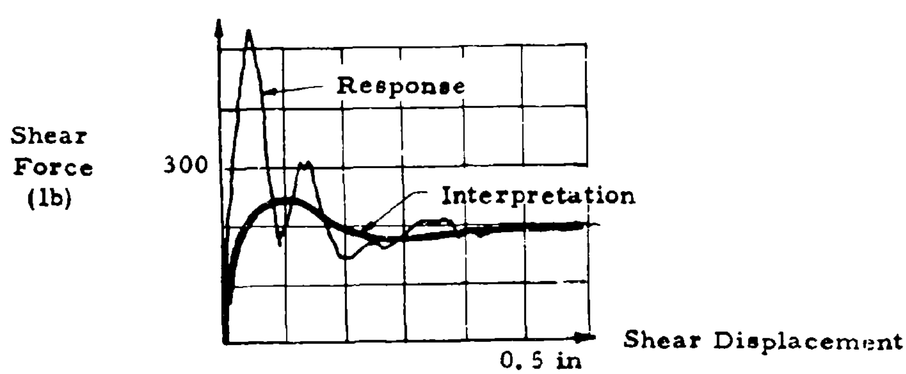

Figure II. 10 Conventional "Dynamic" Dense Sand Shear Force versus Shear Displacement Response

(b) <u>Conventional "Rapid Static" Test.</u>

In the direct shear test the most important response is the shear resistance afforded by the soil. This, however, cannot be associated with a failure criteria unless the applied normal force at the time of maximum shear resistance is known. Figure II. 11 is a tracing of the typical normal force, normal displacement, action shear force, reaction shear force and shear displacement response as a function of time for a "rapid static" test on dense sand.

Analysis of the normal transducer components yields a compression (A = 0.006 in.) upon application of the (B = 240 lb) initial normal force. During the process of developing the shear force at the desired rate, a dilatation (C = 0.005 in.) increases the normal force (D = 30 lb.) to its maximum value (E = 270 lb.) as described in Section a(3) of this appendix. This instantaneous dilatation (F = .024 in.) occurs at the peak normal force allowing the sand to attain its critical void ratio. Once this void ratio has been established there is no longer a tendency toward dilatation and the normal force frictional component reverses its direction and reduces the normal force (G = 25 lb.). Upon release of air pressure in the cylinder the soil expands (H = 0.004 in.) to regain the greatest portion of its initial compression.

The action and reaction shear force responses are seen to be similar throughout. The shear displacement transducer indicates a displacement (I = 0.04 in.) taking place during the shear force application.

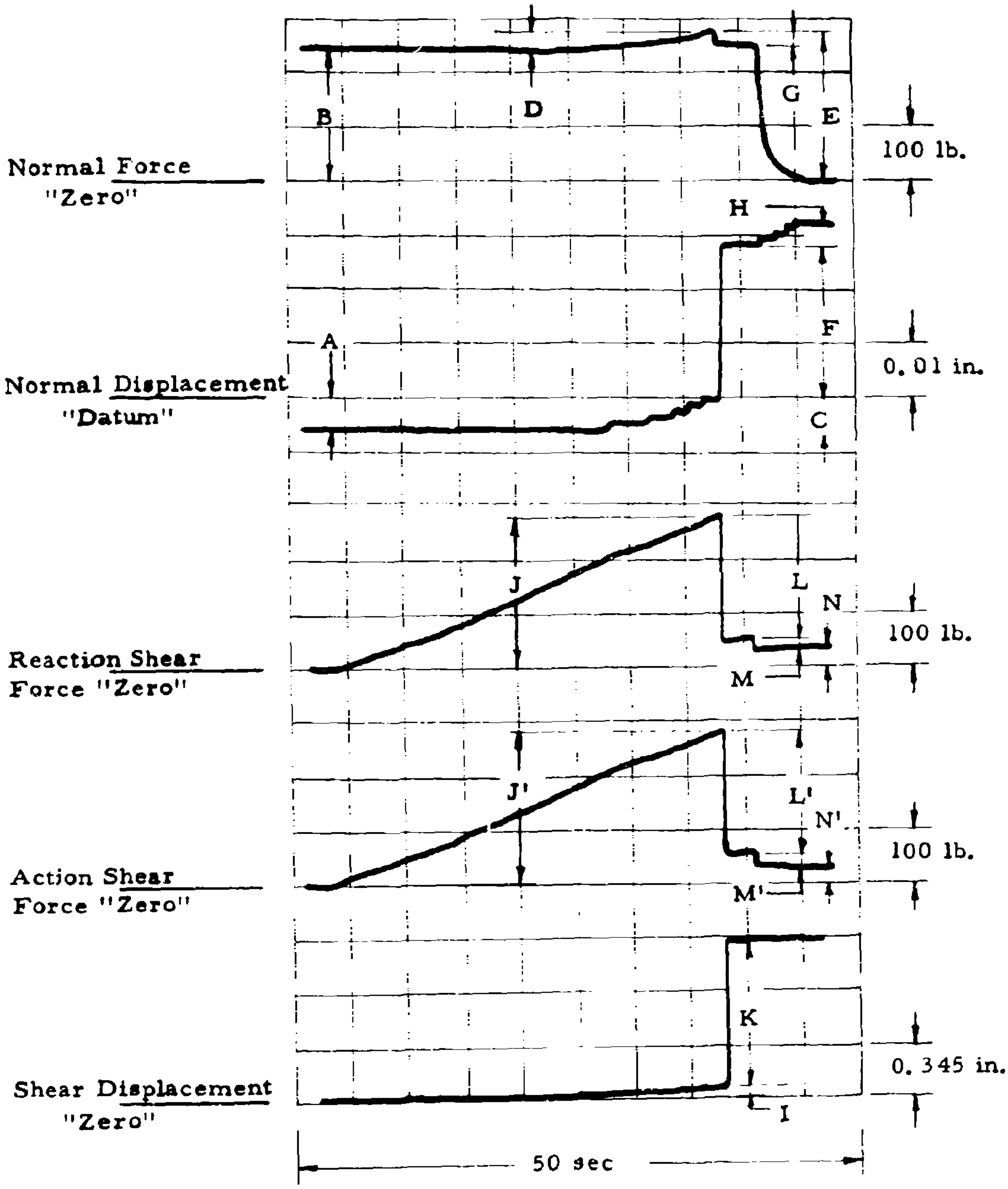

Figure II. 11 Typical Conventional "Rapid Static" Dense Sand Test Results

When the maximum shear force (J = J' = 280 lb.) has been reached the sample shears (K = .935 in.) almost instantaneously and the air pressure exhausts to the atmosphere reducing the shear force by a substantial amount (L = L' = 230 lb.). After the test is completed the air supply is shut off and all air pressure in the cylinder is dissipated (M = M' = 20 lb.). The shear force remaining in the system (N = N' = 20 lb.) is created by the friction force, between the piston ring and cylinder walls, transmitted through the action shear force transducer and the confined soil specimen to the reaction shear force transducer as indicated in Figure II. 12.

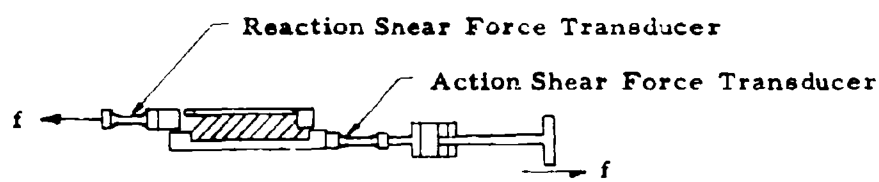

Figure II. 12 Recorded "Shear" Cylinder-Piston Friction Force

The shear force versus shear displacement response indicated in Figure II. 13 was recorded in a test with a normal load comparable to that reported in Figure II. 11. This tracing shows the dense sand's peak

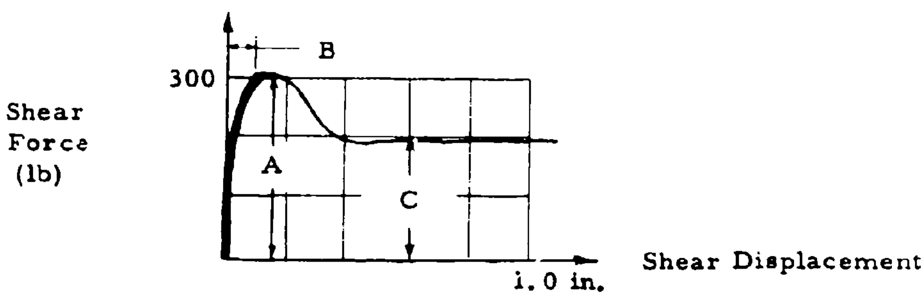

Figure II. 13 Conventiona "Rapid Static" Dense Sand Shear Force vers .. Shear Displacement Response

shear strength (A = 305 lb.), shear displacement at peak shear strength (B = 0.05 in.) and its shear strength (C = 190 lb.) at the critical void ratio. This characteristic trace is to be expected for controlled displacement tests as indicated by Hough[II. 1]. Electronic instrumentation permits the observation of this response for controlled shear force tests.

(3) Loose Cohesionless Material.

Void ratios of 0.69 - 0.70, relative densities of approximately 37%, were reproduceable by using the process described in Appendix III of this report. The following loose sand results were obtained from tests under these conditions.

(a) Conventional "Dynamic" Test.

The typical test results in Figure II. 14 show a variation in the initially applied normal force (A = 355 lb.) upon imposition

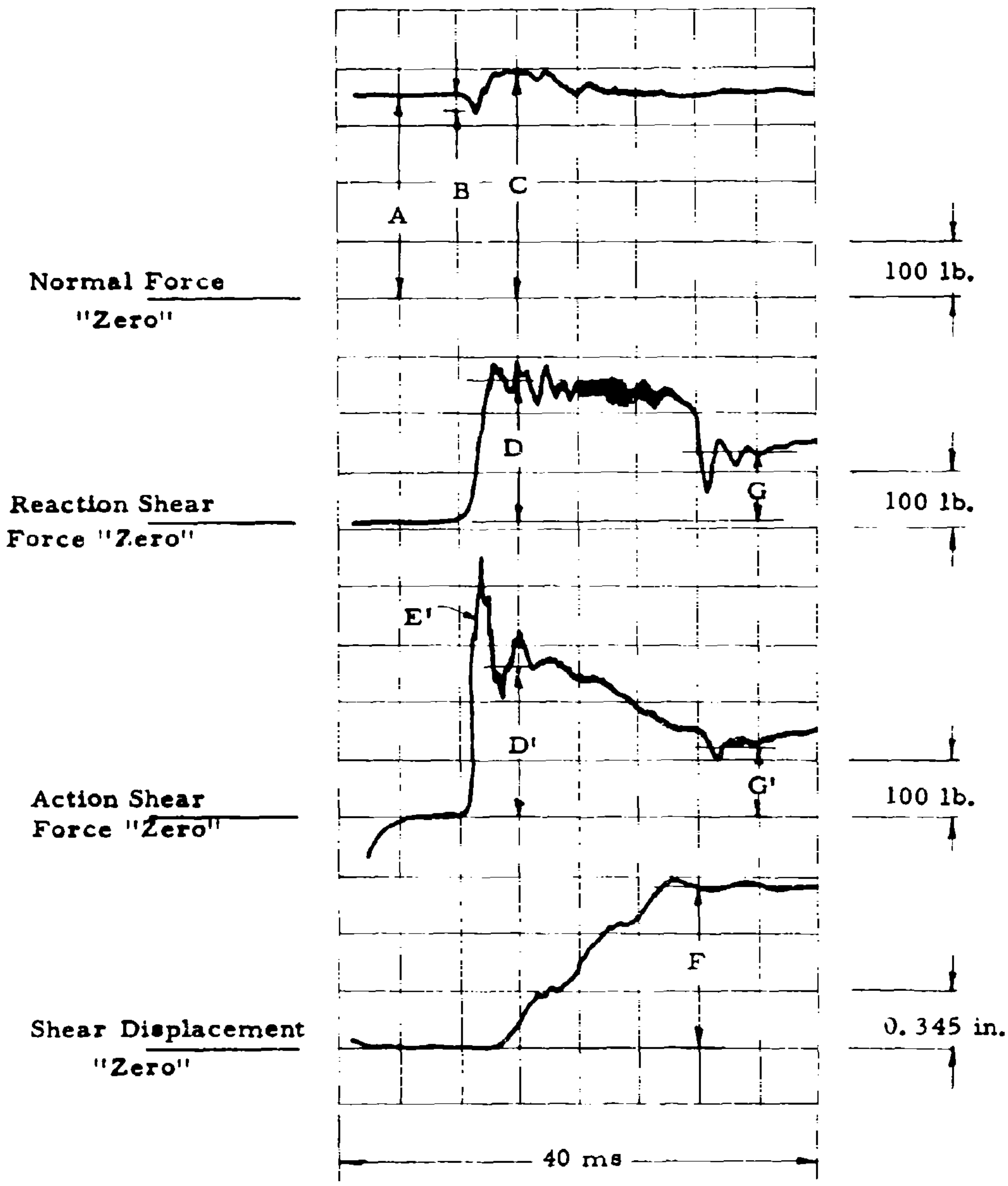

Figure II. 14 Typical Conventional "Dynamic" Loose Sand Test Results

of the shear force and throughout the shearing process. The decrease in normal force (B = 30 lb.) apparently occurs as a result of the instantaneous contraction as discussed in Section a(2) of this appendix. Dilatation subsequently increases the normal force to its value (C = 390 lb.) at the soil's peak shear resistance (D = 250 lb., D' = 260 lb.). It is also necessary to note that the inertial peak (E') in the action force response is virtually eliminated in the reaction force response. After shear displacement ceased (F = 0.96 in.) a shear force (G = G' = 120 lb.) remained on the specimen due to a pressure gradient across the piston created by the flow of air through the cylinder exhausting to the atmosphere.

(b) <u>Conventional "Rapid Static" Test.</u>

The loose sand test results in Figure II.15 indicate that the initially applied normal force (A = 425 lb.) was maintanined virtually constant throughout the entire shearing process. The only deviation (B = 20 lb.) from the constant normal force apparently occurred after a gradual shear displacement (C = 0.138 in.) abruptly changed (D = 0.035 in.) allowing some dilatation of the soil and a reversal of the friction force component in the normal force air cylinder as described in Section a of this appendix. The maximum shear resistance (E = 300 lb., E' = 310 lb.) afforded by the soil under the increased normal force (F = 445 lb.) took place during a sudden shearing (G = 0.90 in.) of the sample. After approximately 0.8 inch displacement the pressure in the air cylinder exhausted

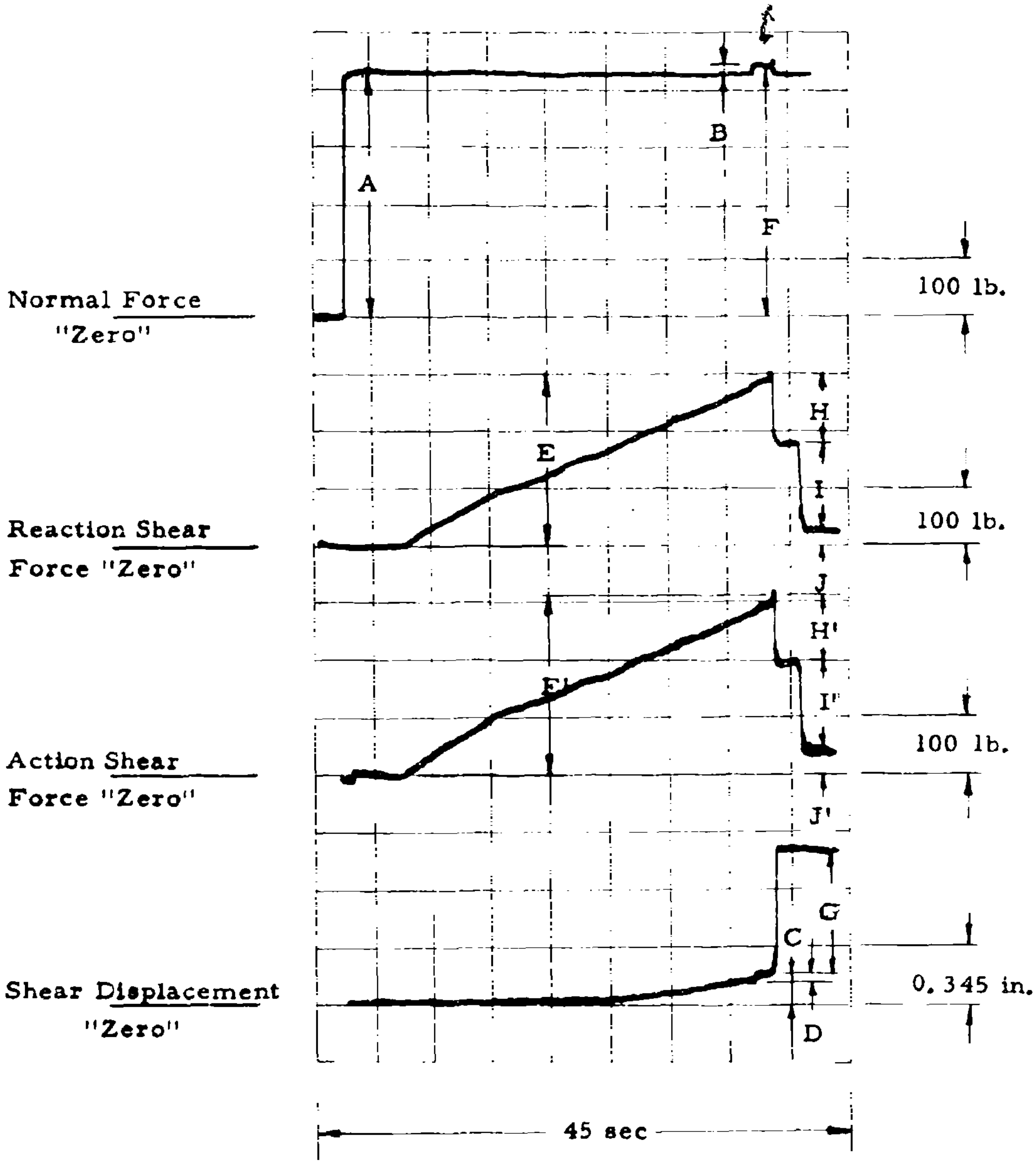

Figure II. 15 Typical Conventional "Rapid Static" Loose Sand Test Results to the atmosphere (H = 120 lb., H' = 120 lb.). The flow of air into the cylinder was shut off (I = 160 lb., I' = 160 lb.) and the air cylinder frictional force (J = 20 lb., J' = 30 lb.) remained.

(4) Cohesive Material.

Test results of all cohesive, fine grained materials indicated similar response characteristics therefore confining the necessary interpretation procedure to a typical soil.

The naturally deposited Chicago Blue clay discussed herein was obtained from Soil Testing Services, Incorporated, of Northbrook, Illinois. Its properties and sample preparation process are described in Appendix III.

(a) Conventional "Dynamic" Test.

The test results in Figure II. 16 show a very slight consolidation (A = 0.001 in.) under the applied normal force (B = 150 lb.) which was established after the sample was seated at its preconsolidation pressure. Upon imposition of the shear force and shear displacement some apparent dilatation, equal to the previous consolidation, took place resulting in a zero net normal displacement throughout the test duration. As previously mentioned, "dynamic" tests on clay give virtually no indication of inertial forces in recording the soils maximum shear resistance (C = 110 lb.).

Figure II. 17 is a tracing of the shear force versus shear displace-

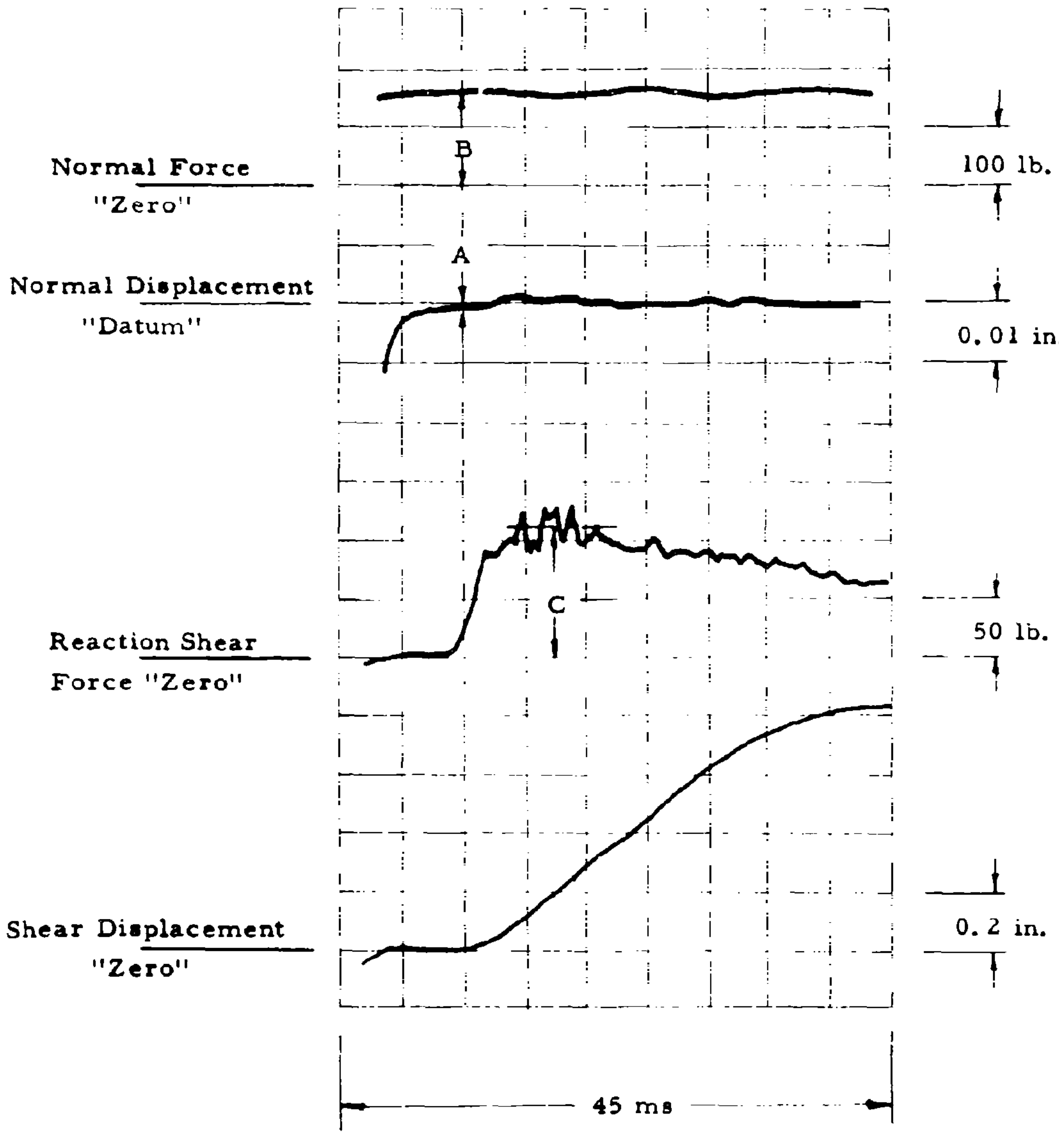

Figure II. 16 Typical Conventional "Dynamic" Test Results on Cohesive Soils

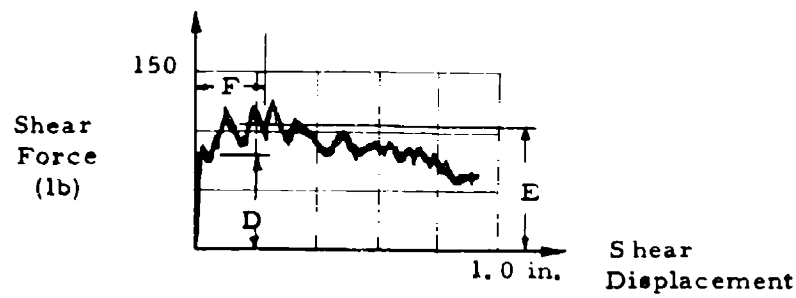

Figure II. 17 Conventional "Dynamic" Shear Force versus Shear Displacement Response for Chicago Blue Clay

ment for the test being discussed. An apparent "threshold" strength (D = 80 lb.) is noted at an extremely small shear displacement. The maximum shear resistance (E = 110 lb.) occurs at a shear displacement (F = 0.24 in.) which is less than the total displacement attained in the "automatic controlled displacement tests."

(b) <u>Conventional "Rapid Static" Test.</u>

A normal force (A = 300 lb.) equal to the pre-consolidation pressure of the Chicago Blue clay was applied to all specimens, including the "rapid static" test indicated in Figure II. 18. This seating force further consolidated the sample (B = 0.003 in.) between measurement of the normal displacement datum, preparation of

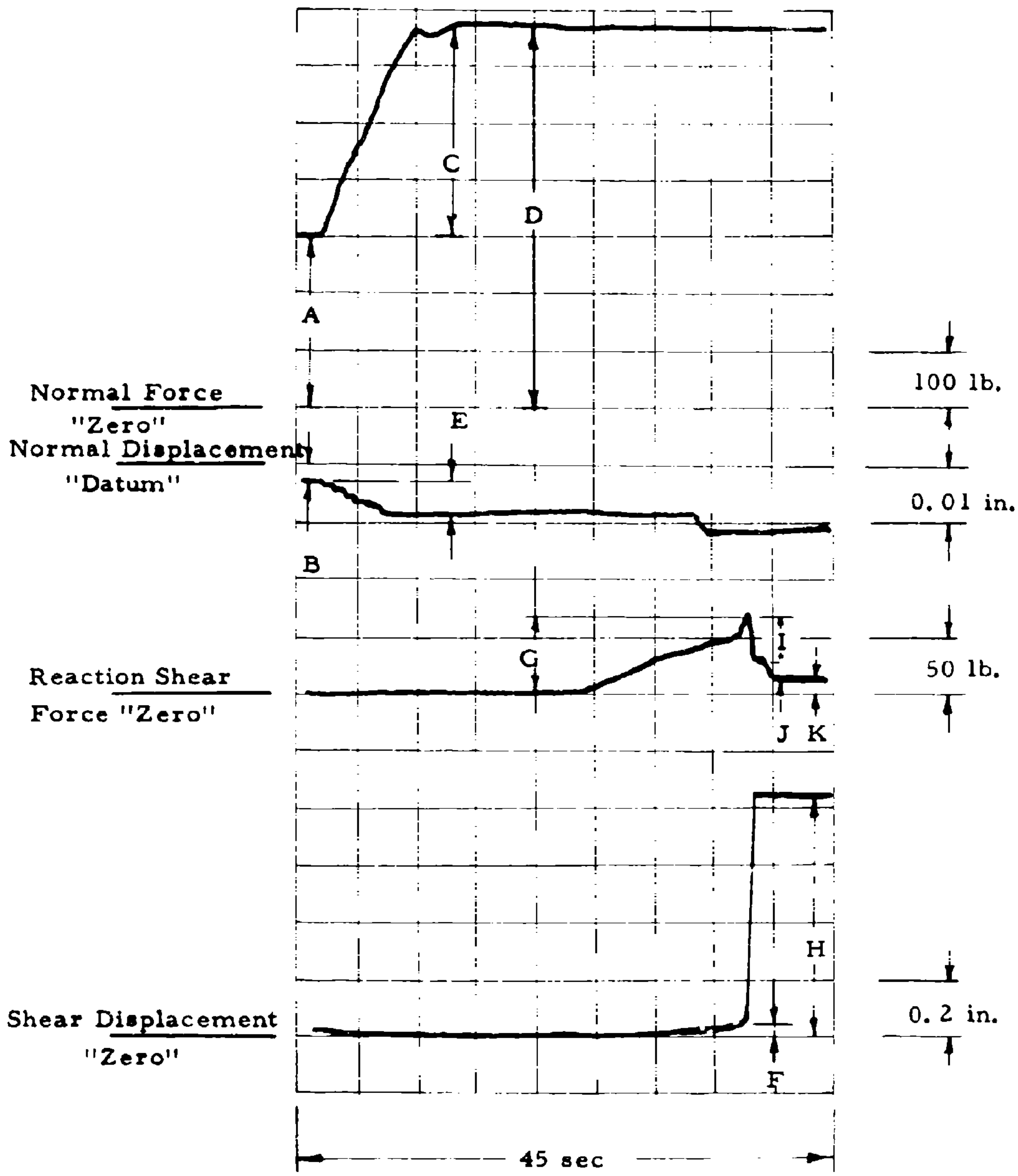

Figure II. 18 Typical Conventional "Rapid Static" Test Results on Cohesive Soils the recording device and release of the traces. The normal force was increased (C = 370 lb.) to the desired value (D = 670 lb.) and an additional consolidation (E = 0.006 in.) took place. During shear force application a gradual shear displacement (F = 0.04 in.) developed whereupon there was a sudden increase in the rate of displacement causing the shear resistance of the soil to assume its ultimate value (G = 65 lb.). The total displacement (H = 0.84 in.) was sufficient to cause a decrease (I = 40 lb.) in applied shear force due to the air supply exhausting to the atmosphere. A further decrease in available shear force (J = 15 lb.) occurs when the flow of air is eliminated. The only remaining force (K = 10 lb.) is a result of friction between the piston and cylinder wall.

Figure II. 19 is a tracing of the shear force versus shear displacement response for the test recorded in Figure II. 18. A "threshold" strength is apparent at incipient "failure" (L), just prior to the increased rate of displacement as indicated by the lower intensity portion of the trace.

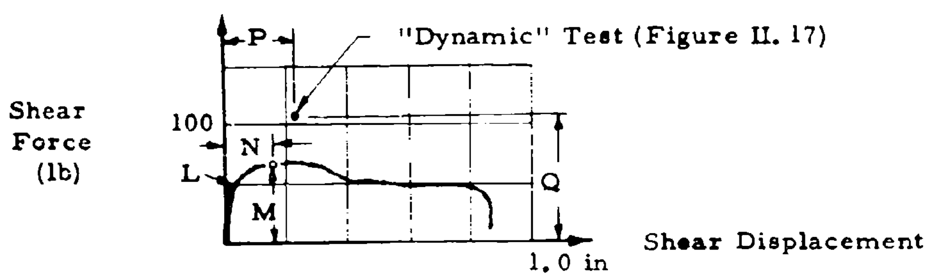

Figure II. 19 Conventional "Rapid Static" Shear Force versus Shear Displacement Response for Chicago Blue Clay

The maximum shear resistance (M = 65 lb.) of the soil is provided at a shear displacement (N = 0.16 in.) which is less than the total displacement produced in the "automatically controlled displacement test."

A comparison of the "dynamic" and "rapid static" shear displacements (respectively P = 0.24 in., N = 0.16 in.) at maximum shear resistance indicates this displacement to be greatest for "dynamic" tests, although the location of maximum resistance is open to interpretation.

(c) <u>Automatically Controlled Displacement Test.</u>

Figure II. 20 is a drawing of the recorded Chicago Blue clay response. There is no difficulty in interpretation of these test results as all traces are continuous with no marked irregularities entering the record. The slight steps in the normal and shear displacement traces are a characteristic of the recording device. Undulations in the shear force trace are a result of variations required to maintain the constant rate of shear displacement. Under the given normal force (A = 340 lb.) contraction (B = 0.012 in.) takes place throughout the duration of the test and requires a slightly increasing shear force (C = 90 lb.) to continue the shearing process at the desired rate (D = 0.04 in./min.). Since the shear displacement varies linearly with time a shear force versus shear displacement plot would yield a trace identical in configuration to the shear force response as a function of time.

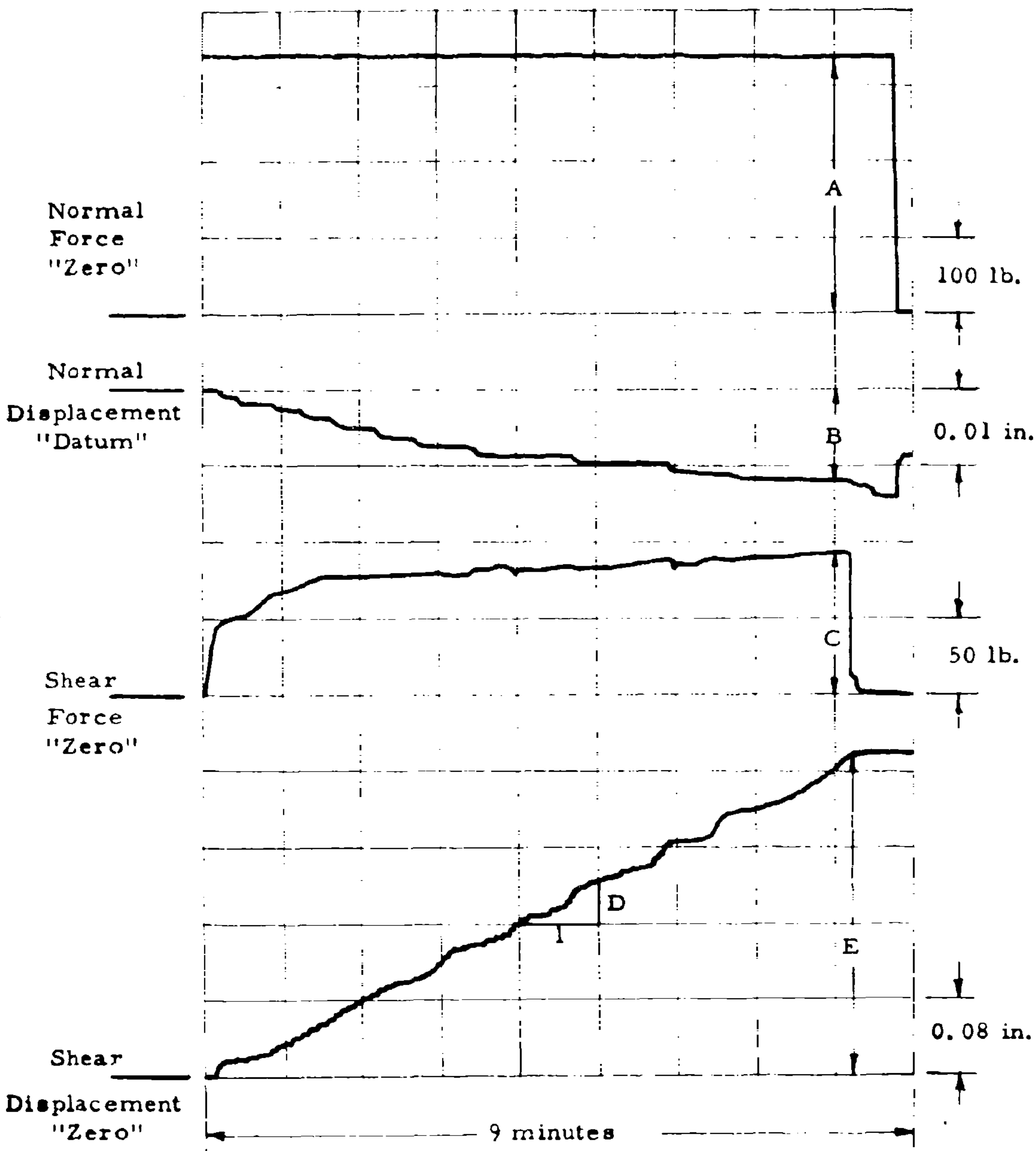

Figure II.20 Typical "Automatic Controlled Displacement" Test Results on Cohesive Soils

Prior to performing "automatic controlled displacement tests" it is necessary to establish a displacement range to guarantee that the maximum shear resistance of the soil has been attained. On the basis of the shear displacement at maximum shear resistance for both "dynamic" and "rapid static" tests, Figure II. 19, a maximum shear displacement of 0.3 in. would seem to be quite sufficient provided no contraction or consolidation takes place. The net displacement (E = 0.34 in.) of the reported test is apparently sufficiently large to satisfy the desired conditions.

APPENDIX II. REFERENCE

II. 1 Hough, B.K., Basic Soils Engineering, The Ronald Press Company, New York, 1957, p. 141.

APPENDIX III. GRAPHICAL ILLUSTRATION AND SUMMARY OF CONVENTIONAL DIRECT SHEAR TEST RESULTS

a. General.

Specific soil properties are presented in this appendix along with graphical illustrations of test results, tabular summaries of individual tests and sample preparation procedures.

Virtually all of the following test results were plotted on the same scale to exemplify the differences in apparent cohesive intercepts and friction angles for the variety of soils tested. In accordance with the previously described test procedures, the following notation has been consistently adopted throughout the test plots.

● "Dynamic" Tests (Time to maximum shear resistance ≈ 5 ms)

o "Rapid Static" Tests (Time to maximum shear resistance ≈ 40 sec)

× Automatic "Controlled Shear Displacement" Tests (Time to maximum shear resistance ≈ 8 min)

The tabular summaries (referenced to figures of the same number) of individual test results include the sample moisture content (w), dry density (γ_d), void ratio (e) and degree of saturation (S). The interpreted values of normal stress (σ_{ff}) and maximum shear stress (τ_m) are presented along with an indication of the direction of normal displacement, Δ_n (no displacement = 0, expansion = +, contraction = -, and no record = NR).

Sample preparation and placement procedures are described following the individual test results.

b. <u>ASTM C-190 Standard Ottawa Sand.</u>

Mineral	pure quartz
Specific Gravity	2.65
Grain Size	0.84 to 0.59 mm
Particle Shape	sub-rounded
Uniformity Coefficient	1.1
Maximum Void Ratio	0.80
Minimum Void Ratio	0.49

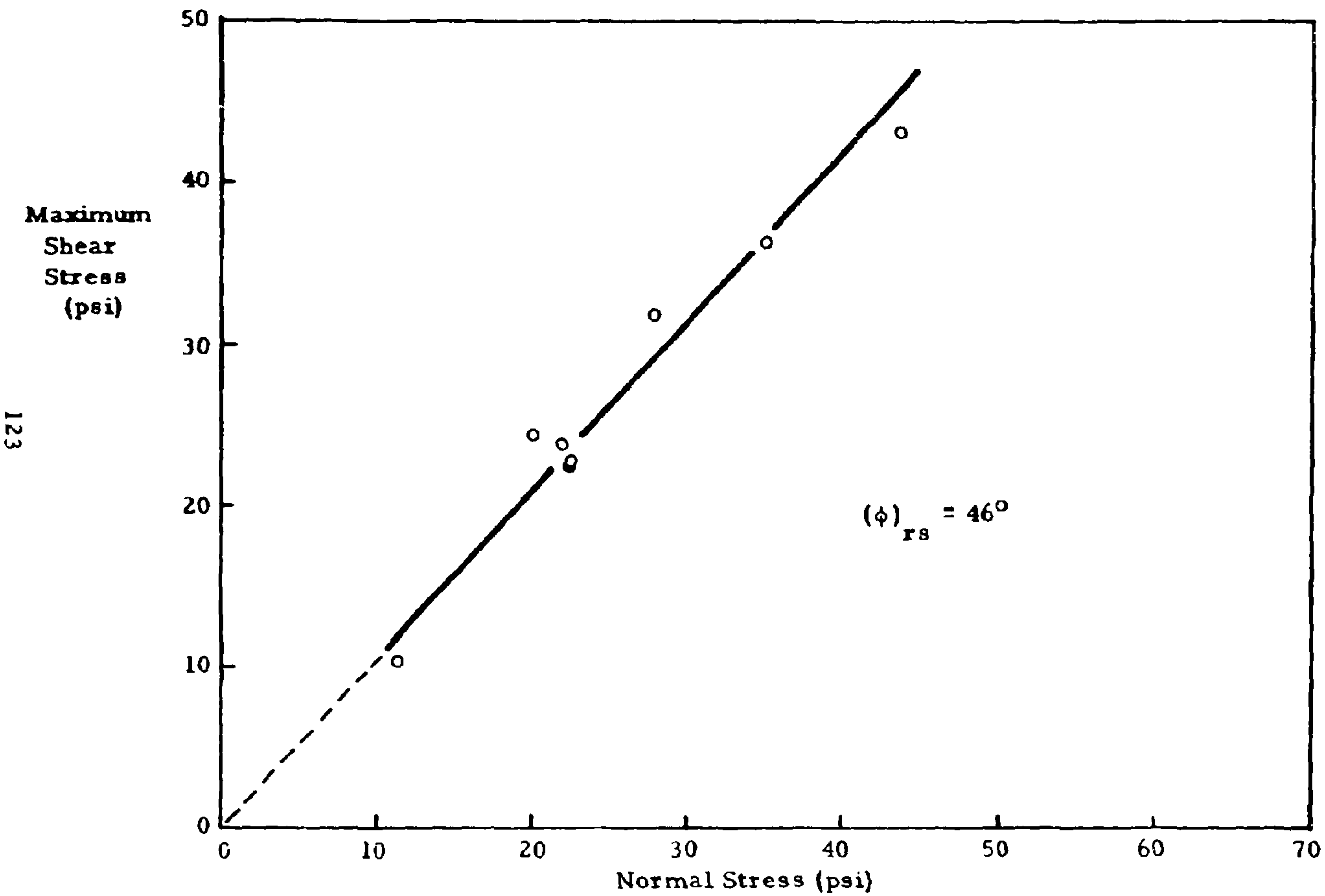

Figure III. 1 "Rapid Static" Failure Envelope for Dense Dry Ottawa Sand

Table III.1 Test Results: Dense Dry Ottawa Sand ("Rapid Static")

Test Type	w (%)	γ_d (pcf)	e	S (%)	σ_{ff} (psi)	τ_m (psi)	Δ_n
Rapid Static	0	≈107.4	≈0.536	0	22.3	22.7	NR
					27.9	31.9	NR
					35.0	36.2	NR
					43.8	43.0	NR
					22.3	22.3	+
					11.1	10.0	+
					21.9	23.9	+
					20.3	24.3	+

Sample Preparation: A known weight of dry sand (257 gm) was sprinkled through a funnel having a 3/8 inch spout. The funnel was rotated in a spiral motion around the shear box and about two inches above it. The upper gripper spacer was placed in position and the handle end of a screw-driver was used to vibrate the sand by tapping the gripper spacer. The sample thickness was measured with respect to the top of the shear box such that density computations could be made.

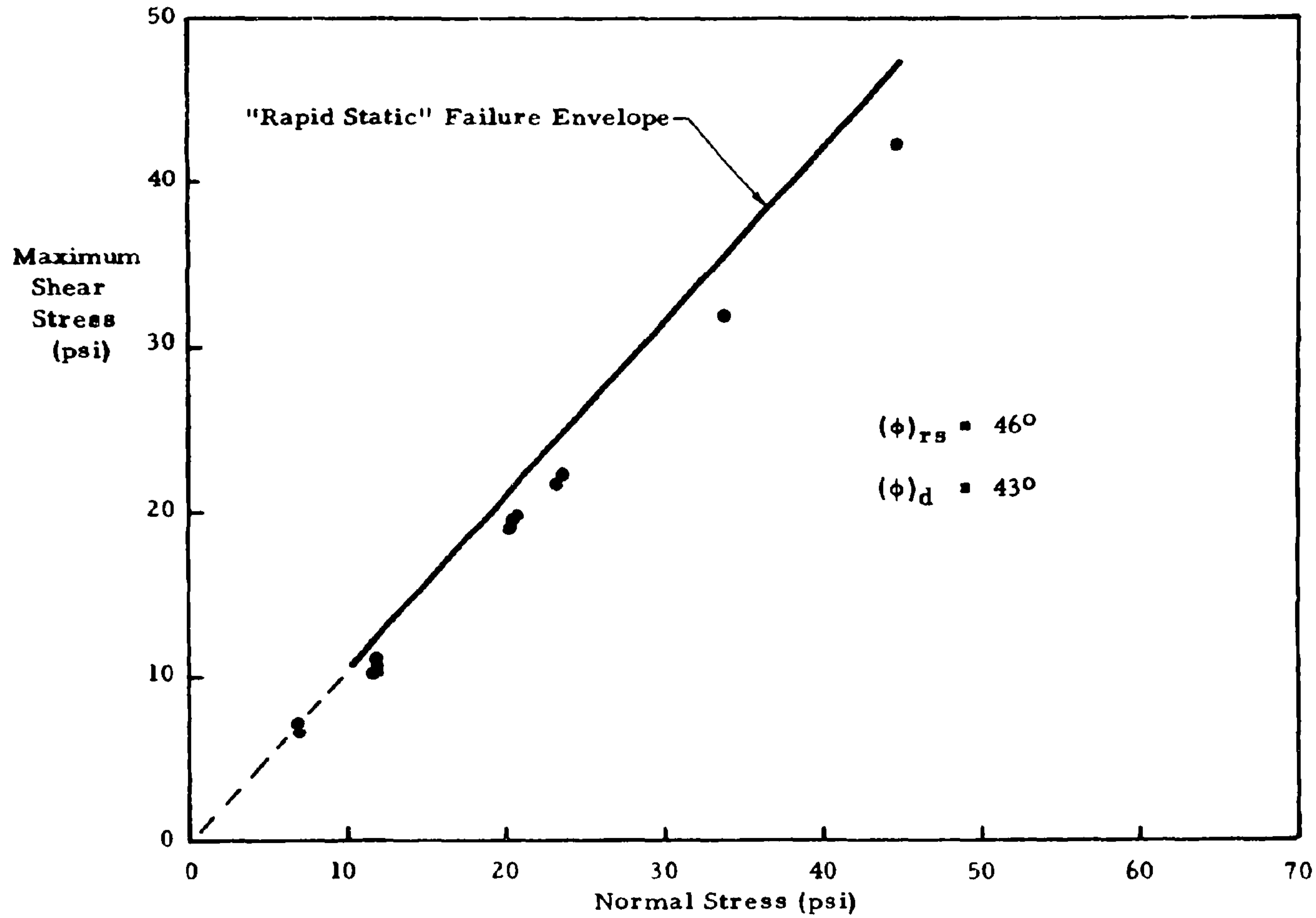

Figure III. 2 "Dynamic" Points Compared with "Rapid Static" Failure Envelope for Dense Dry Ottawa Sand

Table III.2 Test Results: Dense Dry Ottawa Sand ("Dynamic")

Test Type	w (%)	γ_d (pcf)	e	S (%)	σ_{ff} (psi)	τ_m (psi)	Δ_n
Dynamic	0	≈107.4	≈0.536	0	23.9	22.3	NR
					23.1	21.9	NR
					33.9	31.9	NR
					44.6	42.2	NR
					6.8	6.8	+
					6.8	7.2	+
					11.9	10.4	+
					10.9	10.8	+
					11.5	10.4	+
					11.9	11.1	+
					20.7	19.9	+
					20.3	19.1	+
					20.3	19.5	NR

<u>Sample Preparation:</u> See summary of Figure III.1 test results.

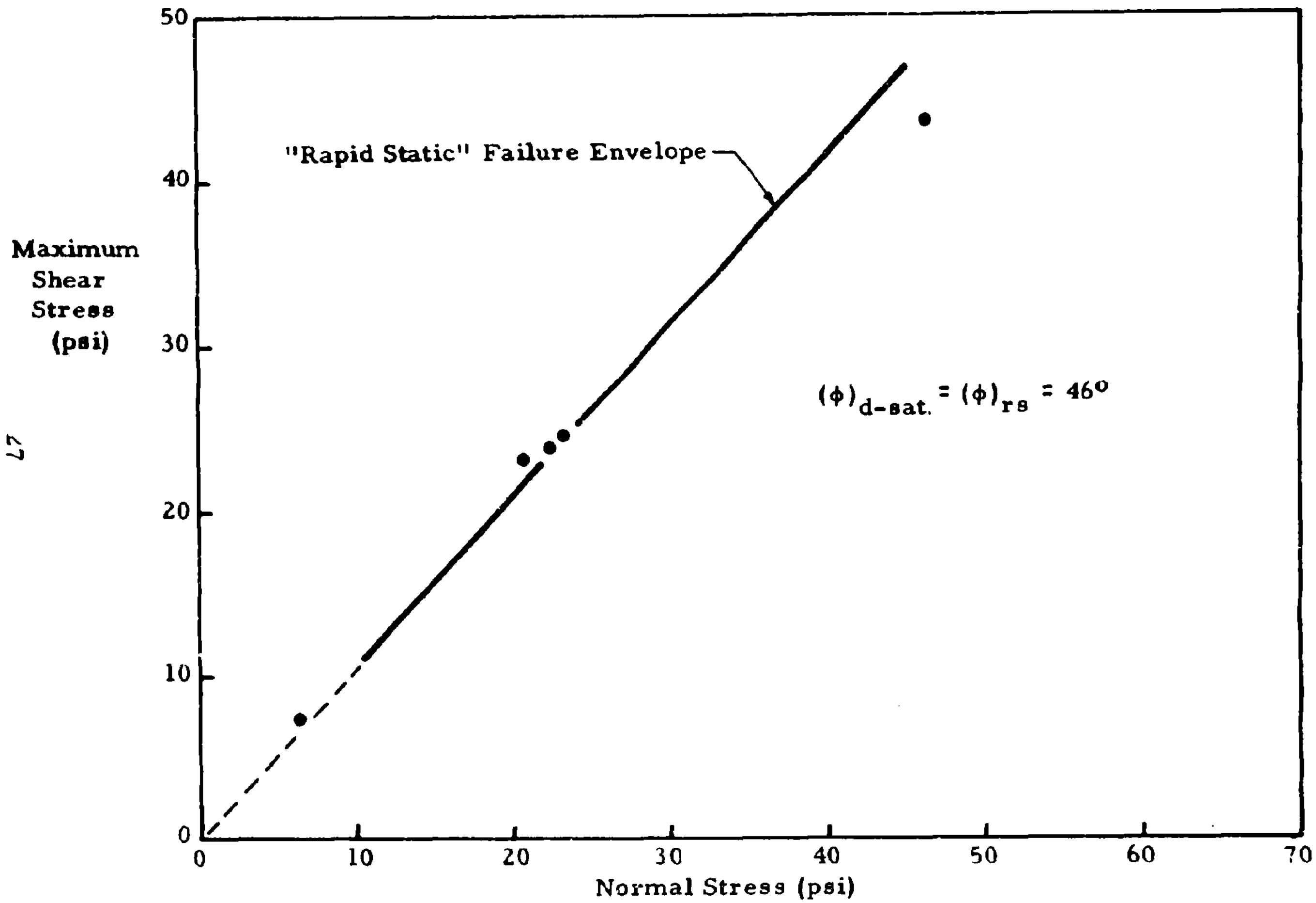

Figure III. 3 "Dynamic" Saturated Points Compared with "Rapid Static" Failure Envelope for Dense Dry Ottawa Sand

Table III.3 Test Results: Dense Saturated* Ottawa Sand ("Dynamic")

Test Type	w (%)	γ_d (pcf)	e	S (%)	σ_{ff} (psi)	τ_m (psi)	Δ_n
Dynamic	≈ 20.2	≈ 107.4	≈ 0.536	≈ 100	23.1	24.7	+
					22.3	23.9	+
					20.7	23.1	+
					6.4	7.2	+
					46.2	43.8	+

Sample preparation: Same as indicated in summary of Figure III.1 with the exception that 52 cc of water were added after vibration but prior to normal force application.

* The shear box drainage is unrestricted.

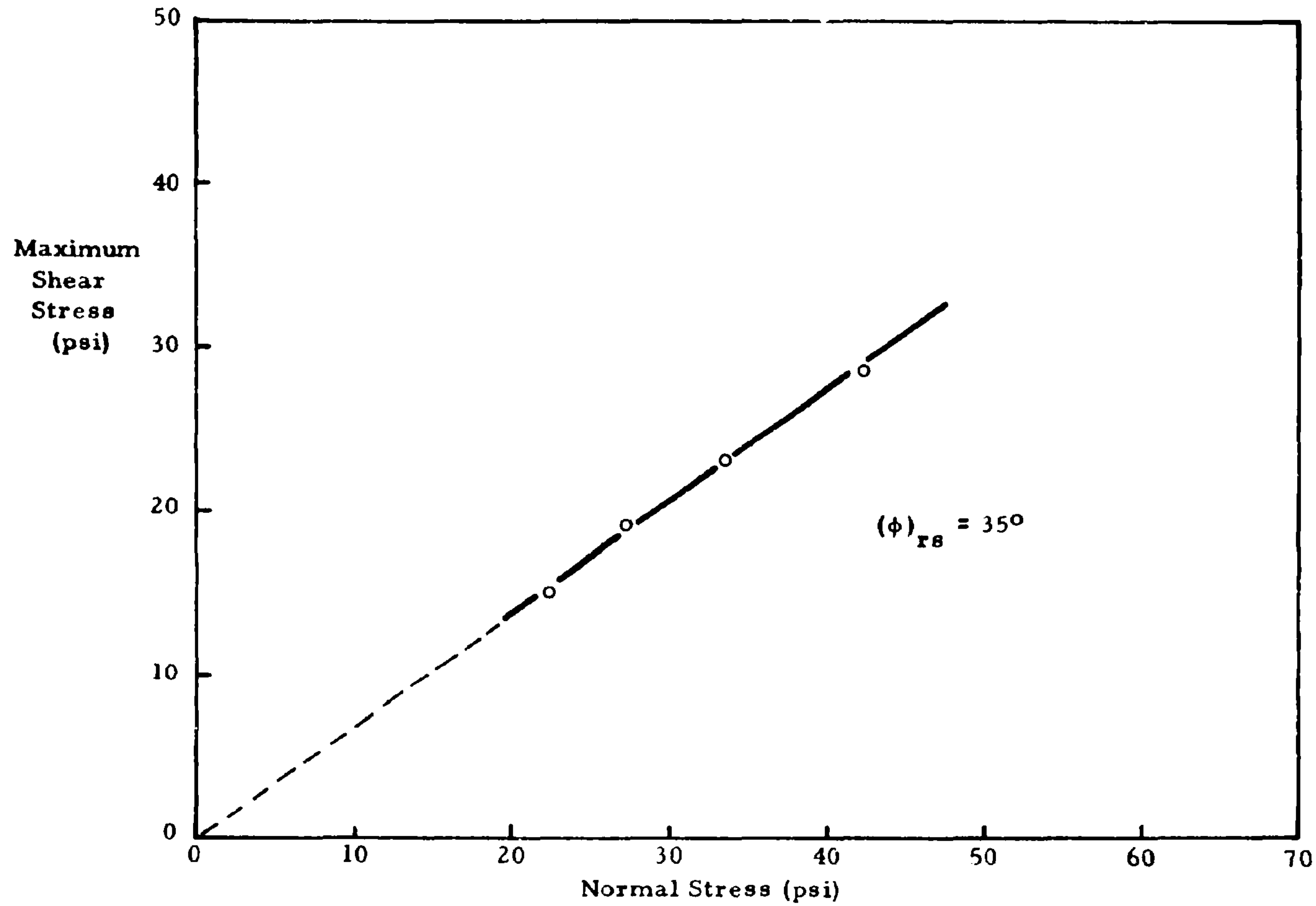

Figure III. 4 "Rapid Static" Failure Envelope for Loose Dry Ottawa Sand

Table III.4 Test Results: Loose Dry Ottawa Sand ("Rapid Static")

Test Type	w (%)	γ_d (pcf)	e	S (%)	σ_{ff} (psi)	τ_m (psi)	Δ_n
Rapid Static	0	≈ 98.1	≈ 0.69	0	22.3	15.1	NR
					27.1	19.1	NR
					33.5	23.1	NR
					42.2	28.7	NR

Sample Preparation: A cup containing 232 gm of sand was held very closely to the shear box and quickly turned over so that the cup with the sand in it was upside down within the shear box. The cup was then raised upwards, creating a loose sand pile. A screed was used to carefully level off the surface and then the sample thickness was determined.

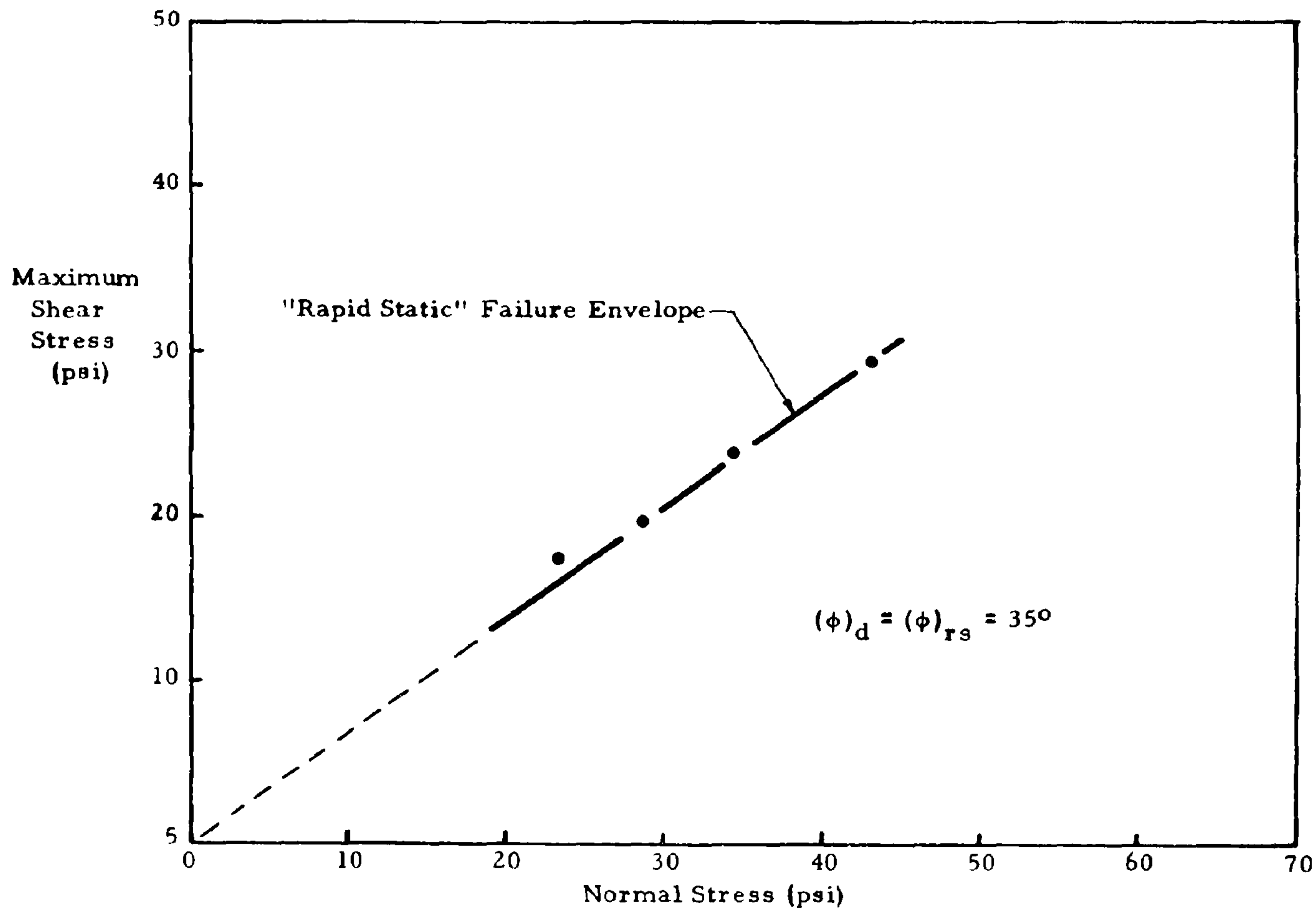

Figure III. 5 "Dynamic" Points Compared with "Rapid Static" Failure Envelope for Loose Dry Ottawa Sand

Table III.5 Test Results: Loose Dry Ottawa Sand ("Dynamic")

Test Type	w (%)	γ_d (pcf)	e	S (%)	σ_{ff} (psi)	τ_m (psi)	Δ_n
Dynamic	0	≈ 98.1	≈ 0.69	0	23.1	17.5	NR
					28.7	19.9	NR
					34.3	23.9	NR
					43.0	29.5	NR

Sample Preparation: See summary of Figure III.4 test results.

c. <u>Jordan Buff Clay.</u>

Soil Characteristics:

Liquid Limit	54.0	%
Plastic Limit	25.9	%
Plasticity Index	28.1	%
Shrinkage Limit	22.2	%
Specific Gravity	2.74	

Chemical Analysis:

Silica (S_iO_2)	67.19	%
Alumina (Al_2O_3)	20.23	%
Iron (Fe_2O_3)	1.73	%
Titania (T_iO_2)	1.18	%
Lime (C_aO)	0.16	%
Magnesia (M_gO)	0.52	%
Soda (Na_2O)	0.23	%
Potash (K_2O)	2.00	%
Ignition	6.89	%
Total	100.13	%
pH (Hydrogen Ion)	4.0	

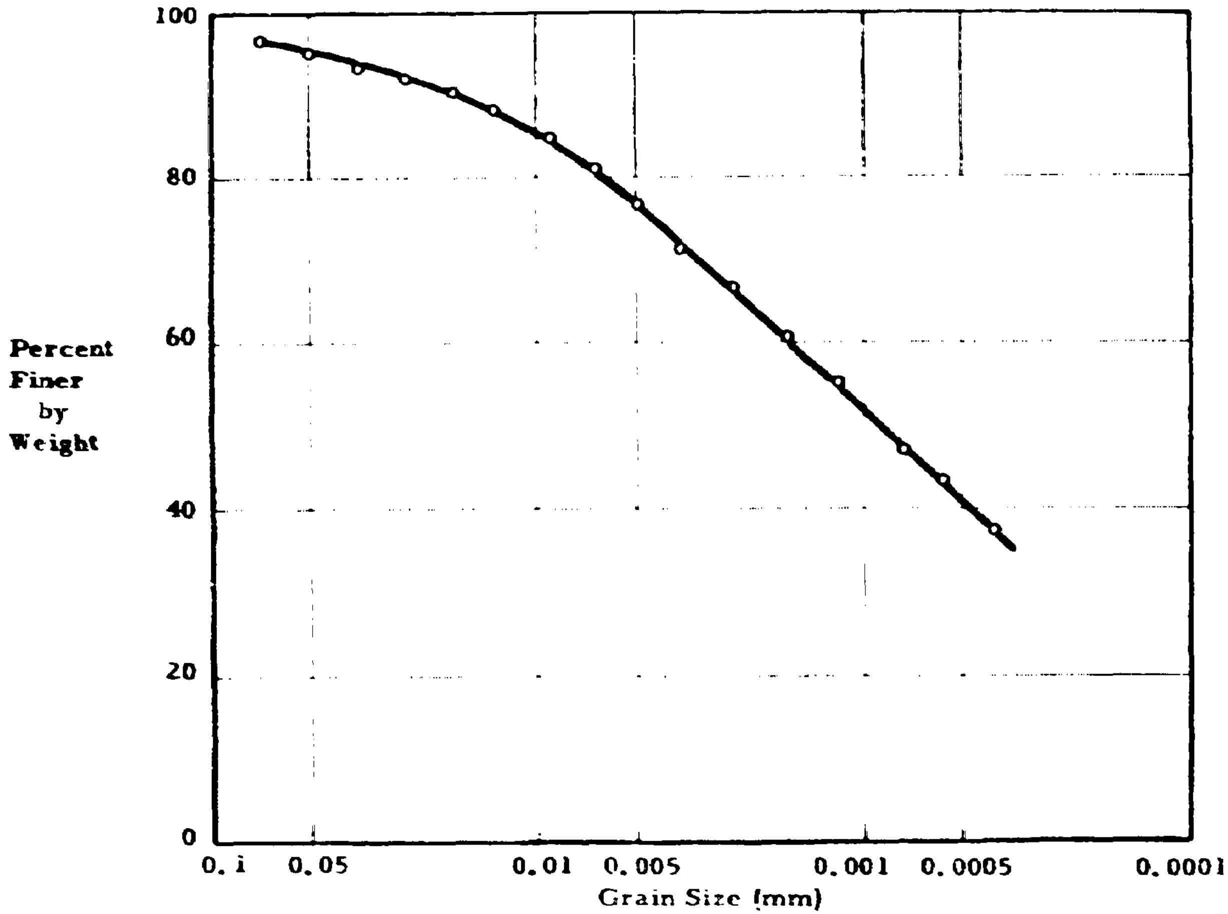

Figure III. 6 Grain Size Distribution Curve for Jordan Buff Clay

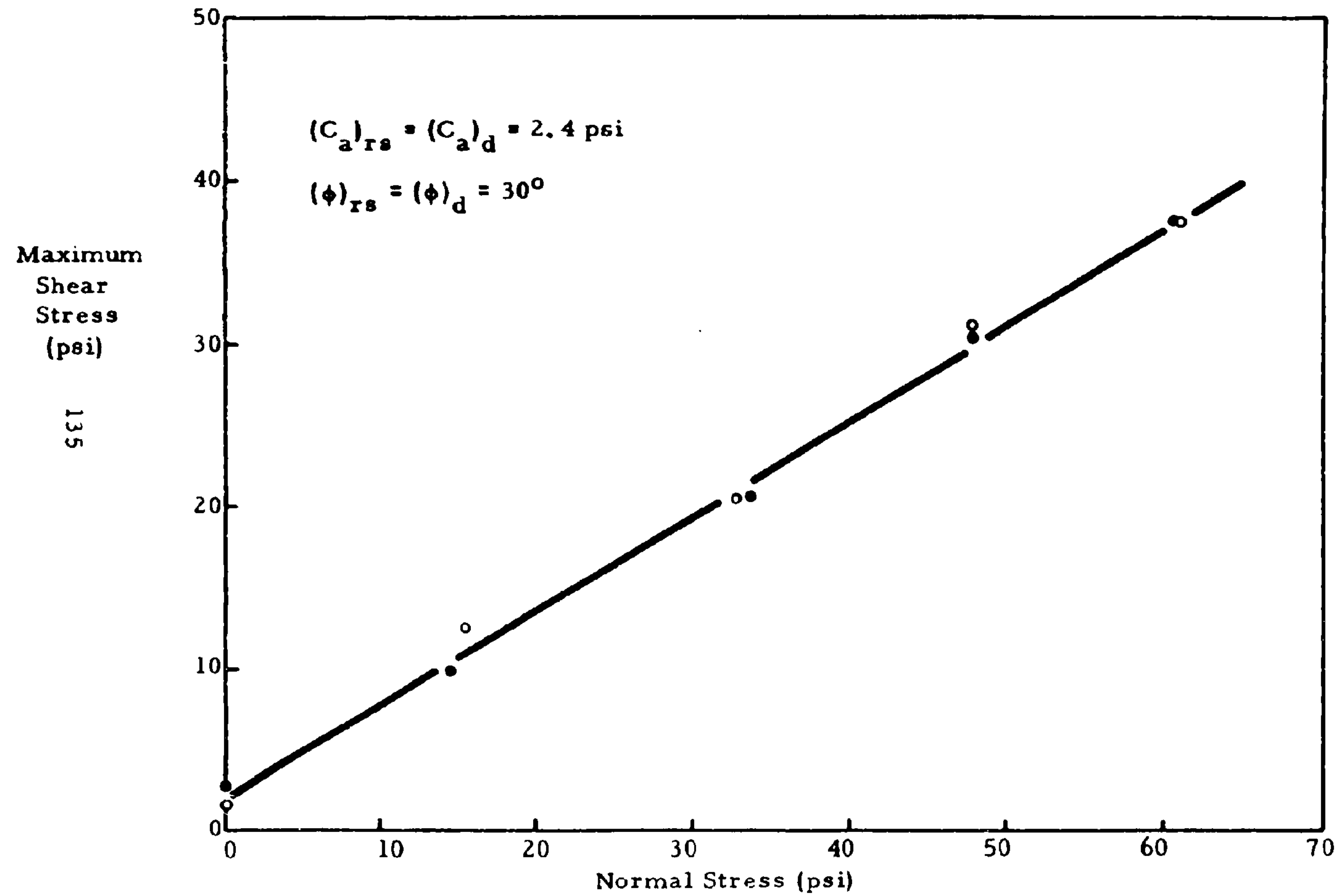

Figure III. 7 Failure Envelope for Air-dried Powdered Jordan Buff Clay: $w \approx 0\%$

Table III.7 Test Results: Jordan Buff Clay $w \approx 0\%$

Test Type	w (%)	γ_d (pcf)	e	S (%)	σ_{ff} (psi)	τ_m (psi)	Δ_n
Rapid Static	0	≈ 74.8	≈ 1.288	0	0	1.6	+
	↓	↓	↓	↓	60.9	37.4	–
					32.7	20.7	–
					15.1	12.7	–
					47.8	31.1	–
Dynamic	0	74.8	1.288	0	0	2.8	+
	↓	↓	↓	↓	14.3	10.0	0
					33.5	20.7	–
					47.8	30.3	–
					60.5	37.4	–

Sample preparation: 180.3 gm of air-dried powdered Jordan Buff clay were placed in the direct shear box and consolidated at a pressure of approximately 50 psi prior to testing.

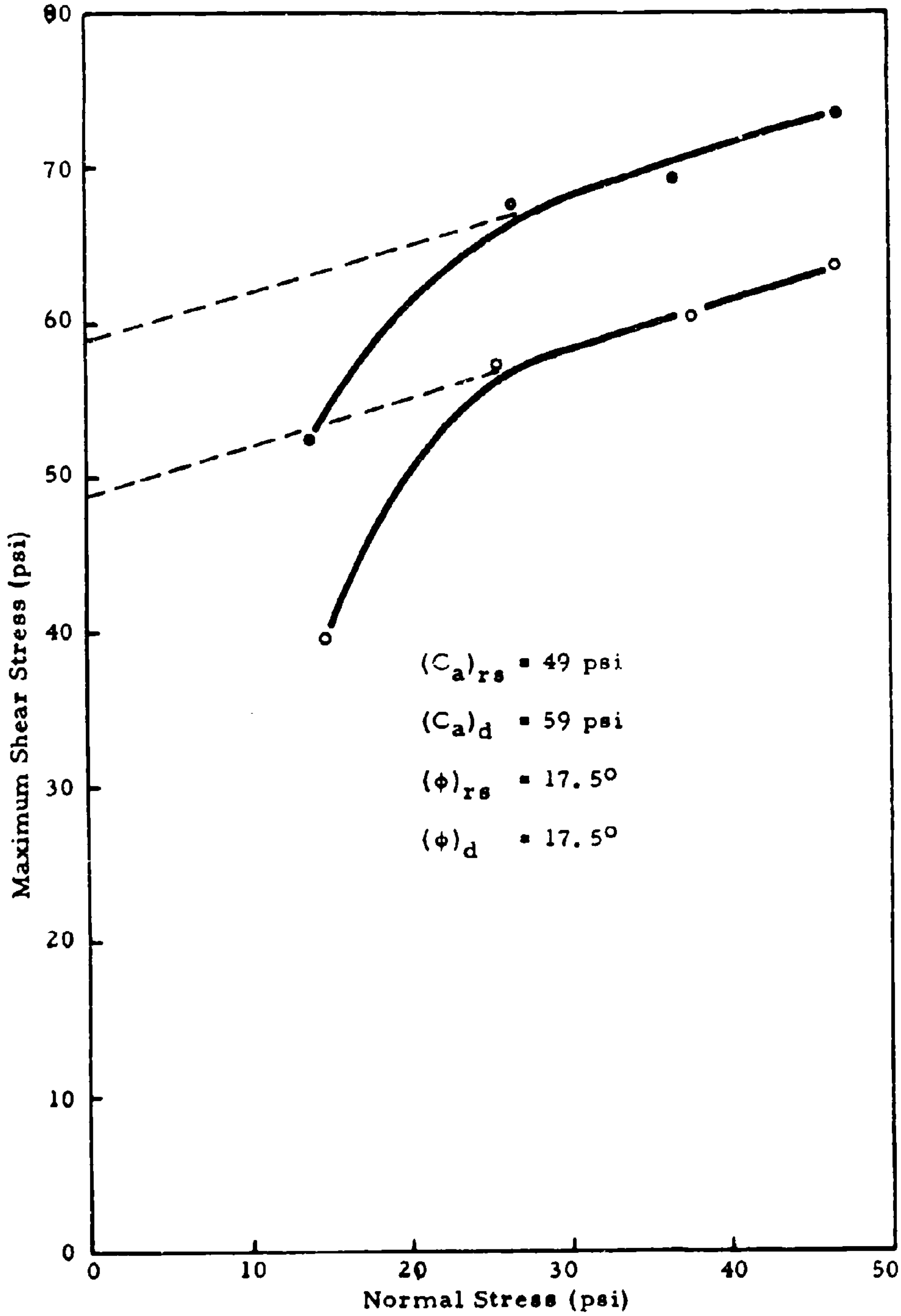

Figure III. 8 Failure Envelopes for Jordan Buff Clay: w ≈ 10%

Table III.8 Test Results: Jordan Buff Clay $w \approx 10\%$

Test Type	w (%)	γ_d (pcf)	e	S (%)	σ_{ff} (psi)	τ_m (psi)	Δ_n
Rapid Static	10.7	95.4	.793	36.0	25.5	57.4	+
	10.2	97.7	.748	38.2	46.6	63.7	+
	9.8	94.9	.799	32.8	14.7	39.8	+
	8.1	96.9	.764	29.6	37.8	60.5	+
Dynamic	10.6	96.2	.777	36.6	26.3	67.9	+
	9.7	94.9	.799	33.2	46.6	73.3	NR
	9.5	94.7	.802	32.4	13.9	52.6	+
	9.5	95.9	.783	33.2	36.6	69.3	0
Average	9.8	95.8	.783	34.0			

Sample Preparation: A batch of air-dried Jordan Buff clay was mixed and passed through a meat grinder at a moisture content of 11%. 270 gm of the material were placed in the shear box and compacted with 21 blows of a standard proctor hammer. This compaction energy is "equal" to the energy applied to the individual test samples obtained from the modified standard proctor compaction described in the summary following Figure III.9. The upper gripper spacer was then seated at a pressure of 80 psi until the normal displacement is less than 0.001 in/min.

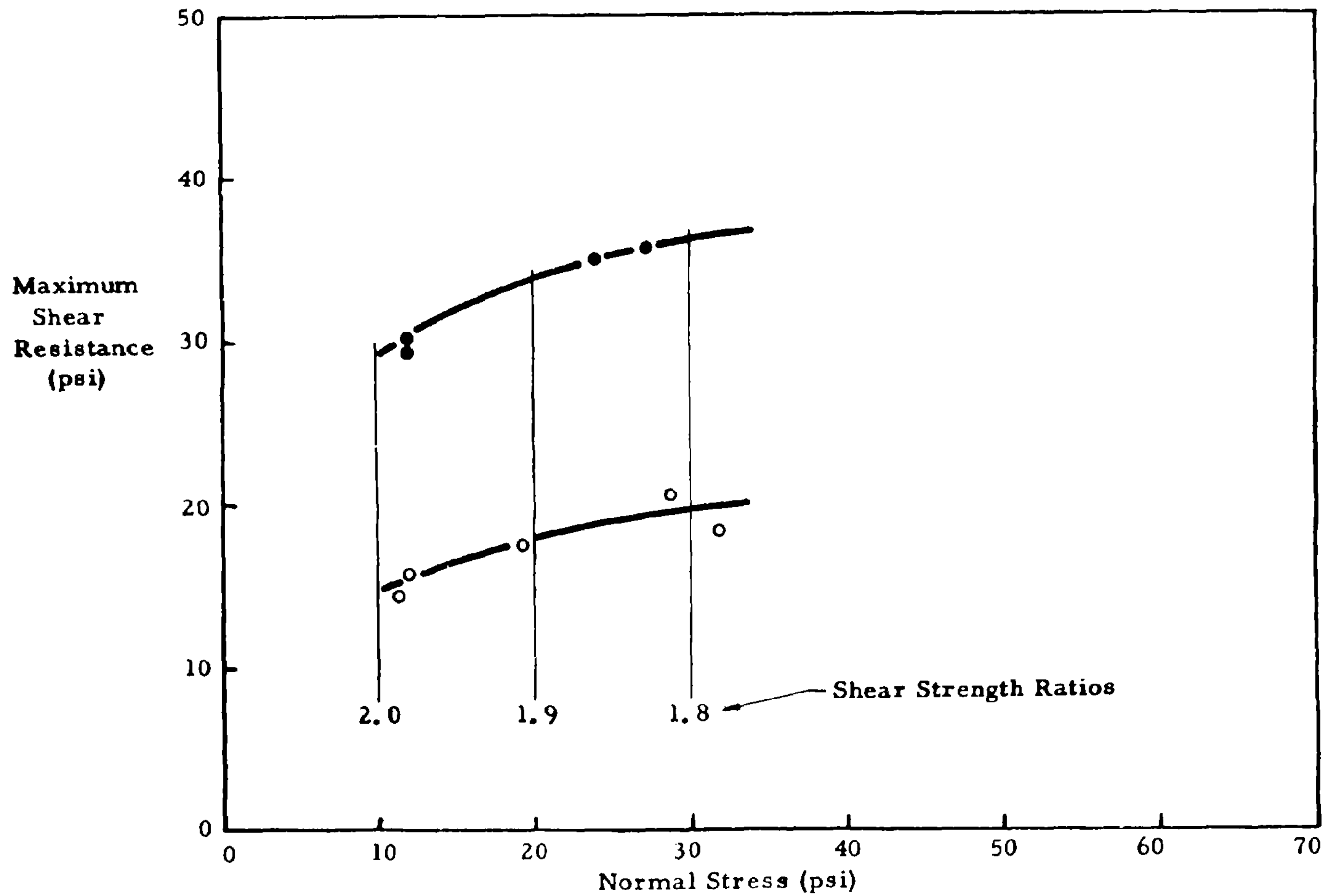

Figure III. 9 Failure Envelopes for Jordan Buff Clay: w≈ 20%

Table III.9 Test Results: Jordan Buff Clay $w \approx 20\%$

Test Type	w (%)	γ_d (pcf)	e	S (%)	σ_{ff} (psi)	τ_m (psi)	Δ_n
Rapid Static	21.0	104.4	.636	90.5	11.9	15.9	NR
	21.3	104.1	.642	91.0	19.1	17.5	↓
	20.9	104.6	.635	90.0	31.9	18.3	↓
	19.9	105.7	.619	88.1	11.1	14.3	↓
	20.1	105.2	.624	88.8	28.7	20.7	↓
Dynamic	21.0	104.4	.636	90.5	11.9	30.3	NR
	21.2	104.2	.640	90.7	23.9	35.0	↓
	21.0	104.4	.636	90.5	27.1	35.8	↓
	19.8	105.8	.598	88.0	11.9	29.5	↓
Average	20.7	104.8	.630	89.8			

Sample Preparation: The soil was mixed and compacted in the following manner. The dry soil was weighed and placed in a large pan. The correct amount of water needed to obtain the desired water content was placed in a bottle with a sprinkler head. The water was added slowly and mixed continuously. When all of the material was wet and had formed into balls it was kneaded to create uniform moisture distribution. The sample was then extruded through a meat grinder yielding spaghetti-like soil aggregates.

Table III.9 Test Results: Jordan Buff Clay $w \approx 20\%$ (continued)

When the entire sample had been extruded, the small soil chunks were mixed by hand. The material was placed in the standard proctor mold in five lifts and compacted using a 5.5 pound proctor hammer dropped 12 inches, 25 times per lift. A cheese cutter was used to cut 3/4 inch thick samples from the cylinder of soil for placement in the shear box.

With the loading head in position a sufficiently large vertical pressure was applied to seat the upper gripper spacer teeth in the soil sample.

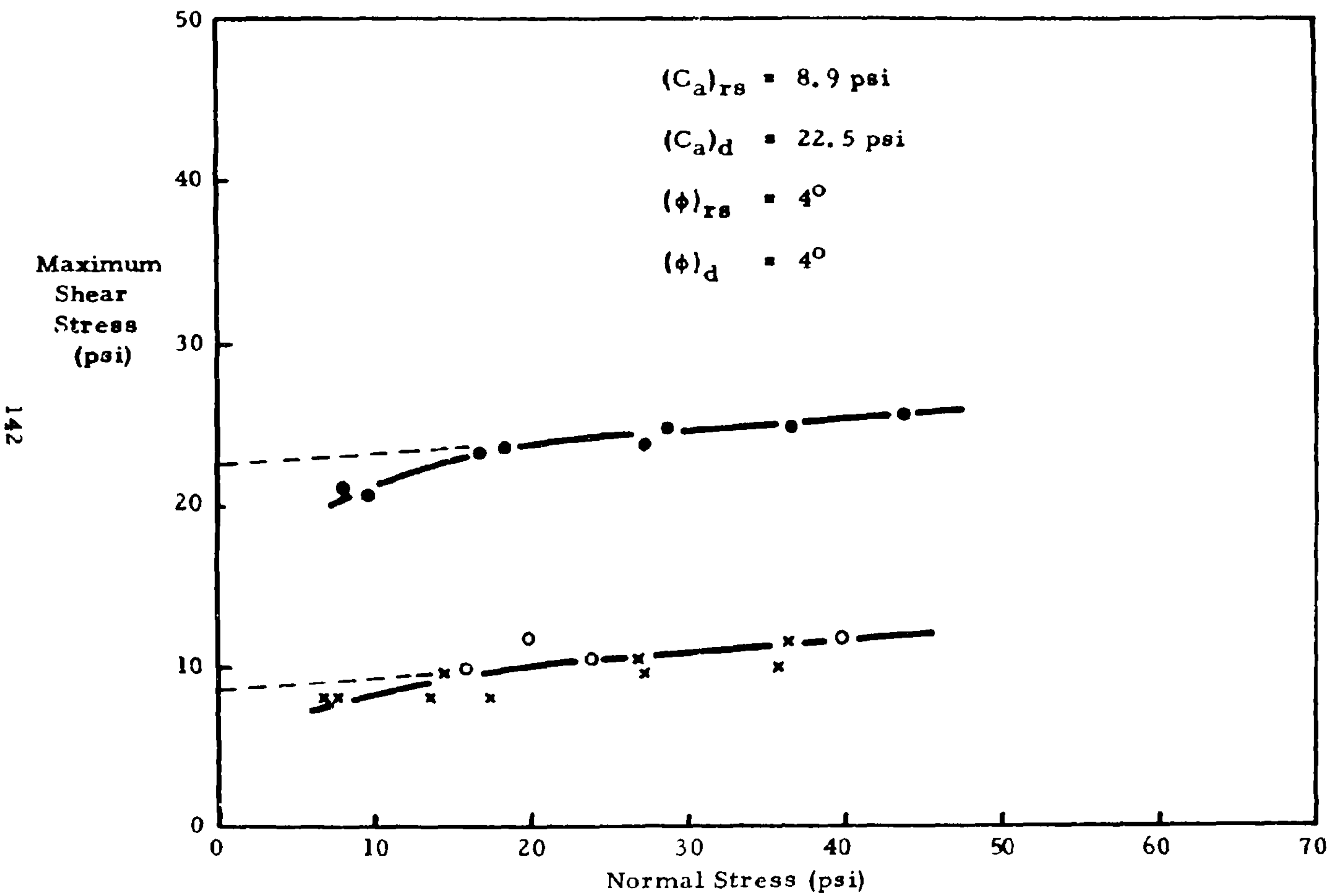

Figure III. 10 Failure Envelopes for Jordan Buff Clay: $w \approx 25\%$

Table III.10 Test Results: Jordan Buff Clay $w \approx 25\%$

Test Type	w (%)	γ_d (pcf)	e	S (%)	σ_{ff} (psi)	τ_m (psi)	Δ_n	Rate of Shear Disp. (in/min)
Automatic Controlled Rate of Shear Displacement	24.5	97.6	.751	89.2	14.3	9.6	-	0.032
	25.2	98.2	.743	93.4	7.6	8.0	0	0.032
	25.9	97.7	.751	94.8	17.1	8.0	-	0.014
	24.6	98.8	.731	92.3	26.7	10.4	-	0.024
	24.5	98.8	.731	92.0	36.2	11.5	-	0.020
	24.8	97.6	.751	90.3	6.8	8.0	0	0.031
	24.6	97.7	.751	89.9	13.5	8.0	-	0.033
	24.3	97.9	.748	89.3	27.1	9.6	-	0.022
	24.4	97.8	.750	89.5	35.8	10.0	-	0.016
Rapid Static	24.2	99.0	.728	91.4	39.8	11.9	NR	
	24.0	99.2	.724	91.1	19.9	11.9	NR	
	23.6	99.3	.722	89.6	23.9	10.4	0	
	24.9	97.5	.755	90.4	15.9	10.0	NR	
Dynamic	25.3	96.9	.767	90.7	9.6	20.7	0	
	25.1	97.0	.764	90.3	43.8	25.5	0	
	24.7	97.5	.755	89.5	16.7	23.1	0	
	24.1	97.9	.748	88.4	28.7	24.[illegible]	0	
	24.4	98.5	.736	91.2	8.0	2[illegible]	[illegible]	
	24.1	98.8	.731	90.6	18.3	2[illegible]	[illegible]	
	24.0	98.9	.728	90.5	27.1	23.[illegible]	0	
	24.0	98.9	.728	90.5	36.6	24.7	0	

Table III.10 Test Results: Jordan Buff Clay $w \approx 25\%$ (continued)

Test Type	w (%)	γ_d (pcf)	e	S (%)
Average	24.5	98.2	.743	90.7

<u>Sample preparation</u>: See summary of Figure III.9 test results.

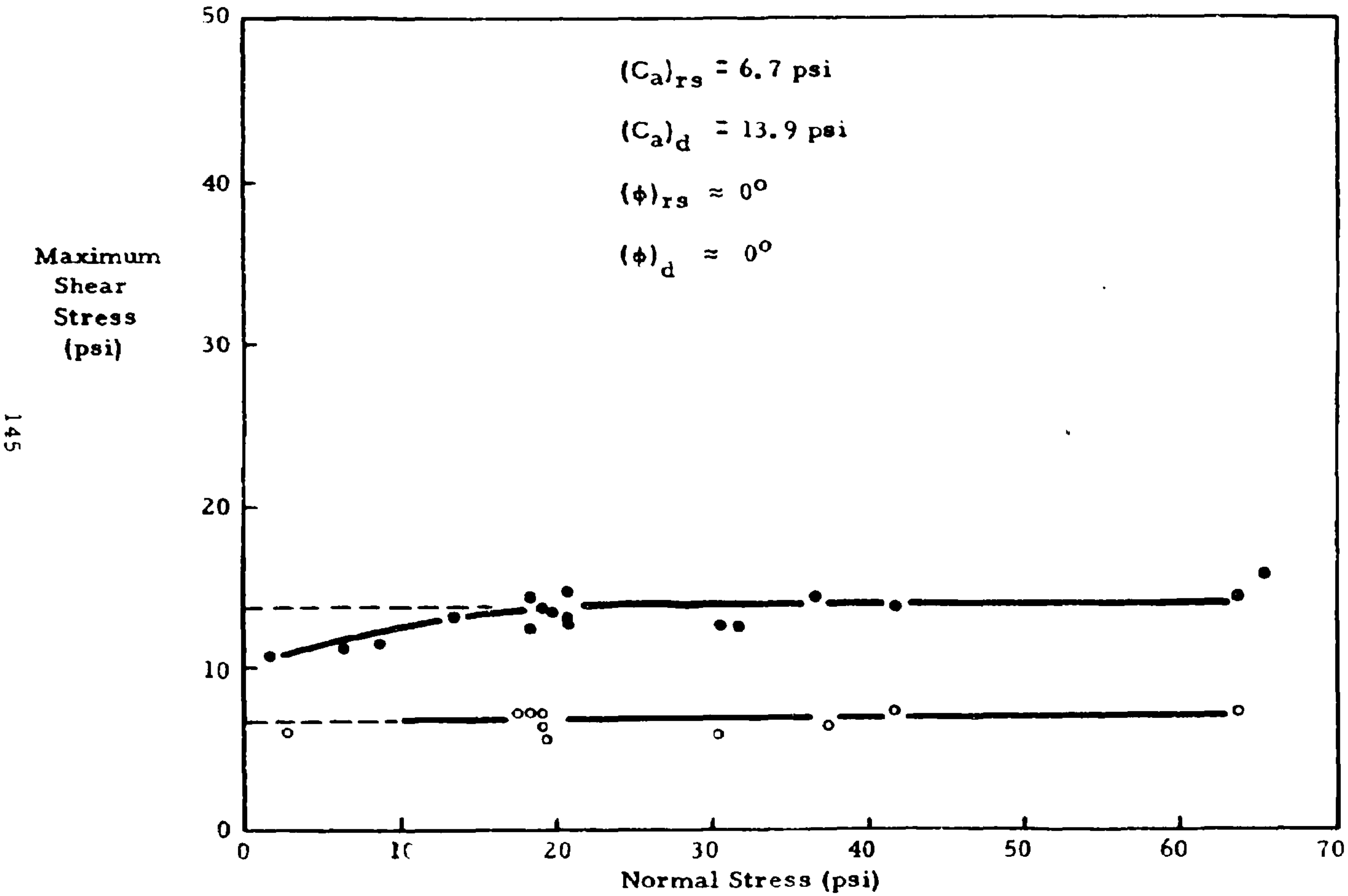

Figure III. 11 Failure Envelopes for Jordan Buff Clay: $w \approx 30\%$

Table III.11 Test Results: Jordan Buff Clay $w \approx 30\%$

Test Type	w (%)	γ_d (pcf)	e	S (%)	σ_{ff} (psi)	τ_m (psi)	Δ_n
Rapid Static	30.4	87.9	.946	86.1	19.1	6.4	NR
	29.6	88.4	.936	87.0	19.1	7.2	NR
	30.0	88.1	.942	87.6	2.8	6.0	NR
	30.5	87.1	.965	86.8	17.5	7.2	NR
	31.4	86.5	.977	88.0	41.8	7.6	NR
	30.6	87.7	.949	88.6	63.7	7.2	NR
	30.0	87.7	.950	86.5	18.3	7.2	NR
	29.6	88.6	.931	87.3	37.4	6.4	0
	29.6	88.6	.931	87.3	19.5	5.6	–
	28.2	90.7	.885	87.5	30.3	6.0	–
Dynamic	29.2	90.0	.901	89.2	8.8	11.5	0
	29.0	90.1	.901	88.9	18.3	12.0	0
	28.8	90.3	.895	88.4	30.3	12.7	0
	30.1	88.2	.939	88.1	20.7	12.7	NR
	30.1	88.2	.939	88.1	31.9	12.7	NR
	28.4	89.2	.920	85.0	20.7	13.1	NR
	30.0	88.1	.942	87.6	19.1	13.9	NR
	31.5	86.4	.981	88.2	41.8	13.9	NR
	31.2	86.5	.977	87.8	1.6	10.8	NR
	32.0	86.9	.970	90.6	63.7	14.3	NR

Table III.11 Test Results: Jordan Buff Clay $w \approx 30\%$ (continued)

Test Type	w (%)	γ_d (pcf)	e	S (%)	σ_{ff} (psi)	τ_m (psi)	Δ_n
Dynamic	31.8	86.6	.974	89.3	19.9	13.5	NR
	31.2	86.8	.970	88.5	20.7	14.7	NR
	30.8	87.2	.961	87.8	18.3	14.3	NR
	30.2	87.8	.949	87.6	36.6	14.3	NR
	30.0	88.0	.944	87.5	13.5	13.1	0
	31.3	87.2	.961	89.5	65.3	15.9	NR
	31.2	87.3	.961	89.4	6.4	11.1	NR
Average	30.2	88.0	.944	88.0			

Sample preparation: See summary of Figure III.9 test results.

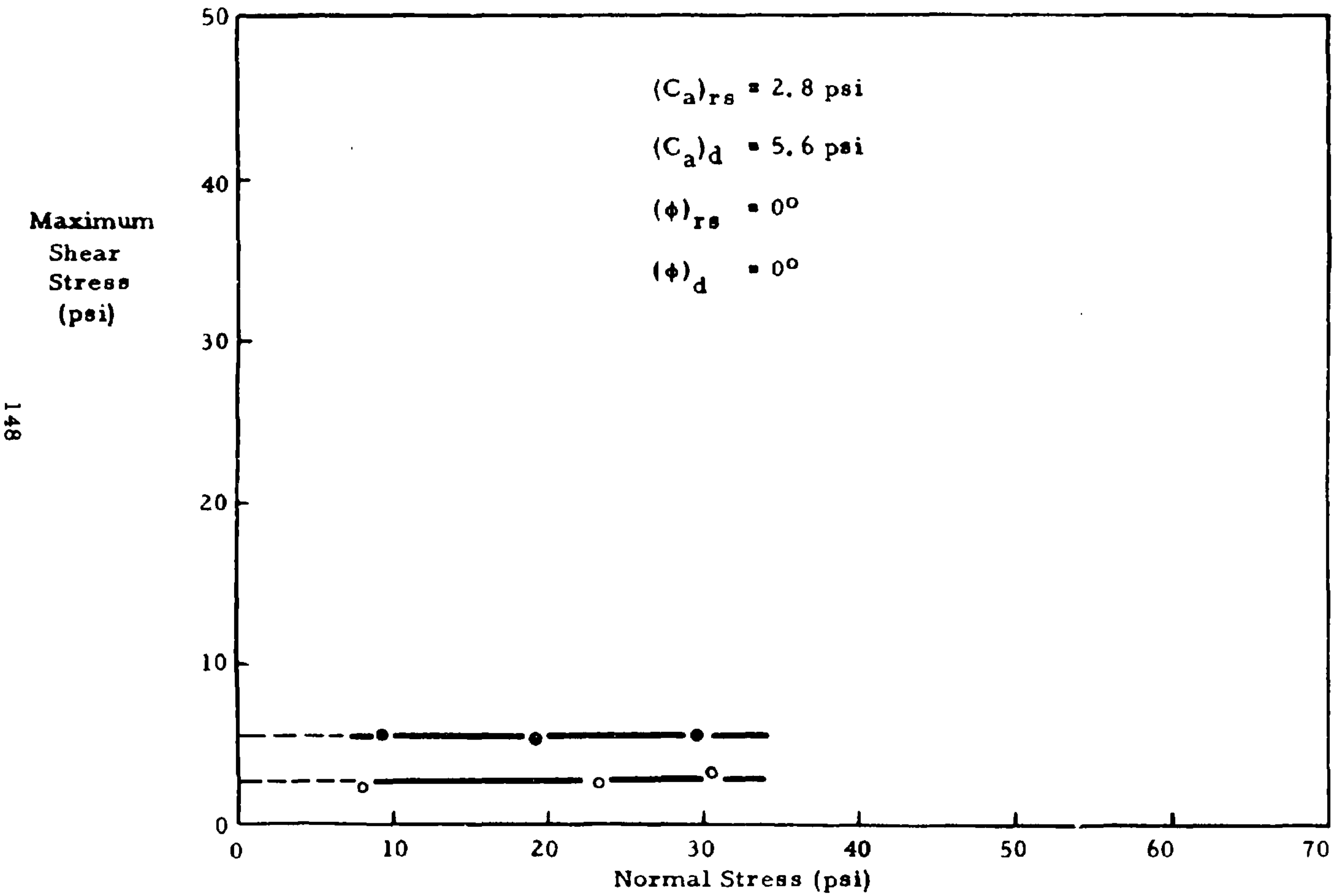

Figure III. 12 Failure Envelopes for Jordan Buff Clay: w ≈ 34%

Table III.12 Test Results: Jordan Buff Clay $w \approx 34\%$

Test Type	w (%)	γ_d (pcf)	e	S (%)	σ_{ff} (psi)	τ_m (psi)	Δ_n
Rapid Static	33.2	83.2	1.055	86.6	8.0	2.4	NR
	32.5	83.8	1.040	85.8	30.7	3.2	NR
	33.7	83.1	1.058	87.3	23.1	2.8	NR
Dynamic	33.9	83.0	1.059	87.6	9.2	5.6	NR
	34.8	82.5	1.071	88.9	29.5	5.6	NR
	34.2	82.6	1.070	88.0	19.1	5.2	NR
Average	33.7	83.0	1.059	87.4			

Sample preparation: See summary of Figure III.9 test results.

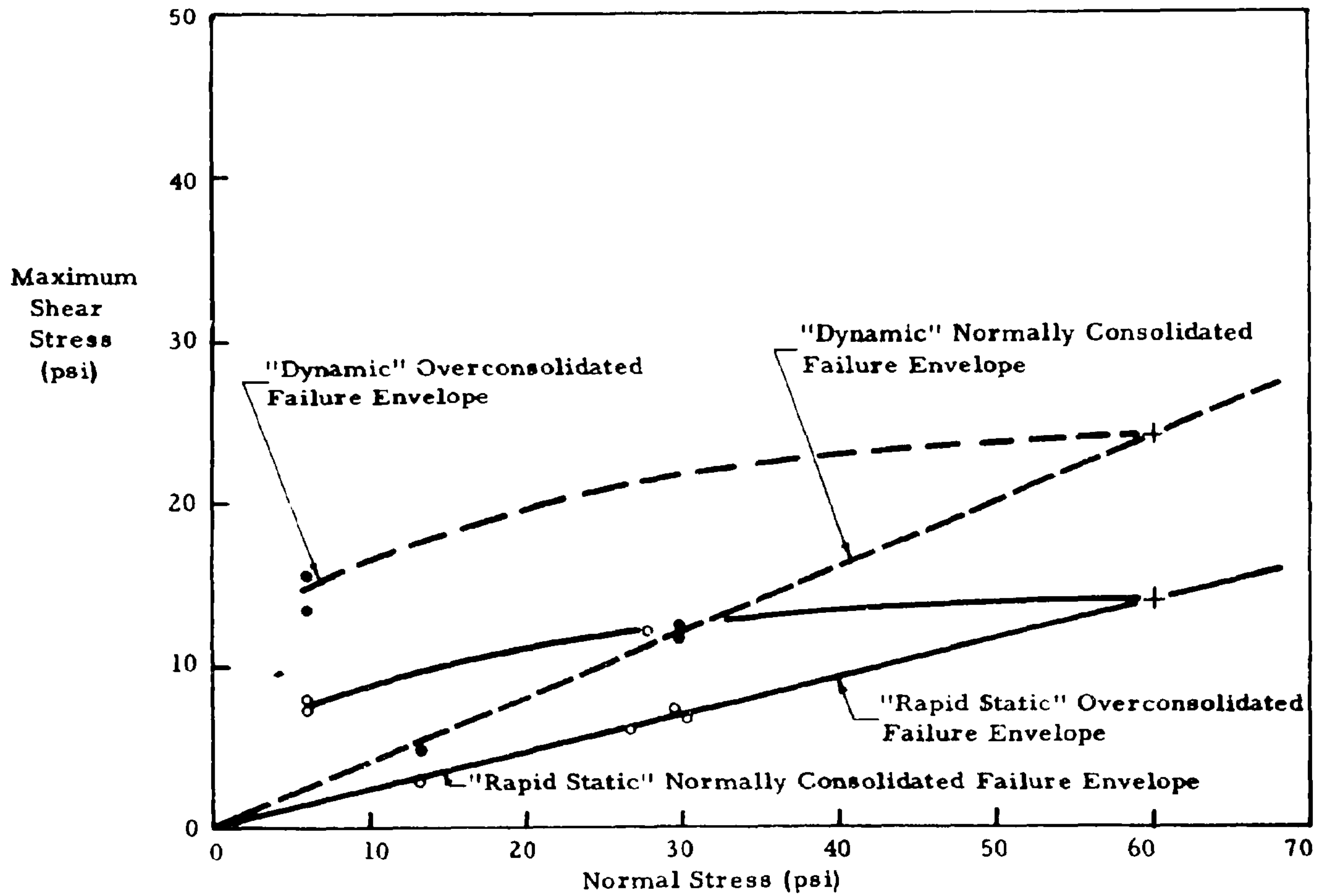

Figure III. 13 Normally Consolidated and Overconsolidated Jordan Buff Clay Test Results

Table III.13a Consolidation Test Results on Jordan Buff Clay

Test Type	w (%)	γ_d (pcf)	e	S (%)	NC (psi)	σ_{ff} (psi)	OCR
Dynamic	48.2	73.9	1.321	100	13.5	13.1	1
Rapid Static	46.3	76.6	1.267	100	13.5	13.1	1
Rapid Static	34.3	88.5	.940	100	26.7	26.7	1
Dynamic	34.5	88.1	.945	100	30.0	29.9	1
Rapid Static	35.2	87.3	.965	100	30.0	30.3	1
Dynamic	35.8	86.4	.982	100	30.0	29.9	1
Rapid Static	35.9	86.4	.983	100	30.0	29.5	1
Rapid Static	32.3	90.8	.886	100	60.0	27.9	2
Rapid Static	34.3	88.3	.938	100	60.0	6.0	10
Dynamic	34.1	88.6	.936	100	60.0	6.0	10
Rapid Static	35.0	87.4	.961	100	60.0	6.0	10
Dynamic	34.3	88.4	.940	100	60.0	6.0	10

Sample preparation: Known weights of dry powdered soil and distilled water were mixed into a slurry having a moisture content of approximately 100%. This mixture was then placed in the consolidomiter (4.3 inch diameter) after which standard consolidation test procedures were utilized to establish the desired normally consolidated or overconsolidated loading conditions.

Table III.13b Test Results: Consolidated Jordan Buff Clay

Test Type	w (%)	γ_d (pcf)	e	S (%)	σ_{ff} (psi)	τ_m (psi)	Δ_n
Dynamic		(quantities below computed			13.1	4.8	-
Rapid Static		from external measurements			13.1	2.8	-
		of shear box after the					
Rapid Static		sample has been placed)			26.7	6.0	0
Dynamic	35.0	87.5	.958	100	29.9	11.5	0
Rapid Static	36.8	85.4	1.002	100	30.3	6.6	0
Dynamic	35.8	86.4	.980	100	29.9	12.3	-
Rapid Static	36.4	86.5	.977	100	29.5	7.2	-
Rapid Static					27.9	12.0	-
Rapid Static	34.4	85.5	1.000	100	6.0	7.2	-
Dynamic	34.3	88.8	.923	100	6.0	13.5	0
Rapid Static					6.0	8.0	-
Dynamic					6.0	15.5	+

Sample preparation: After having removed the sample from the consolidometer a slight impression was made on the surface using the 4 inch diameter trimming ring. The sample was then trimmed slightly oversize with a wire requiring an easy force fit in the shear box. The desired normal pressure (last consolidation pressure) was then established and maintained until the rate of normal displacement was much less than 0.001 in/min (approximately 10 min).

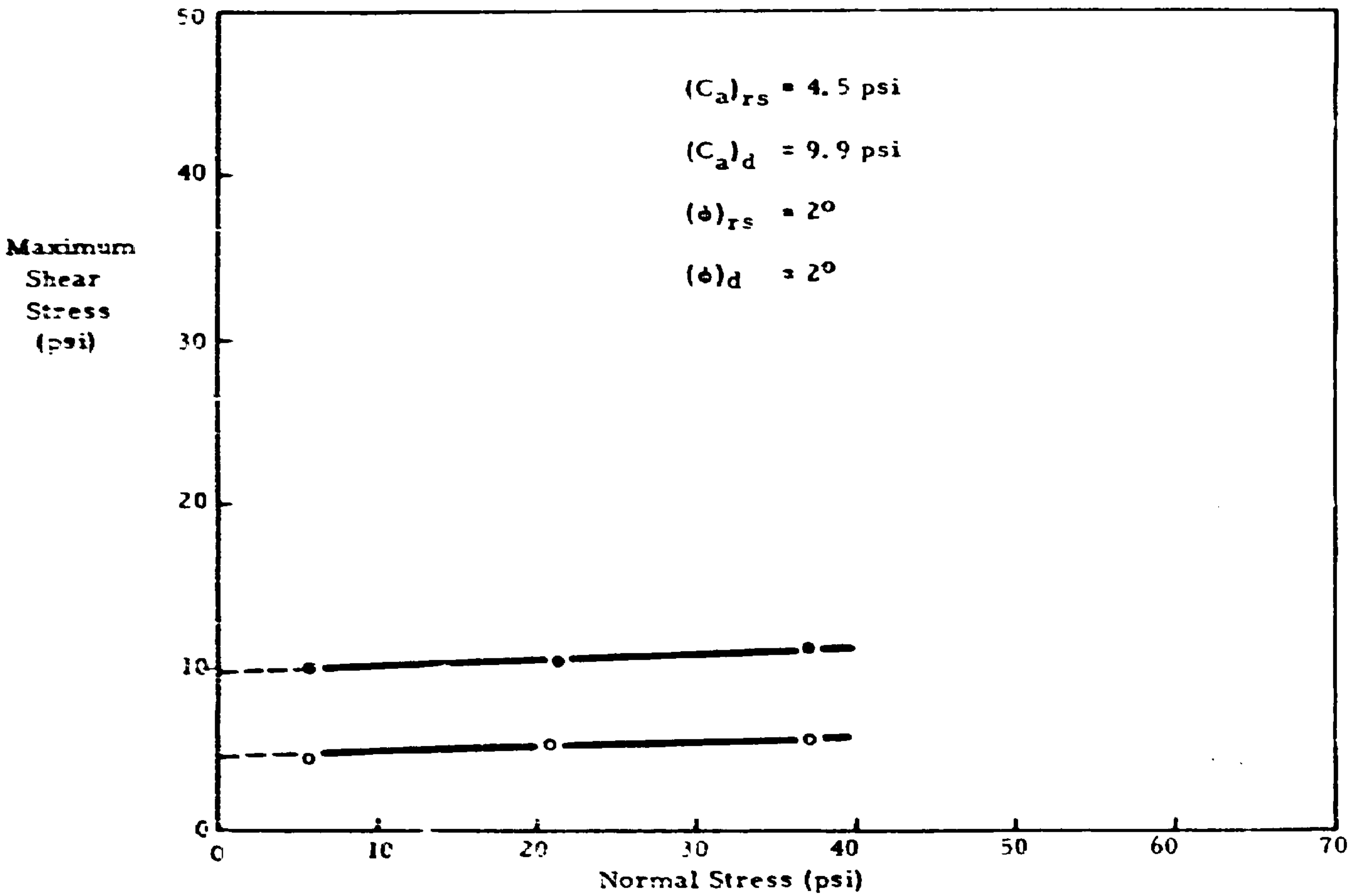

Figure III. 14 Failure Envelopes for Jordan Buff Clay + Salt Water: w ≈ 30%

Table III.14 Test Results: Jordan Buff Clay + Salt Water

Test Type	w (%)	γ_d (pcf)	e	S (%)	σ_{ff} (psi)	τ_n (psi)	Δ_n
Rapid Static	30.4	89.7	.905	92.0	5.6	4.4	NR
	30.1	89.4	.914	89.9	20.7	5.2	NR
	30.0	90.4	.895	91.9	37.0	5.6	NR
Dynamic	29.8	89.1	.919	88.2	5.6	10.0	NR
	29.7	90.1	.901	90.5	21.1	10.4	NR
	29.7	89.0	.923	87.0	37.0	11.1	NR
Average	30.0	89.6	.910	89.9			

Sample preparation: A salt-water solution of 2 gm NaCl per 690 ml water was used with the sample preparation procedure presented in the summary of Figure III.9.

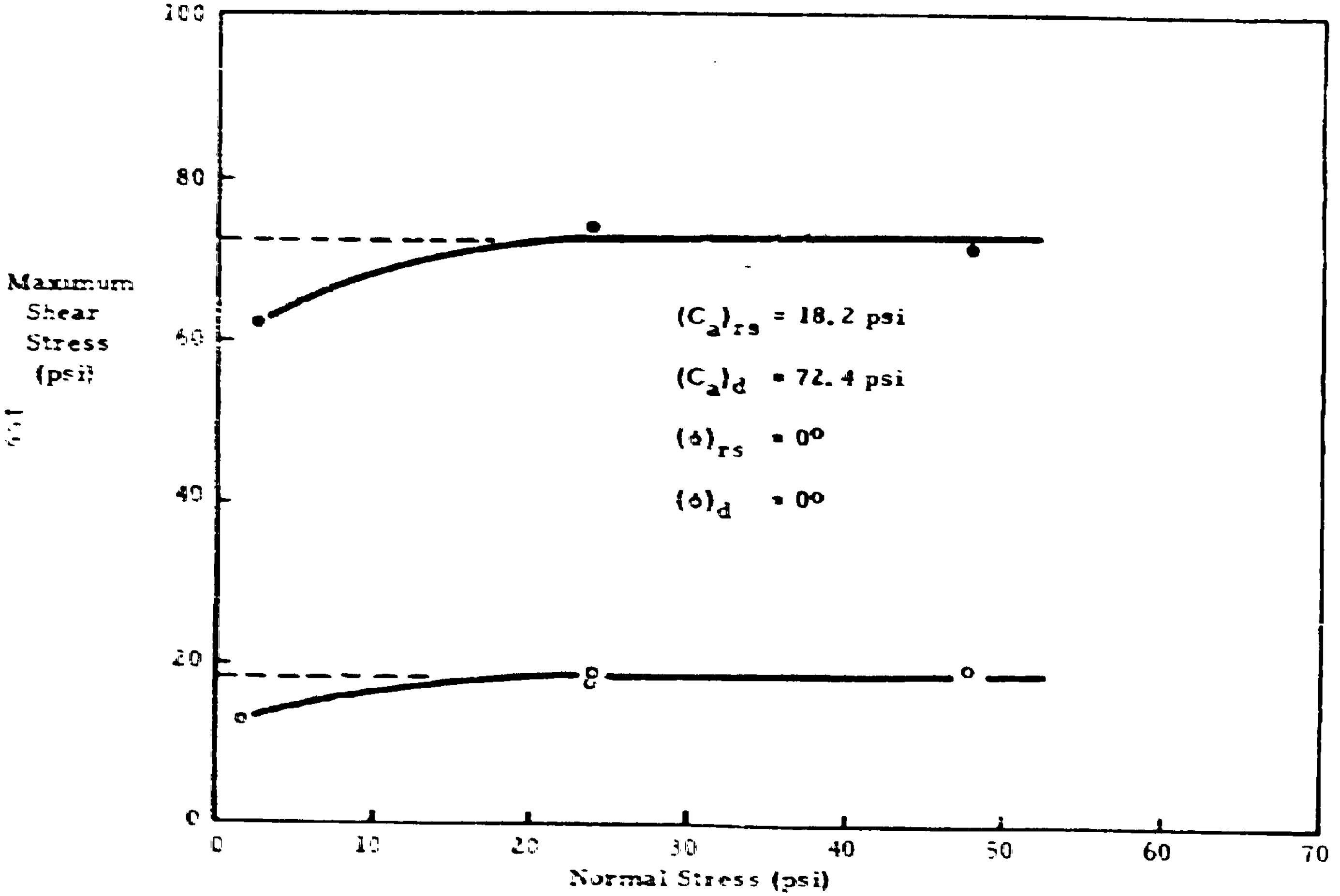

Figure III. 15 Failure Envelopes for Jordan Buff Clay + Glycerin: w = 40%

Table III.15 Test Results: Jordan Buff Clay + Glycerin $w \approx 40\%$

Test Type	w (%)	γ_d (pcf)	e	S (%)	σ_{ff} (psi)	τ_m (psi)	Δ_n
Rapid Static	40.0	84.6	1.020	85.8	1.6	13.1	+
	↓	84.6	1.020	85.8	23.9	18.7	NR
		84.4	1.029	84.9	47.8	17.9	NR
		84.5	1.024	85.4	47.8	19.5	NR
Dynamic	40.0	83.9	1.040	83.7	47.8	71.6	NR
	↓	83.6	1.045	83.8	23.9	74.0	NR
		83.3	1.051	83.1	2.4	62.1	NR
Average	40.0	84.1	1.033	84.6			

<u>Sample preparation:</u> The desired weights of dry material (150 gm) and glycerin for an individual sample were thoroughly mixed with a spatula in an evaporating dish. All material was then worked into the shear box with the spatula and compressed at 60 psi in the air cylinder (about 40 psi on the sample) until the rate of normal displacement was less than 0.001 in/min.

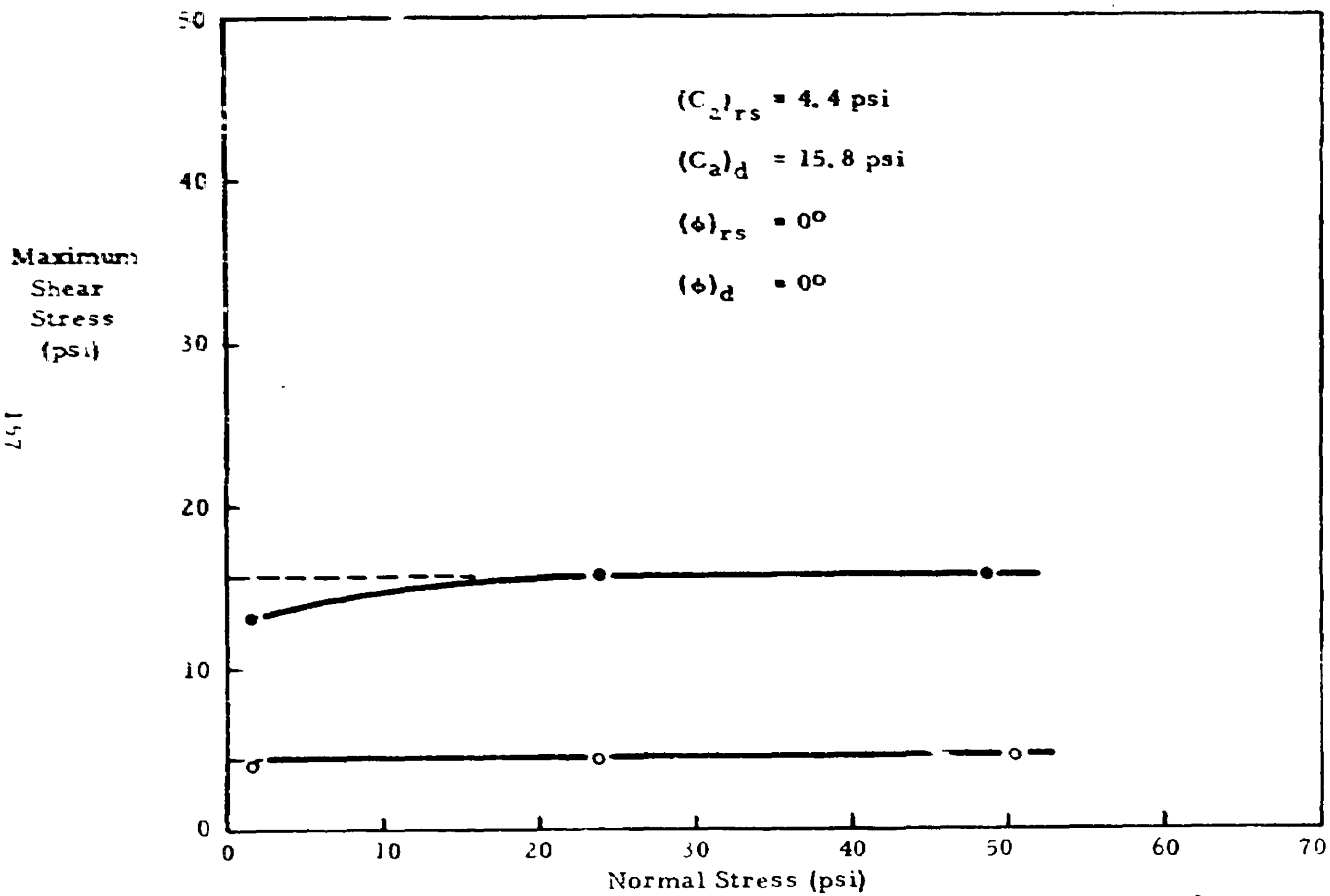

Figure III. 16 Failure Envelopes for Jordan Buff Clay + Glycerin: $w \approx 60\%$

Table III.16 Test Results: Jordan Buff Clay + Glycerin $w \approx 60\%$

Test Type	w (%)	γ_d (pcf)	e	S (%)	σ_{ff} (psi)	τ_m (psi)	Δ_n
Rapid Static	60.0	68.8	1.481	88.1	1.6	4.0	–
		68.8	1.481	88.1	23.9	4.4	–
		68.4	1.500	87.5	50.2	4.8	0
Dynamic	60.0	70.0	1.443	91.6	1.6	13.1	+
		70.1	1.425	91.2	48.6	15.9	0
		68.8	1.481	88.1	23.9	15.9	0
Average	60.0	69.1	1.469	89.1			

Sample preparation: See summary of Figure III.15 test results.

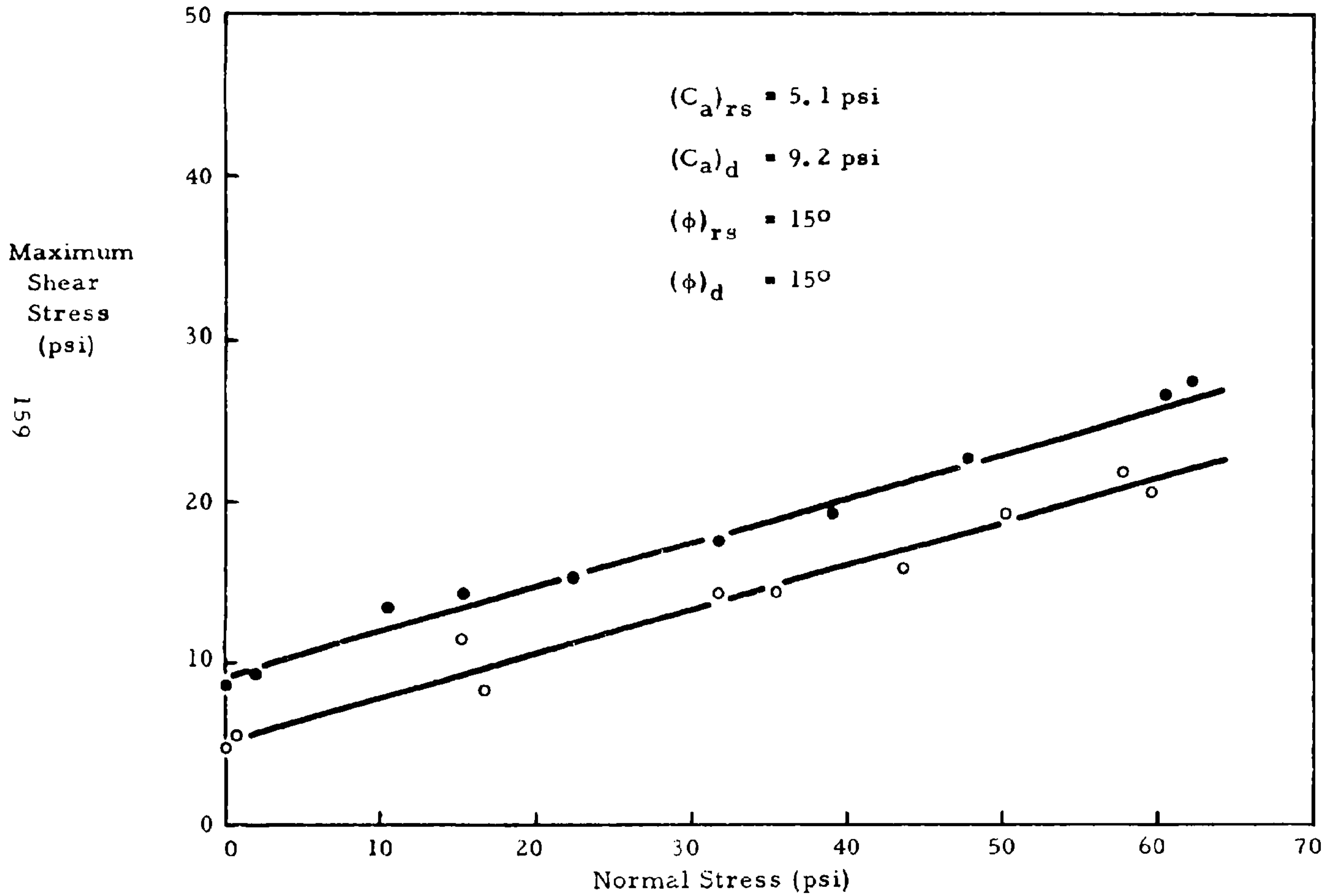

Figure III. 17 Failure Envelopes for Jordan Buff Clay + Kerosene: w≈ 30%

Table III.17 Test Results: Jordan Buff Clay + Kerosene

Test Type	w (%)	γ_d (pcf)	e	S (%)	σ_{ff} (psi)	τ_m (psi)	Δ_n
Rapid Static	≈30.5	≈77.5	≈1.2	≈87	0.8	5.6	+
					59.7	20.7	-
					15.1	11.5	0
					50.2	19.1	-
					35.4	14.3	-
					57.8	21.9	-
					0.0	4.8	+
					31.9	14.3	-
					16.7	8.4	-
					43.8	15.9	-
Dynamic	≈30.5	≈77.5	≈1.2	≈87	52.1	27.1	0
					50.5	26.3	-
					39.0	19.1	-
					22.3	15.1	0
					0.0	8.8	0
					2.0	9.2	+
					10.4	13.5	+
					10.4	13.5	+
					15.1	14.3	0
					31.9	17.5	0
					47.8	22.7	-

Table III.17 Test Results: Jordan Buff Clay + Kerosene (continued)

<u>Sample preparation</u>: The desired weight of dry material (191 gm) and kerosene (64 gm) for an individual sample were mixed thoroughly with a spatula in an evaporating dish. All material was then placed loosely in the shear box and consolidated at an air cylinder pressure of 60 psi (about 40 psi on the sample) until the rate of normal displacement was less than 0.001 in/min.

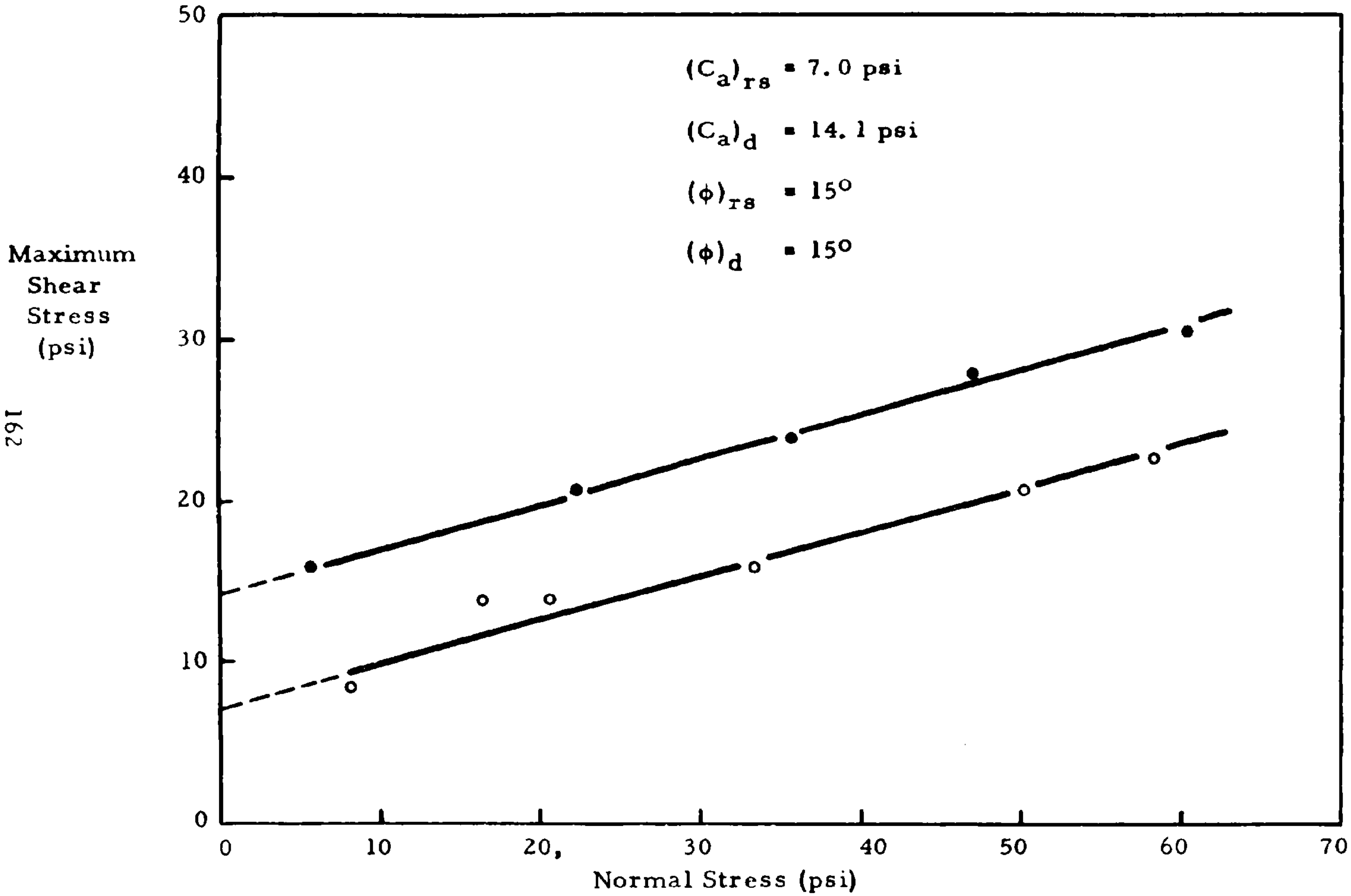

Figure III. 18 Failure Envelopes for Combined "Ideal" Soil: Jordan Buff Clay + Ottawa Sand + Water

Table III.18 Test Results: Combined Soil (Jordan Buff Clay + Ottawa Sand + Water)

Test Type	w (%)	γ_d (pcf)	e	S (%)	σ_{ff} (psi)	τ_m (psi)	Δ_n
Rapid Static	16.5	108.6	.575	79.1	8.0	8.4	NR
	16.4	108.6	.575	79.1	33.5	15.9	NR
	16.3	108.6	.575	79.1	20.7	13.5	NR
	15.8	107.0	.598	72.4	58.2	22.3	-
	15.7	107.1	.594	72.1	50.2	20.7	-
	15.9	106.9	.600	72.6	16.3	13.9	+
Dynamic	16.4	108.6	.575	79.1	5.6	15.9	NR
	16.4	108.6	.575	79.1	22.3	20.7	NR
	16.4	108.6	.575	79.1	35.8	23.9	NR
	15.7	107.1	.594	72.1	60.5	30.3	-
	15.8	107.0	.598	72.4	47.0	27.9	-
Average	16.1	107.9	.585	76.0			

Sample preparation: The sand and clay were mixed in the desired proportions and then prepared as indicated in the summary of Figure III.9 test results.

d. Western Bentonite Clay.

Soil Characteristics:

Liquid Limit	543	%
Plastic Limit	51	%
Plasticity Index	492	%
Specific Gravity	2.79	

X-Ray Analysis:

Montmorillonite	85	%
Quartz	5	%
Feldspars	5	%
Cristobalite	2	%
Illite	2	%
Calcite and Gypsum	1	%
Total	100	%

Chemical Analysis:

Silica (S_i0_2)	55.44	%
Alumina (Al_20_3)	20.14	%
Iron (Fe_20_3)	3.67	%
Lime (C_a0)	0.49	%
Magnesia (M_g0)	2.49	%
Soda (Na_20)	2.76	%
Potash (K_20)	0.60	%
Bound Water	5.50	%
Moisture at 220 °F	8.00	%
Total	99.09	%

pH (6% water suspension) 8.8

Screen Analysis (Ground Material:

passing 100 mesh	99.6	%
passing 200 mesh	91.4	%
passing 325 mesh	76.2	%

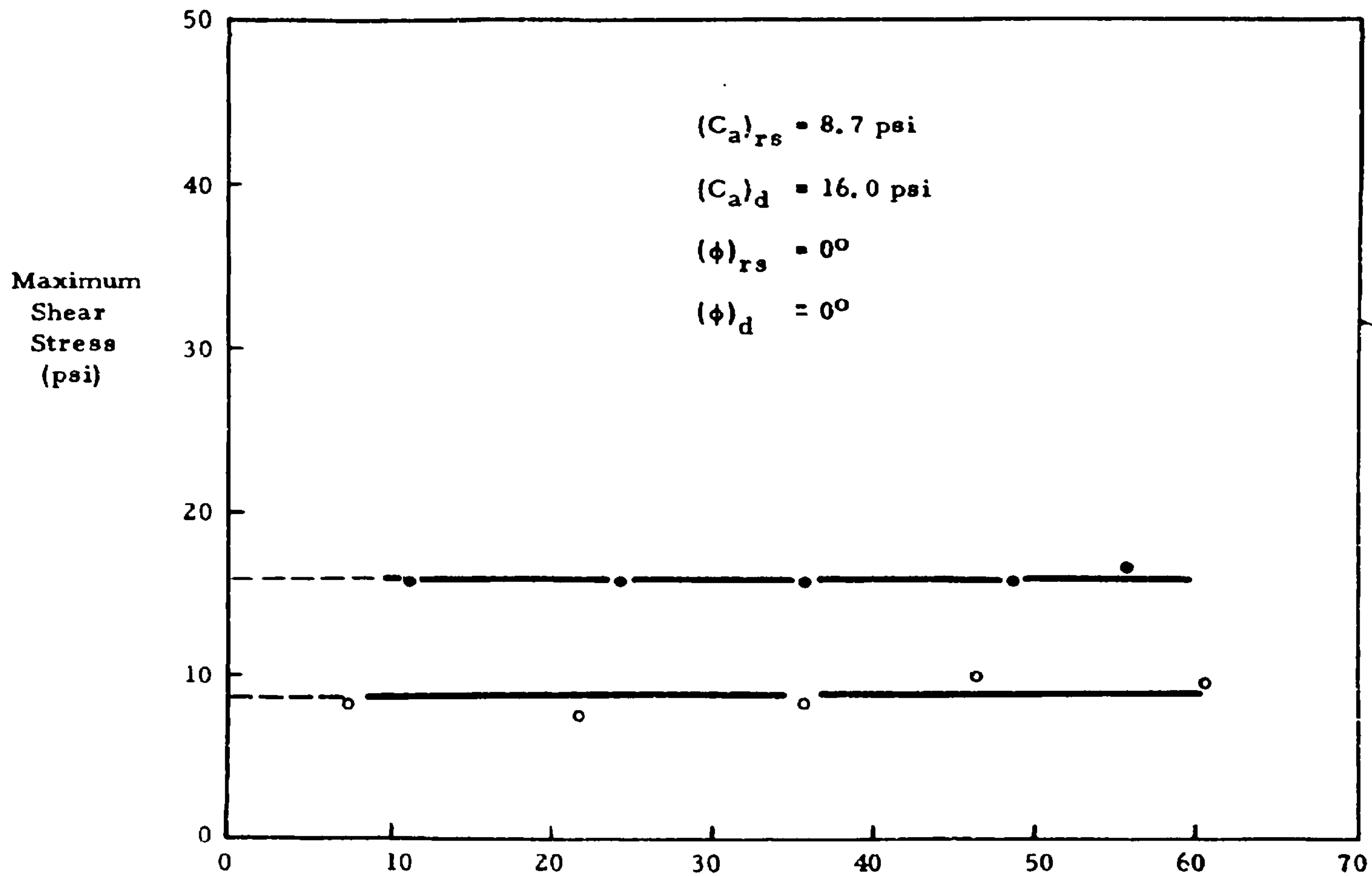

Figure III. 19 Failure Envelopes for Western Bentonite Clay: w ≈ 53%

Table III.19 Test Results: Western Bentonite Clay $w \approx 53\%$

Test Type	w (%)	γ_d (pcf)	e	S (%)	σ_{ff} (psi)	τ_m (psi)	Δ_n
Rapid Static	54.6	64.0	1.718	88.8	7.2	8.4	+
	55.4	63.6	1.731	89.5	21.9	7.6	-
	52.2	67.4	1.626	92.0	35.8	8.4	NR
	52.3	67.4	1.626	92.0	46.2	10.0	-
	52.0	67.6	1.578	91.6	60.5	9.6	-
Dynamic	55.1	63.8	1.731	89.0	35.8	15.9	-
	54.9	63.9	1.722	88.9	11.1	15.9	0
	52.3	67.4	1.626	92.0	24.3	15.9	-
	52.4	67.4	1.626	92.0	48.6	15.9	-
	51.8	67.7	1.570	91.6	55.8	16.7	-
Average	53.3	66.0	1.655	90.7			

<u>Sample preparation</u>: See summary of Figure III.9 test results.

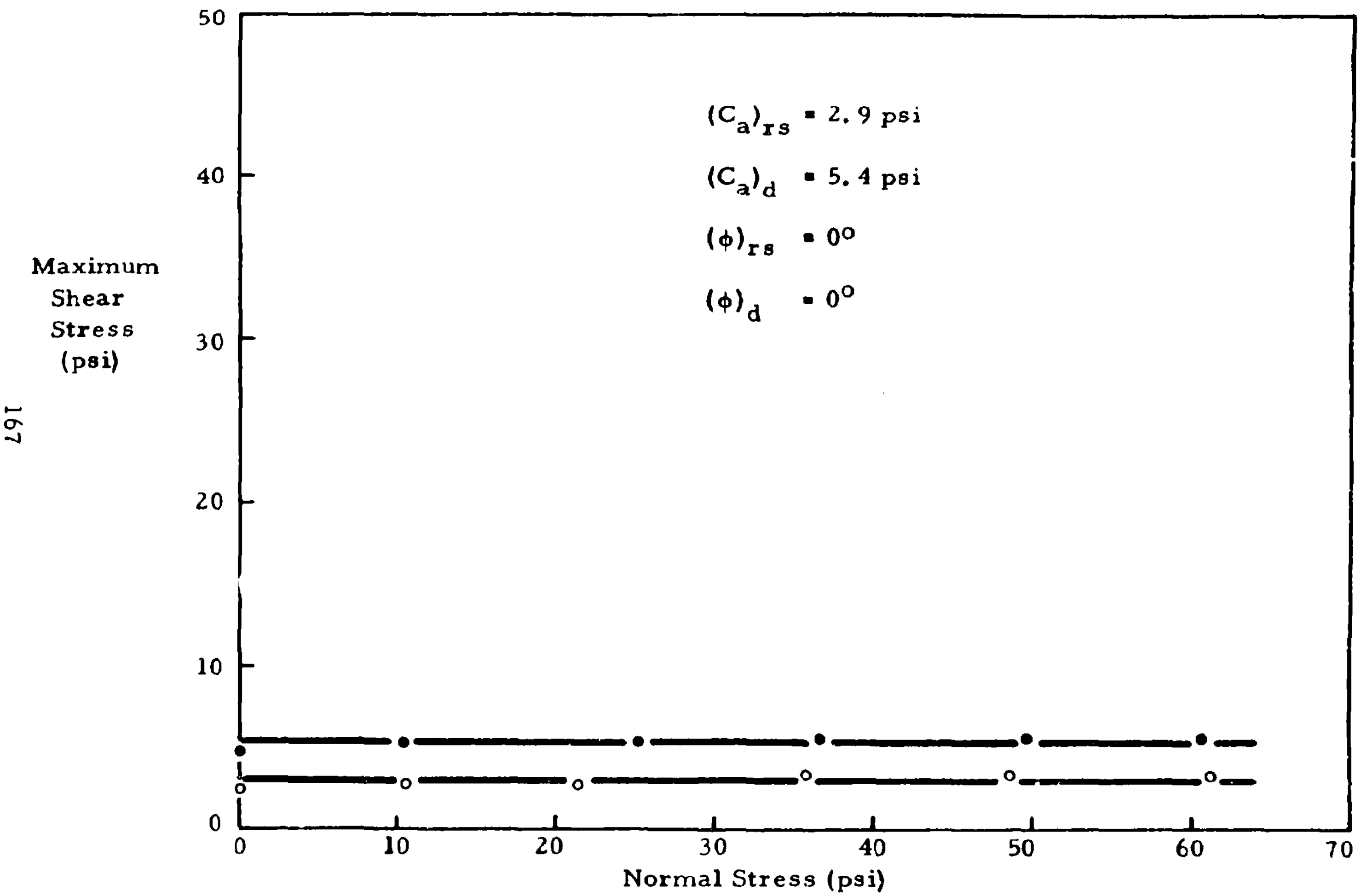

Figure III. 20 Failure Envelopes for Western Bentonite Clay: w ≈ 95%

Table III.20 Test Results: Western Bentonite Clay $w \approx 95\%$

Test Type	w (%)	γ_d (pcf)	e	S (%)	c_{ff} (psi)	τ_m (psi)	Δ_n
Rapid Static	95.2	45.6	2.815	94.5	0.0	2.4	+
	94.3	46.8	2.795	92.2	61.1	3.2	-
	95.4	45.6	2.815	94.5	21.1	2.8	-
	95.0	45.4	2.84-	93.5	48.6	3.2	-
	94.5	45.5	2.82+	93.4	35.8	3.2	-
	97.7	44.8	2.890	94.4	10.4	2.8	-
Dynamic	94.4	46.8	2.795	92.2	0.0	4.8	0
	94.2	46.9	2.79+	92.1	60.5	5.6	-
	95.3	45.6	2.815	94.5	25.1	5.2	0
	94.9	45.5	2.830	94.4	11.1	5.2	0
	95.2	45.3	2.845	93.5	36.6	5.6	-
	95.0	45.4	2.84-	93.5	49.8	5.6	0
Average	95.1	45.8	2.824	93.5			

<u>Sample preparation</u>: See summary of Figure III.9 test results.

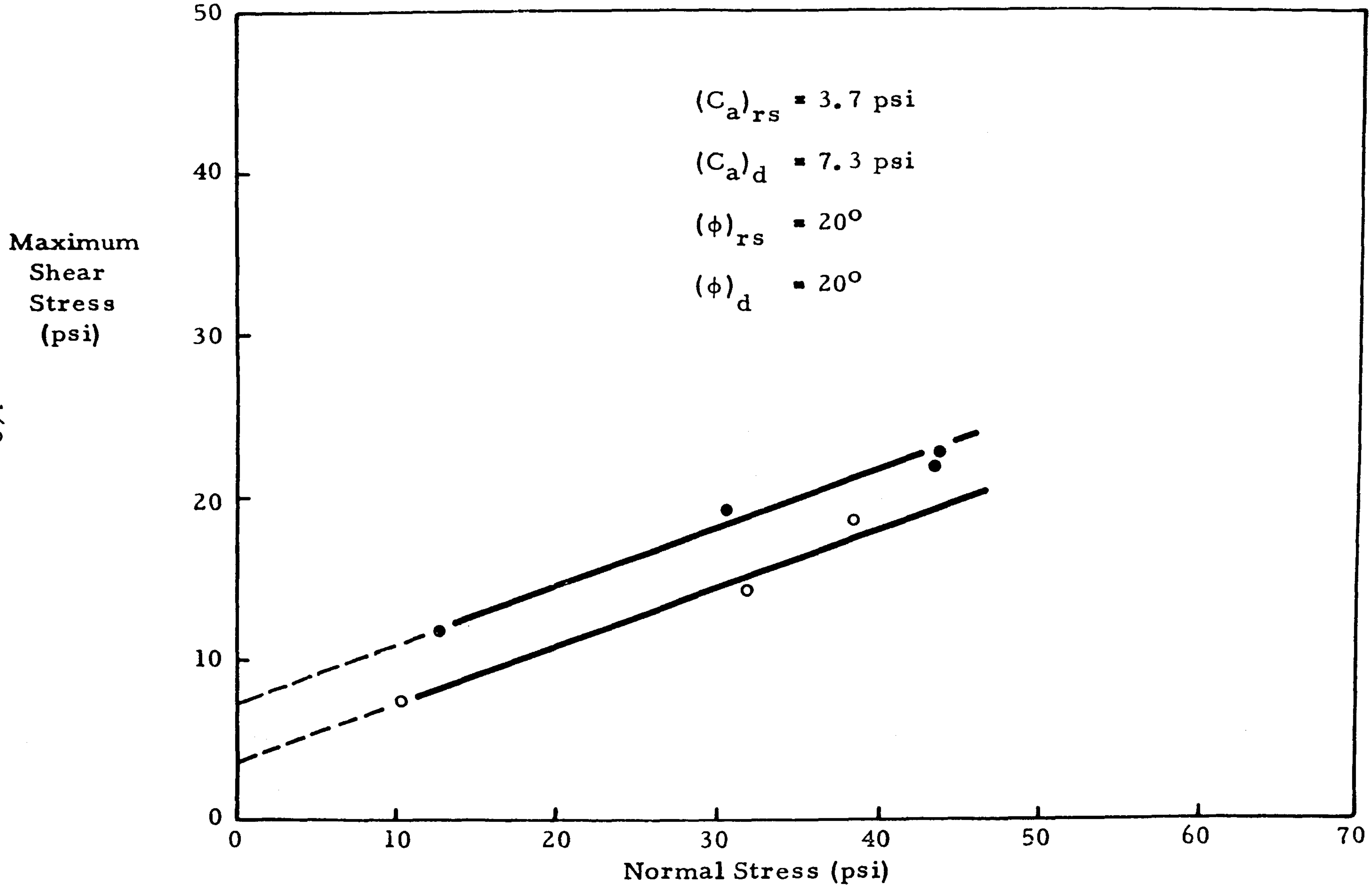

Figure III. 21 Failure Envelopes for Western Bentonite Clay + Benzene: w ≈ 40%

Table III.21 Test Results: Western Bentonite Clay + Benzene $w \approx 40\%$

Test Type	w (%)	γ_d (pcf)	e	S (%)	σ_{ff} (psi)	τ_m (psi)	Δ_n
Rapid Static	≈40	78.1	1.288	100	10.4	7.6	0
		78.3	1.221	100	31.9	14.3	-
		75.8	1.291	97.1	38.2	18.7	-
Dynamic	≈40	77.8	1.237	100	12.7	11.9	0
		76.8	1.269	100	30.3	19.1	-
		76.8	1.269	99.7	43.4	21.9	-
		77.3	1.251	100	43.8	22.7	-
Average	≈40	77.3	1.261	99.5			

Sample preparation: The desired weight of dry material was mixed with benzene at a moisture (benzene) content of 50%. Due to evaporation while mixing it was necessary to add some more to bring it to the desired moisture content (50%) prior to placement of the sample in the shear box. Consolidation at an air cylinder pressure of 60 psi (about 40 psi on the sample) until the rate of normal displacement was less than 0.001 in/min reduced the initial 50% moisture content to approximately 40% at testing.

e. <u>Nevada Test Site Desert Alluvium.</u>

Soil Characteristics:

Specific Gravity	2.76
Grain Size	≈ 70% Finer than 0.05 mm
	≈ 2% Finer than 0.005 mm

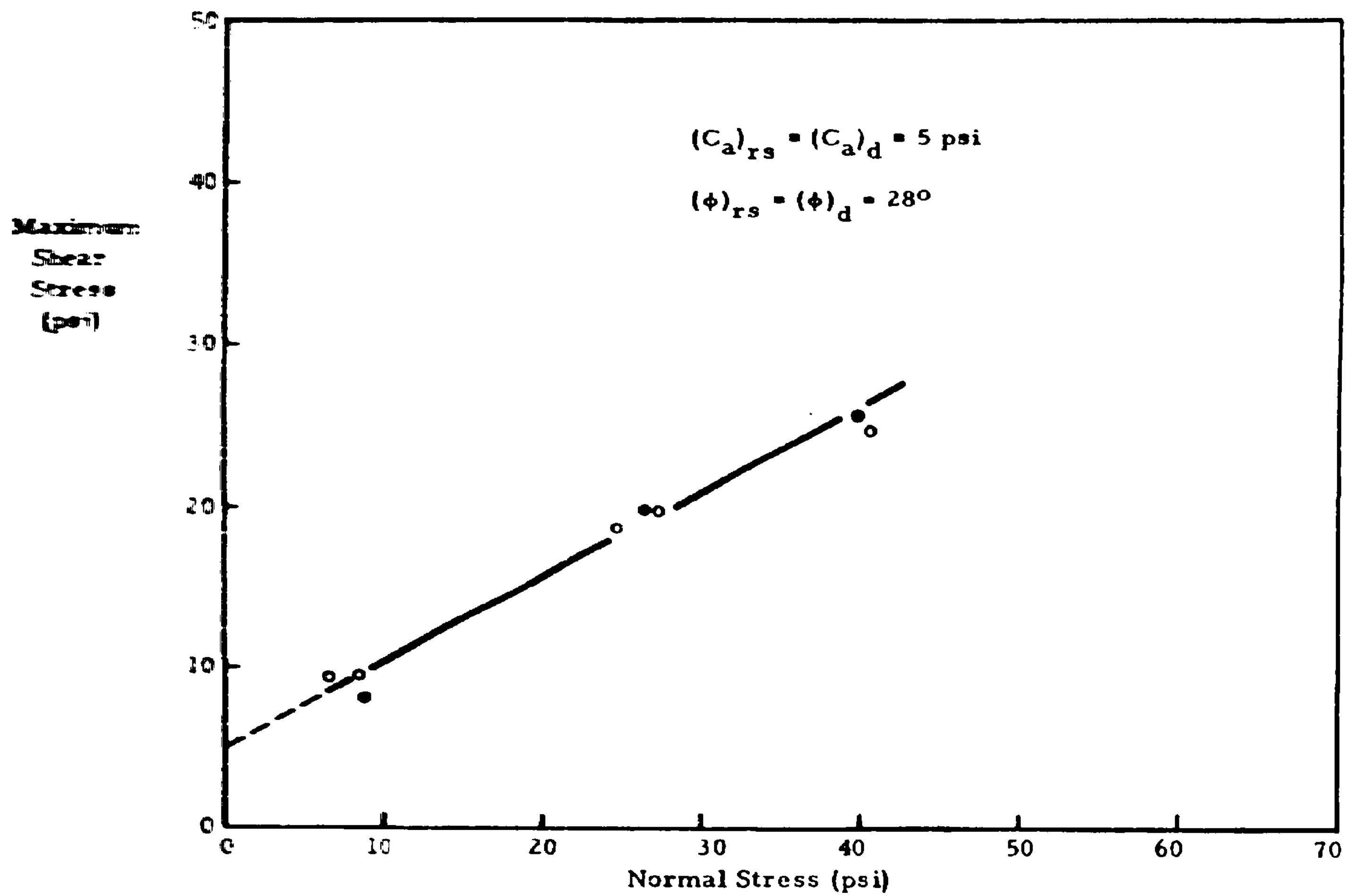

Figure III. 22 Failure Envelope for Remolded Nevada Test Site Desert Alluvium

Table III.22 Test Results: Nevada Test Site Desert Alluvium (Remolded)

Test Type	w (%)	γ_d (pcf)	e	S (%)	σ_{ff} (psi)	τ_m (psi)	Δ_n
Rapid Static	≈ 6.2	≈ 79	≈ 1.2	≈ 15	24.7	18.7	NR
	↓	↓	↓	↓	8.4	9.6	↓
					6.4	9.6	
					27.1	19.9	
					40.6	24.7	
Dynamic	≈ 6.2	≈ 79	≈ 1.2	≈ 15	8.8	8.0	NR
	↓	↓	↓	↓	26.3	19.9	↓
					39.8	25.5	

<u>Sample preparation:</u> 208 gm of material were placed loosely in the shear box and the upper gripper spacer was seated at a pressure of 60 psi in the air cylinder (about 40 psi on the sample).

f. Chicago Blue Clay.

Soil Characteristics:

Liquid Limit	38.6	%
Plastic Limit	15.9	%
Plasticity Index	22.7	%
Specific Gravity	2.83	

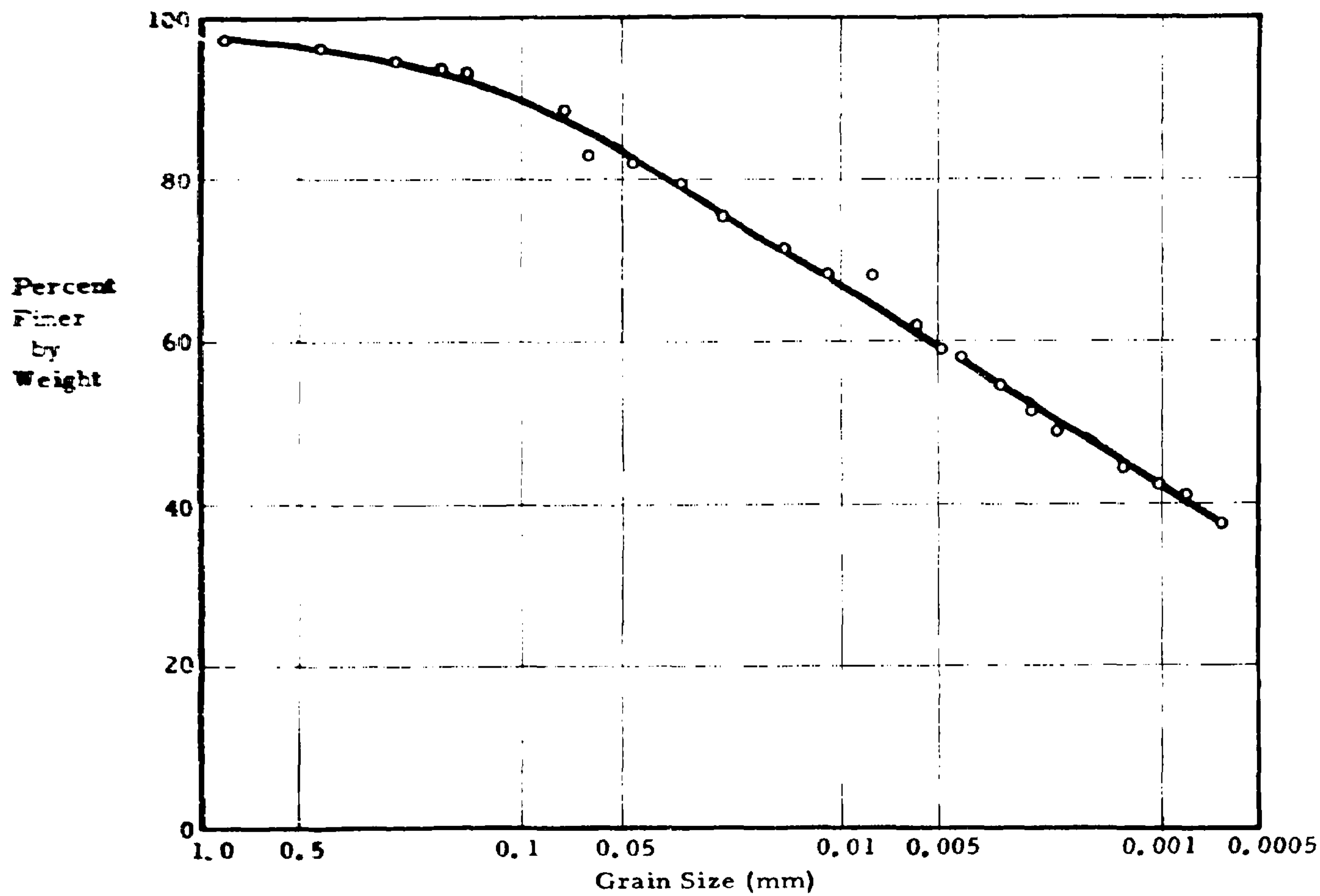

Figure III. 23 Grain Size Distribution Curve for Chicago Blue Clay

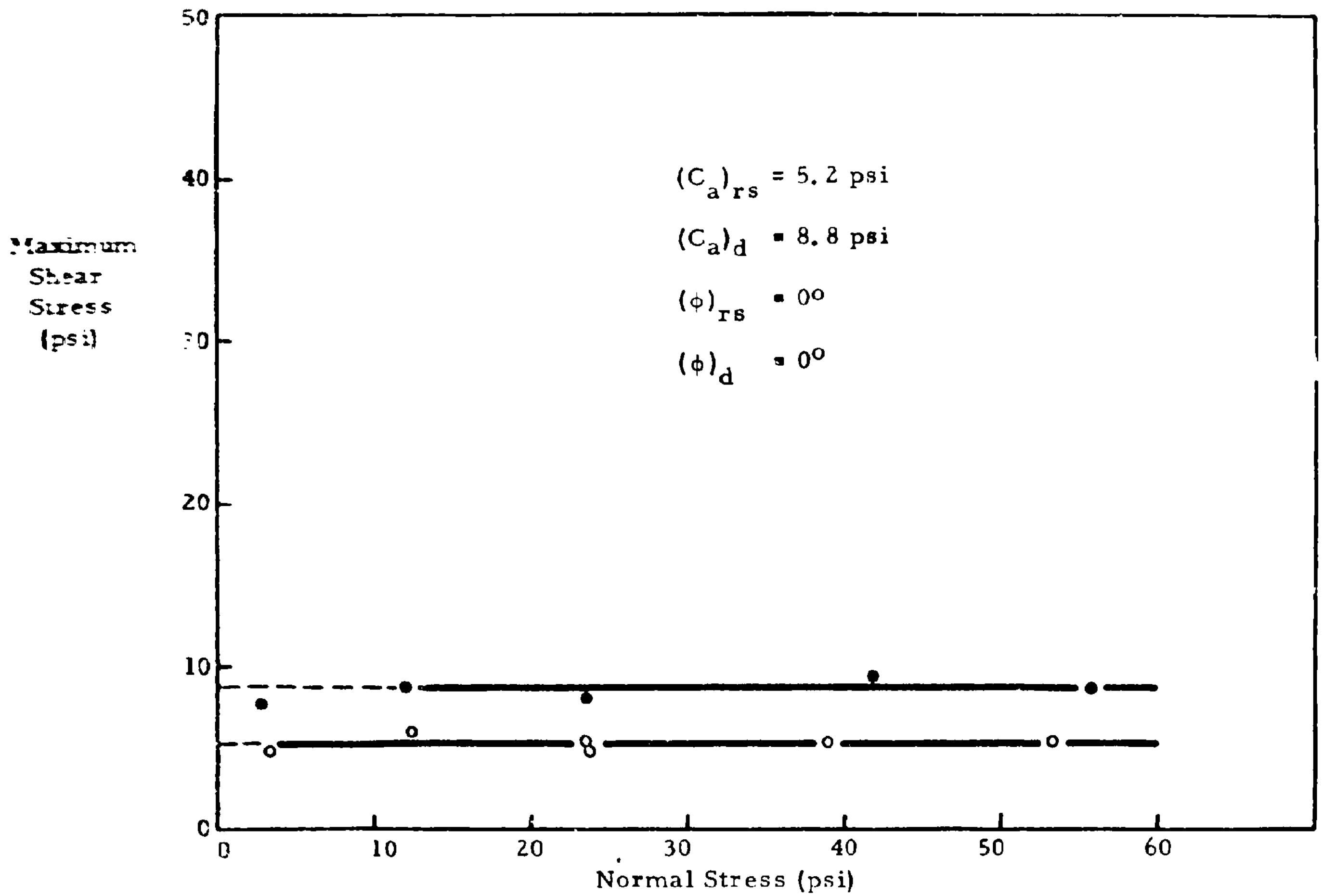

Figure III. 24 Failure Envelopes for "Undisturbed" Chicago Blue Clay

Table III.24 Test Results: Chicago Blue Clay (Undisturbed)

Test Type	w (%)	γ_d (pcf)	e	S (%)	σ_{ff} (psi)	τ_m (psi)	Δ_n
Rapid Static	28.9	94.1	.874	93.0	23.5	5.2	0
	30.5	92.5	.909	94.2	23.9	4.8	-
	30.4	92.6	.905	94.9	39.0	5.2	-
	29.7	94.0	.878	95.4	53.4	5.2	-
	29.6	93.5	.887	93.8	12.3	6.0	-
	30.0	92.6	.905	93.4	3.2	4.8	0
Dynamic	30.2	92.6	.905	94.5	23.5	8.0	-
	29.2	93.6	.887	93.3	41.8	9.2	-
	30.1	93.1	.897	94.9	55.8	8.8	NR
	30.2	93.1	.897	94.9	2.8	7.6	+
	30.2	92.4	.910	93.6	11.9	8.8	0
Average	29.9	93.1	.896	94.2			

<u>Sample preparation:</u> The soil was removed from the sampling tube by cutting the tube lengthwise on opposing diameters. It was then cut into slices sufficiently thick such that the sample could be trimmed to the proper height with a 4 inch diameter 3/4 inch thick trimming ring. Once inserted in the shear box the soil was compressed to its preconsolidation pressure (23.6 psi on the sample) until the rate of normal displacement was less than 0.001 in/min.

g. <u>Rochester Sandy Silt.</u>

Soil Characteristic:

Specific Gravity	2.70

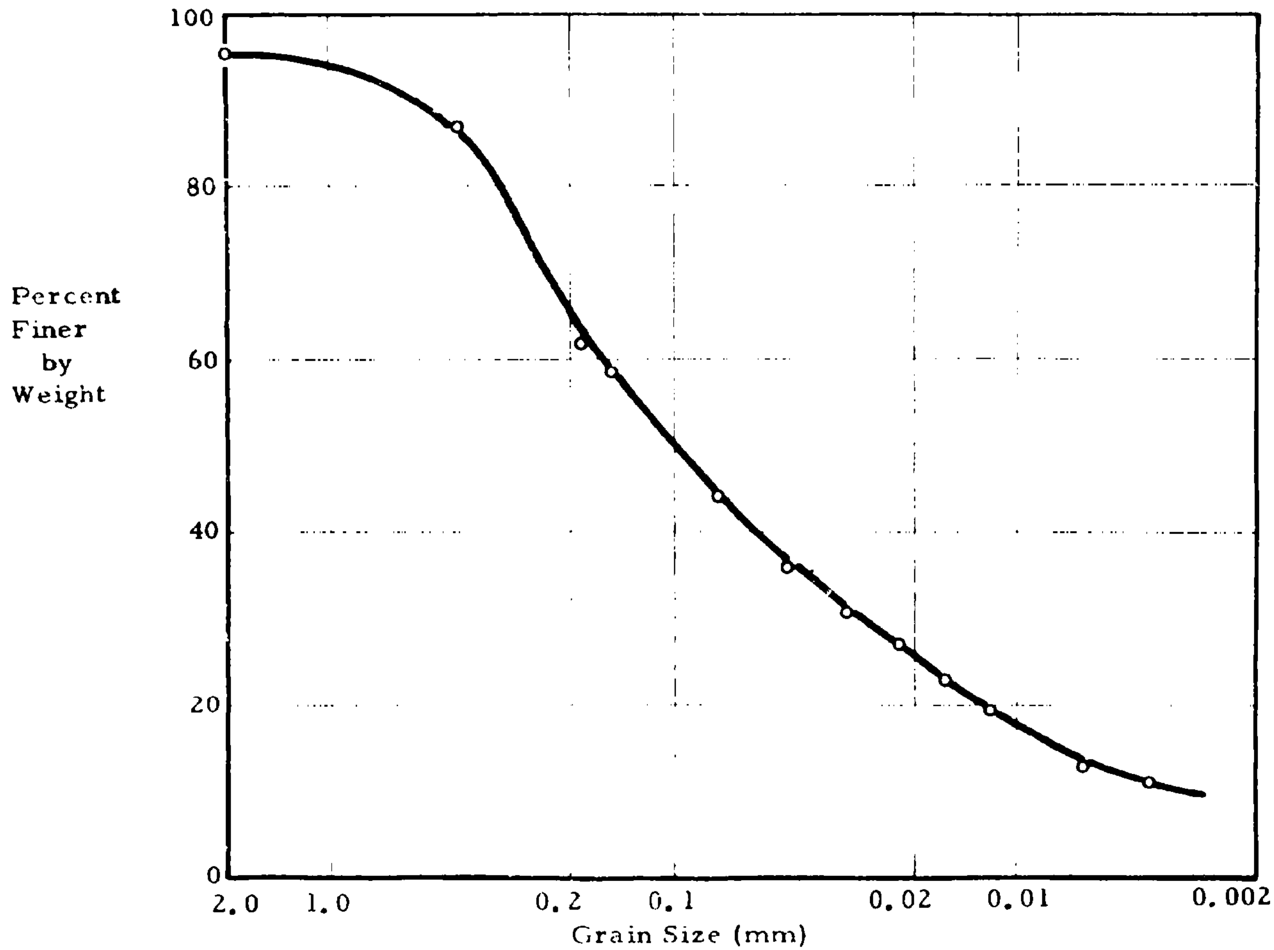

Figure III. 25 Grain Size Distribution Curve for Rochester Sandy Silt

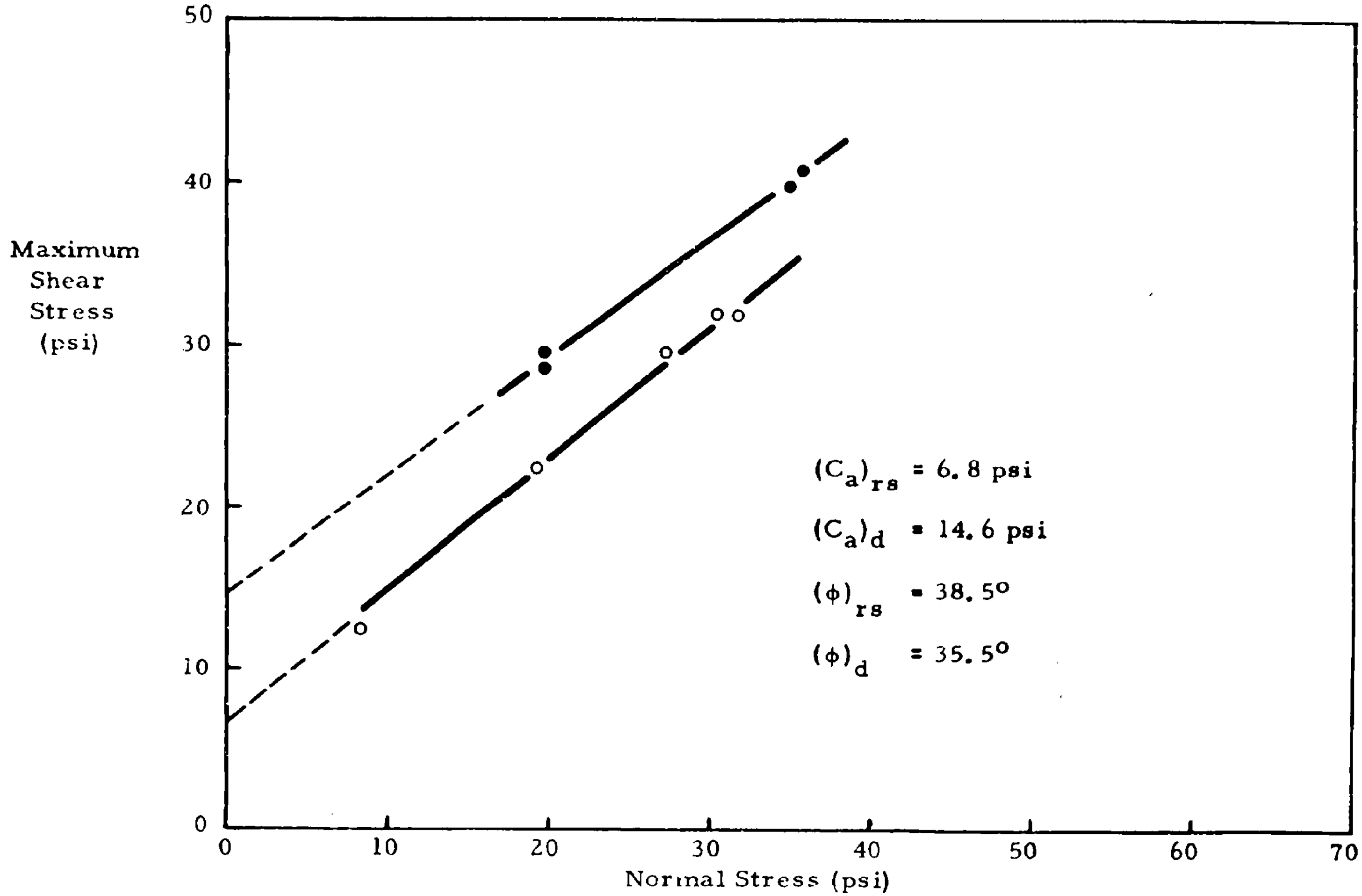

Figure III. 26 Failure Envelopes for "Undisturbed" Rochester Sandy Silt

Table III.26 Test Results: Rochester Sandy Silt (Undisturbed)

Test Type	w (%)	γ_d (pcf)	e	S (%)	σ_{ff} (psi)	τ_m (psi)	Δ_n
Rapid Static	14.5	≈ 106	≈ .60	≈ 61	19.1	22.3	-
	11.8				8.3	12.3	+
	13.2				30.3	31.9	NR
	13.3				27.2	29.5	-
	13.5				31.9	31.9	-
Dynamic	13.4	≈ 106	≈ .60	≈ 61	19.9	28.7	+
	14.5				19.9	29.5	+
	13.0				35.8	40.6	0
	--				35.0	39.8	NR
Average	13.4						

Sample preparation: An undisturbed sample was obtained by the test pit method. Individual specimens were cut from the large block of soil using a thin steel ring which was the same diameter as the shear box and 3/4 inch thick. This ring was set into the surface of the soil block to surround the desired sample. The soil was removed from the outside perimeter of the ring to enable a cheese cutter blade to be slipped underneath the steel ring and sample thus freeing the intended specimen. The ring and sample were placed over the shear box cavity and a 4 inch diameter metal disk was used to force the specimen from the ring into the shear box. To seat the upper gripper spacer a 60psi air cylinder pressure (40 psi on the sample) was established and removed.

h. <u>Notre Dame Lake Marl.</u>

Soil Characteristics:

Liquid Limit	99.5	%
Plastic Limit	73.3	%
Plasticity Index	26.2	%
Shrinkage Limit	55.0	%
Specific Gravity	2.63	

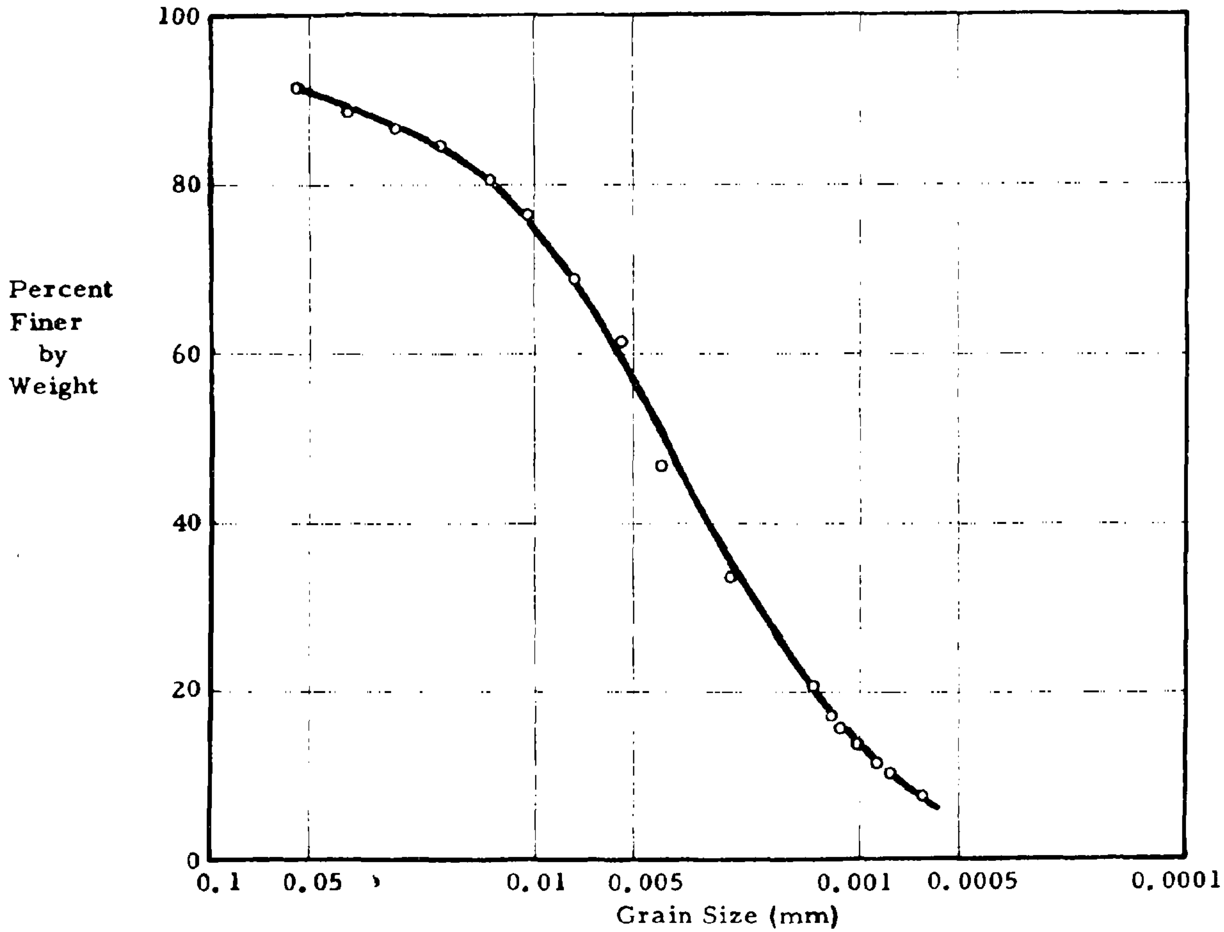

Figure III. 27 Grain Size Distribution Curve for Notre Dame Lake Marl

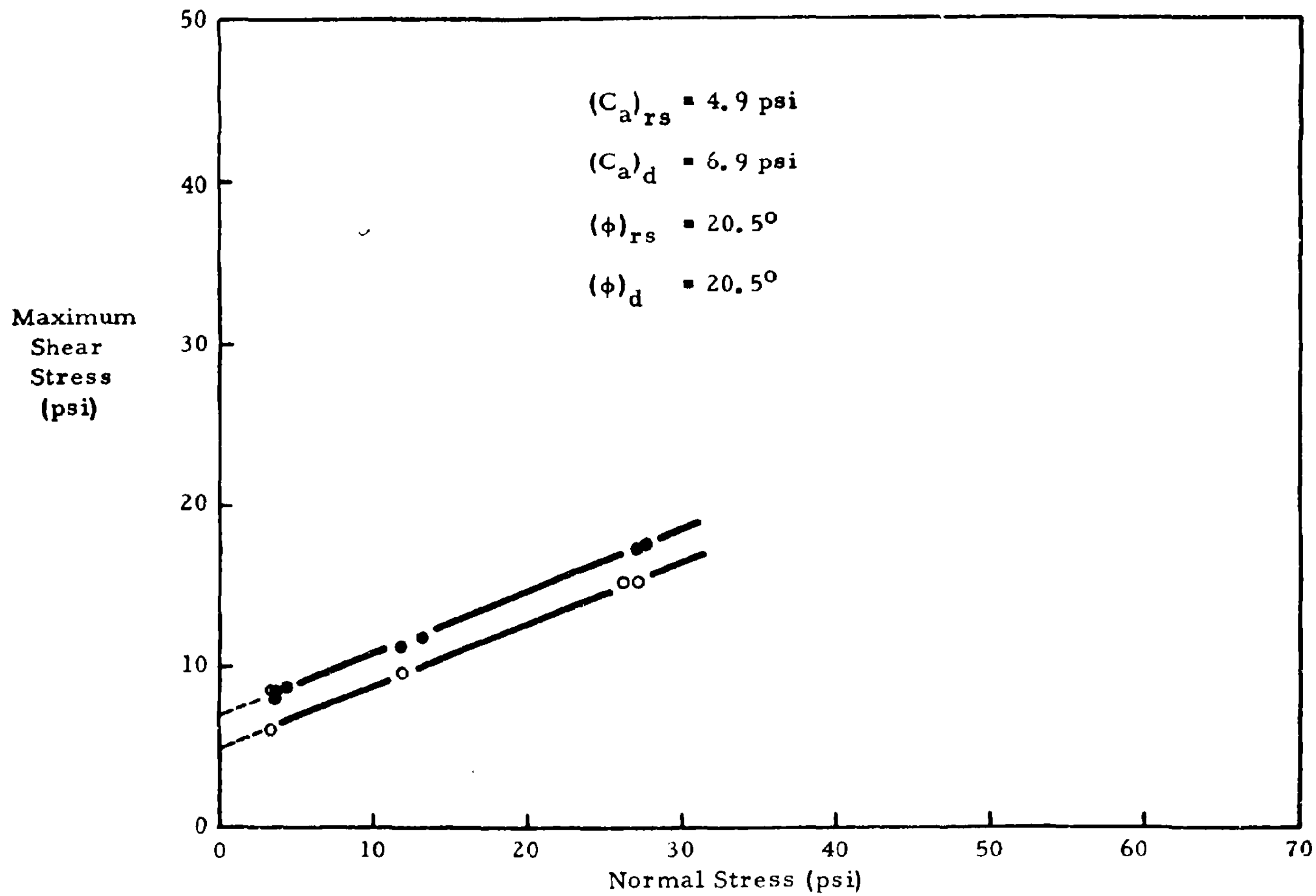

Figure III. 28 Failure Envelopes for "Undisturbed" Notre Dame Lake Marl

Table III.28 Test Results: Notre Dame Lake Marl (Undisturbed)

Test Type	w (%)	γ_d (pcf)	e	S (%)	σ_{ff} (psi)	τ_m (psi)	Δ_n
Rapid Static	89.5	≈ 40	≈ 3.1	≈ 74	3.2	6.0	0
	88.4				26.3	15.1	-
	84.2				27.1	15.1	-
	85.8				11.9	9.6	-
Dynamic	--	≈ 40	≈ 3.1	≈ 74	3.2	8.4	0
	94.0				4.4	8.8	+
	93.5				3.6	8.0	+
	94.8				3.6	8.4	+
	89.7				11.9	11.1	0
	90.9				13.1	11.9	-
	85.4				27.1	17.1	-
	87.0				27.9	17.5	-
Average	89.4						

Sample preparation: An undisturbed sample was obtained by the test pit method. Individual specimens were obtained as indicated in the summary of Figure III.26 test results. With the sample in the shear box the upper gripper spacer was seated by hand. The normal force at which the specimen was to be sheared was applied three minutes before applying the shear force. At the end of this period the rate of normal displacement was less than 0.001 in/min.

APPENDIX IV. SPECIAL TEST RESULTS

Table IV.1 Test Results: Inertial Confinement of ASTM C-190 Standard Ottawa Sand

Test Type	w (%)	γ_d (pcf)	e	S (%)	σ'_{ff} (psi)	τ_m (psi)	Δ_n
"Dynamic" with PNEUMATIC Normal Force	0	107.4	.536	0	6.8	6.8	+
					6.8	7.2	+
					11.9	10.4	+
					11.9	10.8	+
					11.5	10.4	+
					11.9	10.4	+
					11.9	11.1	NR
					20.7	19.9	+
					23.9	22.3	NR
"Dynamic" with MASS Normal Force	0	107.4	.536	0	11.9	19.9	NR
					11.9	19.9	
					11.9	21.5	
					5.5	11.1	
					5.5	10.4	
					2.4	4.4	
					8.0	14.3	
					10.4	18.3	
					14.3	23.9	

Sample preparation: See summary of Figure III.1 test results.

Table IV.2 Test Results: Simultaneous "Dynamic" Loading of Jordan Buff Clay

Test Type	w (%)	γ_d (pcf)	e	S (%)	σ_{ff} (psi)	τ_m (psi)	Δ_n
Rapid Static	29.6	92.3	.852	94.9	15.9	13.9	NR
	29.5	91.6	.865	92.2	40.6	13.9	-
Dynamic	29.6	92.3	.852	94.9	19.1	25.9	+
	29.6	91.5	.869	93.2	41.8	27.5	0
Simultaneous	29.6	91.5	.869	93.2	14.3	23.5	+
"Dynamic"	29.6	91.6	.865	93.6	46.2	26.3	-
Application	30.1	91.5	.869	94.8	67.7	27.1	-
of	29.7	92.1	.856	93.6	12.7	25.5	+
Shear	29.7	92.1	.856	93.6	31.9	25.5	+
and	29.6	91.9	.862	93.8	10.4	26.3	+
Normal	29.6	91.9	.862	93.8	47.0	26.3	+
Forces	29.4	91.6	.869	92.7	48.6	27.1	-
	29.3	91.7	.866	93.2	10.4	24.3	+
Average	29.6	91.8	.862	93.7			

<u>Sample preparation</u>: See summary of Figure III.9 test results.

Table IV.3 Test Results: Repetitive Loading of Jordan Buff Clay

Test Type	w (%)	γ_d (pcf)	e	S (%)	σ_{ff} (psi)	τ^* (psi)	Plastic Shear Disp. per Pulse (in)
Square wave pulsed shear force application at frequency of 1 cps	28.2	91.5	.870	97.1	15.9	2.8	.0016
					15.9	4.8	.0026
					15.9	8.4	.0200
					15.9	9.6	.0448
					15.9	10.0	.0349
	28.4	90.9	.884	97.0	15.9	3.6	.0005
	28.3	91.0	.880	96.9	15.9	0.9	.0002
	28.4	90.9	.884	97.0	15.9	5.2	.0010
	28.3	91.0	.880	96.9	15.9	8.0	.0157
	28.3	91.0	.880	96.9	15.9	5.6	.0054
	28.2	91.1	.877	96.6	15.9	10.0	.0560
Average	28.2	90.9	.875	97.0			

<u>Sample preparation:</u> See summary of Figure III.9 test results.

*Shear force pulsed from zero to the indicated value

DISTRIBUTION

No. cys

HEADQUARTERS USAF

1 Hq USAF (AFCOA), Wash, DC 20330

1 Hq USAF (AFOCE), Wash, DC 20330

1 Hq USAF (AFNIN), Wash, DC 20330

1 USAF Dep, The Inspector General (AFIDI), Norton AFB, Calif 92409

1 USAF Directorate of Nuclear Safety (AFINS), Kirtland AFB, NM 87117

MAJOR AIR COMMANDS

AFSC, Andrews AFB, Wash, DC 20331

1 (SCT)
1 (SCLT)

1 TAC (DORQ-M), Langley AFB, Va 23365

1 SAC (DORQM), Offutt AFB, Nebr 68113

1 AUL, Maxwell AFB, Ala 36112

1 USAFIT, Civil Engineering Center, Wright-Patterson AFB, Ohio 45433

1 USAFA, Colo 80840

AFSC ORGANIZATIONS

1 AFSC Scientific and Technical Liaison Office, Research and Technology Division, AFUFO, Los Angeles, Calif 90045

1 FTD (TDBTL), Wright-Patterson AFB, Ohio 45433

1 ASD, Wright-Patterson AFB, Ohio 45433

1 RTD (RTS), Bolling AFB, Wash, DC 20332

1 AFMTC (MU-135, Tech Library), Patrick AFB, Fla 32925

BSD, Norton AFB, Calif 92409

1 (BSQ)
1 (BSR)
1 (BSOT)

DISTRIBUTION (cont'd)

No. cys	
1	ESD (ESTI), L.G. Hanscom Fld, Bedford, Mass 01731
1	RADC (EMLAL-1), Griffiss AFB, NY 13442
	KIRTLAND AFB ORGANIZATIONS
1	AFSWC (SWEH), Kirtland AFB, NM 87117
	AFWL, Kirtland AFB, NM 87117
15	(WLIL)
15	(WLDC)
1	SAC Res Rep (SACLO), AFSWC, Kirtland AFB, NM 87117
1	TAC Liaison Office (TACLO-S), AFSWC, Kirtland AFB, NM 87117
	OTHER AIR FORCE AGENCIES
1	Director, USAF Project RAND (RAND Library), via: Air Force Liaison Office, The RAND Corporation, 1700 Main Street, Santa Monica, Calif 90406
	ARMY ACTIVITIES
1	Chief of Research and Development, Department of the Army (Special Weapons and Air Defense Division), Wash, DC 20310
1	Director, US Army Waterways Experiment Sta (WESRL), P.O. Box 631, Vicksburg, Miss 39181
2	Director, US Army Engineer Research and Development Laboratories, ATTN: STINFO Branch, Ft Belvoir, Va 20260
1	US Army Engineer Division, Ohio River, Corps of Engineers, Ohio River Division Laboratories (ORDLBVR), 5851 Mariemont Avenue, Mariemont, Cincinnati 27, Ohio
	NAVY ACTIVITIES
1	Chief of Naval Research, Department of the Navy, Wash, DC 20390
1	Bureau of Yards and Docks, Department of the Navy, Code 22.102, (Branch Manager, Code 42.330), Wash 25, DC
1	Commanding Officer, Naval Research Laboratory, Wash, DC 20390
1	Superintendent, US Naval Postgraduate School, ATTN: George R. Luckett, Monterey, Calif
3	Commanding Officer and Director, Naval Civil Engineering Laboratory, Port Hueneme, Calif

DISTRIBUTION (cont'd)

No. cys	
1	Commander, Naval Ordnance Laboratory, ATTN: Dr. Rudlin, White Oa , Silver Spring, Md 20910
	OTHER DOD ACTIVITIES
2	Director, Defense Atomic Support Agency (Document Library Branch), Wash, DC 20301
1	Commander, Field Command, Defense Atomic Support Agency (FCAG3, Special Weapons Publication Distribution), Sandia Base, NM 87115
1	Director, Advanced Research Projects Agency, Department of Defense, The Pentagon, Wash, DC 20301
30	DDC (TIAAS), Cameron Station, Alexandria, Va 22314
	AEC ACTIVITIES
2	Sandia Corporation (Information Distribution Division), Box 5800, Sandia Base, NM 87115
1	Sandia Corporation (Technical Library), P.O. Box 969, Livermore, Calif 94551
1	University of California Lawrence Radiation Laboratory, ATTN: Director's Office, Technical Information Division, P.O. Box 808, Livermore, Calif 94551
1	Director, Los Alamos Scientific Laboratory (Helen Redman, Report Library), P.O. Box 1663, Los Alamos, NM 87554
	OTHER
1	Office of Assistant Secretary of Defense (Civil Defense), Wash, DC 20301
1	Central Intelligence Agency (OCR), 2430 E Street NW, Wash, DC 20505
5	AF Shock Tube Facility, ATTN: Dr. Zwoyer, Box 188, University Station, Albuquerque, NM
2	IIT Research Institute, ATTN: Dr. Eben Vey, 3422 S. Dearborn St, Chicago 15, Illinois
2	Massachusetts Institute of Technology, Dept of Civil Engineering, ATTN: Dr. Robert Whitman, 77 Massachusetts Ave, Cambridge 39, Mass
20	University of Notre Dame, Dept of Civil Engineering, ATTN: Dr. Harry Saxe, Dr. Bruce Schimming, Notre Dame, Indiana

DISTRIBUTION (cont'd)

No. cys	
2	Purdue University, Dept of Civil Engineering, ATTN: Dr. G.A. Leonards, Lafayette, Indiana
1	Shannon & Wilson, Soil Mechanics & Foundation Engineers, 1105 N. 38th Street, Seattle 3, Washington
1	Teledyne, Inc UED Earth Sciences Division, P.O. Box 1650, Library, Pasadena, California
2	Stanford Research Institute, ATTN: F.M.Sauer, G.K. Fowles, 333 Ravens Wood, Menlo Park, California
1	Iowa State University, Dept of Theoretical & Applied Mechanics, ATTN: Glen Murphy, Ames, Iowa
2	University of Illinois, Dept of Civil Engineering, ATTN: Dr. N.M. Newmark, 111 Talbot Laboratory, Urbana, Illinois
1	Princeton University, Dept of Civil Engineering, Princeton, New Jersey
1	University of Washington, ATTN: Dr. I.M. Fyfe, Seattle 5, Washington
1	West Virginia University, Dept of Civil Engineering, ATTN: Dr. James H. Schaub, Morgantown, West Virginia
1	Northrop-Ventura, ATTN: Dr. J.G. Trulio, 1950 Cotner Ave, West Los Angeles, California
1	Physics International, ATTN: Dr. Charles Godfrey, 2700 Merced,San Leandro, California
1	The Boeing Company, Suite 802, First National Bank Building, Albuquerque, New Mexico
1	The Boeing Company, ATTN: H.G. Leistner, M/S47-47, P.O. Box 3707, Seattle, Washington
1	Official Record Copy (WLDC, Lt Seknicka)

UNCLASSIFIED
Security Classification

DOCUMENT CONTROL DATA - R&D

(Security classification of title, body of abstract and indexing annotation must be entered when the overall report is classified)

1. ORIGINATING ACTIVITY (Corporate author) Department of Civil Engineering University of Notre Dame Notre Dame, Indiana	2a. REPORT SECURITY CLASSIFICATION Unclassified 2b. GROUP

3. REPORT TITLE
A Comparison of the Dynamic and Static Shear Strengths of Cohesionless, Cohesive and Combined Soils

4. DESCRIPTIVE NOTES (Type of report and inclusive dates)
March 1962 through May 1965

5. AUTHOR(S) (Last name, first name, initial)
Schimming, B.B.; Haas, H.J.; Saxe, H.C.

6. REPORT DATE	7a. TOTAL NO. OF PAGES	7b. NO. OF REFS
August 1965	210	40

8a. CONTRACT OR GRANT NO. AF29(601)-5174 b. PROJECT NO. 5710 c. DASA Subtask 13.4' d. Program Element 7.60.06.01.5	9a. ORIGINATOR'S REPORT NUMBER(S) AFWL TR-65-48 9b. OTHER REPORT NO(S) (Any other numbers that may be assigned this report)

10. AVAILABILITY/LIMITATION NOTICES
Qualified users may obtain copies of this report from DDC.
Distribution is limited because of the technology discussed in the report.

11. SUPPLEMENTARY NOTES	12. SPONSORING MILITARY ACTIVITY
	Air Force Weapons Laboratory Kirtland AFB, New Mexico

13. ABSTRACT A direct shear device capable of applying maximum shear stresses to soil specimens in a period of time ranging from 1 millisecond to 20 minutes has been utilized to test a wide variety of soils. The cohesionless materials, an Ottawa sand in the loose and dense condition, a powdered Nevada silt and a dry powder clay, did not exhibit any increase in maximum shear resistance due to an impact type dynamic shear force application as compared to a static force application. An increase of apparent friction angle from 45 degrees to approximately 60 degrees due to inertial confinement was observed in a dense Ottawa sand. Cohesive materials, which included undisturbed and remolded clays and combined soils (mixtures of sand and clay), demonstrated an increase in maximum shear resistance under impact loads described solely by the apparent cohesion intercept of the failure envelope. The friction angle was essentially insensitive to test duration. The ratio of the apparent cohesion for a failure envelope involving failure times of 5 milliseconds to the corresponding intercept for failure times of nearly 1 minute was approximately 2. This ratio appeared to be relatively insensitive to moisture content, dry density, grain size and soil structure (flocculated or dispersed) for degrees of saturation in excess of 85%. The apparent cohesion ratio appeared to decrease on the dry side of optimum for compacted soils. Investigation of different pore fluids indicated that pore fluid viscosity was not primarily responsible for the increases in strength. The simultaneous dynamic application of normal and shear forces did not alter the apparent cohesion ratio of the clays studied. A preliminary discussion of repetitive force results on clays is included in the report.

DD FORM 1 JAN 64 1473

UNCLASSIFIED
Security Classification

UNCLASSIFIED

Security Classification

14 KEY WORDS	LINK A		LINK B		LINK C	
	ROLE	WT	ROLE	WT	ROLE	WT
Dynamic Soil Response						
Dynamic Shear Strength of Soil						
Dynamic Direct Shear of Soil						
Soil Mechanics						
Foundation Engineering						

INSTRUCTIONS

1. ORIGINATING ACTIVITY: Enter the name and address of the contractor, subcontractor, grantee, Department of Defense activity or other organization *(corporate author)* issuing the report.

2a. REPORT SECURITY CLASSIFICATION: Enter the overall security classification of the report. Indicate whether "Restricted Data" is included. Marking is to be in accordance with appropriate security regulations.

2b. GROUP: Automatic downgrading is specified in DoD Directive 5200.10 and Armed Forces Industrial Manual. Enter the group number. Also, when applicable, show that optional markings have been used for Group 3 and Group 4 as authorized.

3. REPORT TITLE: Enter the complete report title in all capital letters. Titles in all cases should be unclassified. If a meaningful title cannot be selected without classification, show title classification in all capitals in parenthesis immediately following the title.

4. DESCRIPTIVE NOTES: If appropriate, enter the type of report, e.g., interim, progress, summary, annual, or final. Give the inclusive dates when a specific reporting period is covered.

5. AUTHOR(S): Enter the name(s) of author(s) as shown on or in the report. Enter last name, first name, middle initial. If military, show rank and branch of service. The name of the principal author is an absolute minimum requirement.

6. REPORT DATE: Enter the date of the report as day, month, year; or month, year. If more than one date appears on the report, use date of publication.

7a. TOTAL NUMBER OF PAGES: The total page count should follow normal pagination procedures, i.e., enter the number of pages containing information.

7b. NUMBER OF REFERENCES: Enter the total number of references cited in the report.

8a. CONTRACT OR GRANT NUMBER: If appropriate, enter the applicable number of the contract or grant under which the report was written.

8b, 8c, & 8d. PROJECT NUMBER: Enter the appropriate military department identification, such as project number, subproject number, system numbers, task number, etc.

9a. ORIGINATOR'S REPORT NUMBER(S): Enter the official report number by which the document will be identified and controlled by the originating activity. This number must be unique to this report.

9b. OTHER REPORT NUMBER(S): If the report has been assigned any other report numbers *(either by the originator or by the sponsor)*, also enter this number(s).

10. AVAILABILITY/LIMITATION NOTICES: Enter any limitations on further dissemination of the report, other than those imposed by security classification, using standard statements such as:

(1) "Qualified requesters may obtain copies of this report from DDC."

(2) "Foreign announcement and dissemination of this report by DDC is not authorized."

(3) "U. S. Government agencies may obtain copies of this report directly from DDC. Other qualified DDC users shall request through ________________."

(4) "U. S. military agencies may obtain copies of this report directly from DDC. Other qualified users shall request through ________________."

(5) "All distribution of this report is controlled. Qualified DDC users shall request through ________________."

If the report has been furnished to the Office of Technical Services, Department of Commerce, for sale to the public, indicate this fact and enter the price, if known.

11. SUPPLEMENTARY NOTES: Use for additional explanatory notes.

12. SPONSORING MILITARY ACTIVITY: Enter the name of the departmental project office or laboratory sponsoring *(paying for)* the research and development. Include address.

13. ABSTRACT: Enter an abstract giving a brief and factual summary of the document indicative of the report, even though it may also appear elsewhere in the body of the technical report. If additional space is required, a continuation sheet shall be attached.

It is highly desirable that the abstract of classified reports be unclassified. Each paragraph of the abstract shall end with an indication of the military security classification of the information in the paragraph, represented as *(TS)*, *(S)*, *(C)*, or *(U)*.

There is no limitation on the length of the abstract. However, the suggested length is from 150 to 225 words.

14. KEY WORDS: Key words are technically meaningful terms or short phrases that characterize a report and may be used as index entries for cataloging the report. Key words must be selected so that no security classification is required. Identifiers, such as equipment model designation, trade name, military project code name, geographic location, may be used as key words but will be followed by an indication of technical context. The assignment of links, rules, and weights is optional.

AFSC (KAFB NM) 1965

UNCLASSIFIED

Security Classification